Quaternary Science Reviews 30 (2011) 3542–3574

Contents lists available at SciVerse ScienceDirect

Quaternary Science Reviews

journal homepage: www.elsevier.com/locate/quascirev

Invited review

Sea level and shoreline reconstructions for the Red Sea: isostatic and tectonic considerations and implications for hominin migration out of Africa

Kurt Lambeck [a,b,*,1], Anthony Purcell [a], Nicholas. C. Flemming [c], Claudio Vita-Finzi [e], Abdullah M. Alsharekh [f], Geoffrey N. Bailey [d]

[a] Research School of Earth Sciences, The Australian National University, Canberra 0200, Australia
[b] Département des Géosciences, École Normale Supérieure, 24, rue Lhomond, 75231 Paris, CEDEX 05, France
[c] National Oceanography Centre, Southampton SO14 3ZH, UK
[d] Department of Archaeology, University of York, the King's Manor, York YO1 7EP, UK
[e] Natural History Museum, Cromwell Road, London SW7 5BD, UK
[f] Department of Archaeology, King Saud University, P.O. Box 2627, Riyadh 12372, Saudi Arabia

ARTICLE INFO

Article history:
Received 24 March 2011
Received in revised form
5 August 2011
Accepted 12 August 2011
Available online 21 October 2011

ABSTRACT

The history of sea level within the Red Sea basin impinges on several areas of research. For archaeology and prehistory, past sea levels of the southern sector define possible pathways of human dispersal out of Africa. For tectonics, the interglacial sea levels provide estimates of rates for vertical tectonics. For global sea level studies, the Red Sea sediments contain a significant record of changing water chemistry with implications on the mass exchange between oceans and ice sheets during glacial cycles. And, because of its geometry and location, the Red Sea provides a test laboratory for models of glacio-hydro-isostasy. The Red Sea margins contain incomplete records of sea level for the Late Holocene, for the Last Glacial Maximum, for the Last Interglacial and for earlier interglacials. These are usually interpreted in terms of tectonics and ocean volume changes but it is shown here that the glacio-hydro-isostatic process is an additional important component with characteristic spatial variability. Through an iterative analysis of the Holocene and interglacial evidence a separation of the tectonic, isostatic and eustatic contributions is possible and we present a predictive model for palaeo-shorelines and water depths for a time interval encompassing the period proposed for migrations of modern humans out of Africa. Principal conclusions include the following. (i) Late Holocene sea level signals evolve along the length of the Red Sea, with characteristic mid-Holocene highstands not developing in the central part. (ii) Last Interglacial sea level signals are also location dependent and, in the absence of tectonics, are not predicted to occur more than 1–2 m above present sea level. (iii) For both periods, Red Sea levels at 'expected far-field' elevations are not necessarily indicative of tectonic stability and the evidence points to a long-wavelength tectonic uplift component along both the African and Arabian northern and central sides of the Red Sea. (iv) The observational evidence is consistent with tectonic and isostatic processes both operating over the past 300,000 years without requiring changes in the time averaged (over a few thousand years) tectonic rates. (v) Recent bathymetric data for the Bab al Mandab region have been compiled to confirm the location and depth of the sill controlling flow in and out of the Red Sea. Throughout the last 400,000 years the Red Sea has remained open to the Gulf of Aden with cross sectional areas at times of glacial maxima about 2% of that today. (vi) The minimum channel widths connecting the Red Sea to the Gulf of Aden at times of lowstand occur south of the Hanish Sill. The channels are less than 4 km wide and remain narrow for as long as local sea levels are below −50 m. This occurs for a number of sustained periods during the last two glacial cycles and earlier. (vii) Periods suitable for crossing between Africa and Arabia without requiring seaworthy boats or seafaring skills occurred periodically throughout the Pleistocene, particularly at times of favourable environmental climatic conditions that occurred during times of sea level lowstand.

© 2011 Elsevier Ltd. All rights reserved.

* Corresponding author. Research School of Earth Sciences, The Australian National University, Canberra ACT 0200, Australia. Tel.: +61 2 6125 5161; fax: +61 2 6125 5443.
E-mail addresses: kurt.lambeck@anu.edu.au, lambeck@geologie.ens.fr (K. Lambeck).
[1] Tel.: +33 1 4432 2201.

0277-3791/$ – see front matter © 2011 Elsevier Ltd. All rights reserved.
doi:10.1016/j.quascirev.2011.08.008

1. Introduction

The history of Red Sea relative sea level change and of the concomitant migration of its shorelines is of interest and importance for a number of reasons. One is the understanding of possible pathways of human dispersal out of Africa and this provided the original motivation for this study (Bailey et al., 2007a,b; Bailey, 2009). The current estimate for the sill depth at the southern end of the Red Sea is close to the maximum sea level regression during past glacial maxima, and a close examination of the changing geometry of the channel with changes in sea level during the glacial-interglacial cycle is therefore critically important for evaluating the relative ease or difficulty of human transit at different periods in the human evolutionary sequence. Another interest is that sea level change can provide a quantitative constraint, through estimates of long-term rates of vertical tectonics, on models for Red Sea rifting (Bosworth et al., 2005). A third is that the Red Sea sediments contain a long and significant record of changing water chemistry that has implications for global sea level change (Rohling et al., 1998; Siddall et al., 2004). Fourthly, because of the geometry and location of the Red Sea basin, a complex spatial pattern of this sea level change can be expected – even in the absence of tectonics – such that the region provides a potentially important laboratory for testing models of sea level change that have been developed for other parts of the world.

Coral reef growth has been important along much of the Red Sea coast during recent interglacials and has provided ready indicators of changes in the relative disposition of land and sea surfaces. This has been recognised at least since the time when Darwin wrote: '*The nature of the formations round the shores of the Red Sea, as described by several authors, shows that the whole of this large area has been elevated within a very recent tertiary epoch*' (Darwin, 1842, p. 136). He made reference to Eduard Rüppell's observations in his *Reise in Abyssinien* published in 1838 that (in Darwin's words) '*the tertiary formation, of which he has examined the organic remains, forms a fringe along the shores with a uniform height of from 30 and 40 feet, from the mouth of the Gulf of Suez to about Lat. 26°; but that south of 26°, the beds attain only the height of from 12 to 15 feet*'. Furthermore, Darwin notes that '*there may be a decrease in the elevation of the shores in the middle parts of the Red Sea, for Dr. Malcolmson (as he informs me) collected from the cliffs of Camaran Island (Lat. 15° 30' S.)* (Kamaran Island, off Yemen) *shells and corals, apparently recent, at a height between 30 and 40 feet; and Mr. Salt (Travels in Abyssinia) describes a similar formation a little southward on the opposite shore at Amphila*' (Anfile Bay, Eritrea). Darwin concluded: '*The entire area of the Red Sea appears to have been upraised within a modern period*' (p. 138).

Others have reached a different view, concluding that while there are some areas of active tectonic uplift, as in the Gebel el Zeit region, much of the African coast of the Red Sea has been tectonically stable since some time after the penultimate interglacial and before the Last Interglacial (e.g. Plaziat et al., 1998). This conclusion is based on the observation that Late Holocene and Last Interglacial (LIg) reefs occur at elevations where they are 'expected to be' in the absence of tectonics. 'Expected to be' in this case refers to the elevations at which such reefs are typically observed in other parts of the globe and on the assumption that spatial variation in the earth's response to changing ice-water loads during successive glacial cycles is unimportant. The inference of a cessation of tectonic uplift before the LIg and the neglect of the ice-water loading effects on relative sea level change are both unsatisfactory and a realistic evaluation of the Red Sea sea level evidence requires a relaxation of both these constraints before realistic reconstructions of shorelines and bathymetry during the past glacial cycle and earlier are attempted.

The aims of this paper are therefore to:

- Examine critically the field evidence for relative sea level in the Red Sea at different epochs, including the Holocene, the Last and earlier Glacial Maximum (LGM), and the earlier interglacials, notably Marine Isotope Stage (MIS) 5.5.
- Combine this field data with models for the glacio-hydro-isostatic response of the crust over this time range.
- Arrive at a more realistic assessment of the contribution made by rifting and tectonic uplift to relative sea level change by extracting the glacio-hydro-isostatic component from the observed sea levels.
- Make a critical re-assessment of the bathymetric data for the shallowest part of the seabed in the vicinity of the Hanish Sill and use the above models to map palaeo-shorelines at the southern end of the Red Sea.
- Assess the implications of the resulting palaeogeographic reconstructions for the relative ease or difficulty of human transit across the southern end of the Red Sea, and the likely timing of such crossings.

Section 2 of this paper gives a brief overview of the tectonic setting of the region with an emphasis only on aspects that are relevant to the interpretation of the sea level data. Section 3 deals with the evidence and the analysis of the sea level data itself through a sequence of steps outlined in Fig. 1. The Holocene evidence is dealt with first, applying first-order tectonic corrections where this is said to be important, based on the observed elevations of LIg reefs. Inversion of this data for earth-model parameters (E_1) is then attempted in order to establish whether the effective response parameters for this region are significantly different from those found for other regions. In the next step, the sparse LGM evidence is discussed and compared with model predictions based on this preliminary E_1 solution. In the third step the LIg data is examined and compared with model predictions based on the E_1 parameters and on LIg ice volumes inferred from far-field analyses of sea level. This comparison establishes whether the original assumption made about the LIg elevations in the Holocene analysis was sufficient, whether tectonic uplift has been important and whether the resulting rates of uplift are consistent with the observed elevations of the older marine terraces observed at a number of locations. If results consistent with the latter can be found, the original Holocene sea level data is corrected for these site-specific tectonic components, a new solution for earth-model parameters $E2$ is made, assuming that the tectonic rates of vertical movement are constant over the time interval, and the cycle of analysis is repeated. When convergence occurs, the palaeo-bathymetry and palaeo-shorelines are constructed at specific epochs for the critically important region of the Hanish Sill and Bab al Mandab Strait at the southern end of the Red Sea, using a new bathymetric data set, to provide a basis for the assessment of the likely importance of the 'southern dispersal route' for migrations out of Africa (Lahr and Foley, 1994; Petraglia and Alsharekh, 2003; Macaulay et al., 2005; Beyin, 2006; Petraglia and Rose, 2009) (Section 5).

2. Tectonic context

The Red Sea has a complex history of episodic extension and rifting with the most recent phase of spreading having occurred only since the Miocene, with a total opening of approximately 80–100 km during the past 4–5 Ma (Girdler and Styles, 1974; Hötzl, 1984; Hempton, 1987; Purser and Bosence, 1998), recorded also on both its flanks (e.g. Bohannon et al., 1989; Drury et al., 1994). The major tectonic units are the Arabian and African Plates in the east and west, respectively, both of which have 'normal' shield crust and upper mantle structure (Stern and Johnson, 2010) (Fig. 2). In addition, the seismicity of the region (e.g. Ambraseys et al., 1995;

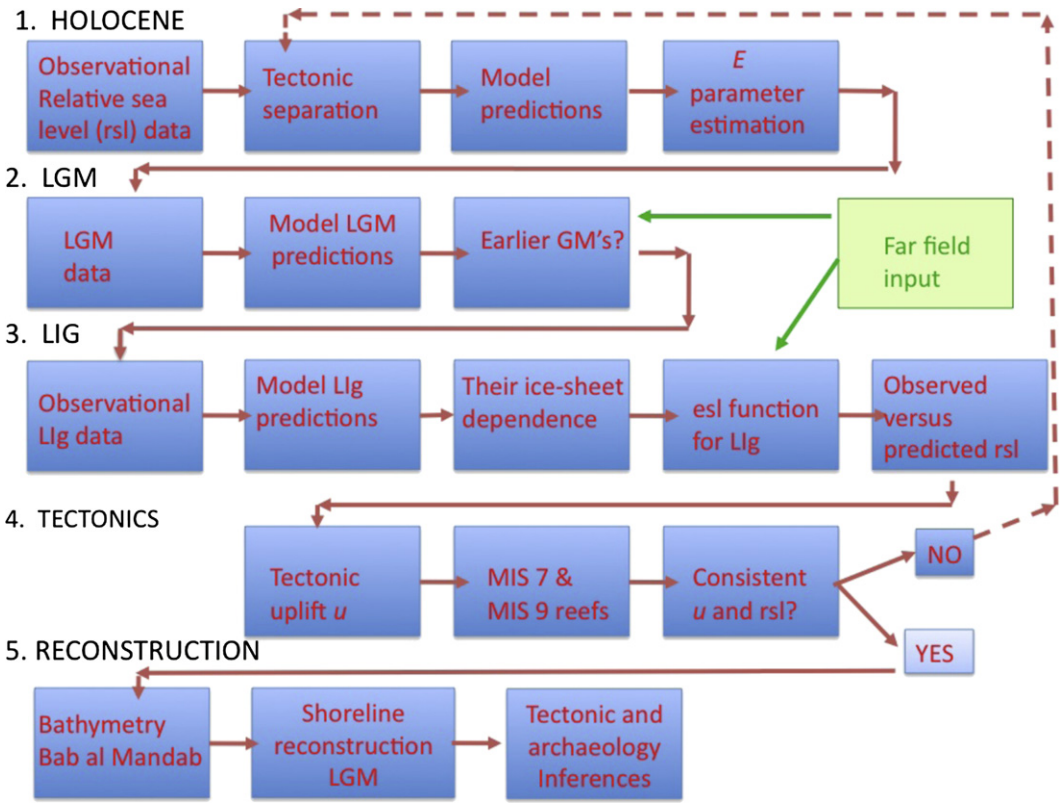

Fig. 1. Flow diagram for the sequence of data analysis and model calculations. In the first step the Red Sea Holocene field evidence for relative sea-level (rsl) change and vertical tectonic movement is evaluated and compared with the predicted isostatic signals followed by a first approximation solution for the Earth-model parameters *E*. In the second step the Last Glacial Maximum (LGM) evidence from the Red Sea is discussed and for the earlier glacial maxima (GM) evidence external to the Red Sea is introduced. In step 3 the observational evidence for the Last Interglacial (LIg) is discussed along with models for the predicted isostatic signals, introducing external data for estimates of ice volumes during the LIg. In step 4 the original assumptions for vertical tectonic movements are tested against the observational evidence for earlier interglacials. If the inferences for tectonics are not consistent with those adopted in step 1 then the steps 1–3 are repeated, using the new tectonic rates from this step. When internally consistent results are achieved the palaeo reconstructions for the entrance to the Red Sea follow.

Bosworth et al., 2005) defines the Sinai and Danakil microplates in the north and south, respectively (Chu and Gordon, 1998). The key boundaries between the tectonic units are the constructive plate boundary represented by the axial graben and central deeps of the Red Sea, a transform boundary along the Gulf of Aqaba and the Dead Sea rift and, according to Bosworth and Taviani (1996), an 'aborted' continental rift along the Gulf of Suez. In the south, the Red Sea links tectonically to the Gulf of Aden via the Afar with the zone of seismic activity coming onshore in the vicinity of Abdur and the Danakil depression (Fig. 2). We have limited the analysis of the sea level evidence to the Red Sea proper and the tectonics of the Gulf of Tadjoura is excluded here.

The Red Sea proper is characterised by three different sections: late stage continental rifting north of about 23°N, active ocean spreading south of about 20°N, and a central transition zone in between (Cochran, 1983). The northern section is characterised by low levels of seismicity (e.g. Ambraseys et al., 1995; Bosworth et al., 2005) and the sea floor is underlain by stretched and variably magma-intruded continental crust. In the central and southern sections, the sea floor of the axial graben and central deeps are underlain by oceanic crust (Rihm and Henke, 1998). Active seismicity within the ocean spreading zone extends along the central axis of the Red Sea only to ~15°N, with a bifurcation of activity occurring at ~17°N, one branch continuing southwards and possibly dying out at ~15°N and the second branch traversing the Danakil Depression to the Afar Triangle, such that all extension is transferred to this latter branch (McClusky et al., 2010). Seismic activity is low along the western coast of the Red Sea south of ~27°N as far as the Danakil plate boundary at ~16°N, along much of the Arabian Red Sea coast south of about 27°N, and on both sides of Bab al Mandab.

Geodetic evidence for the relative motions of the Nubian and Arabian plates is available for only the last decade (McClusky et al., 2003; ArRajehi et al., 2010) but the geodetic relative pole of rotation for these plates is in good agreement with the average palaeomagnetic estimates for the past 3 Ma of Chu and Gordon (1998). The same applies to the location of the pole for the Arabian and Sinai plates (compare the palaeomagnetic pole of Joffe and Garfunkel, 1987, with the geodetic pole of ArRajehi et al., 2010) although the geodetic rate of rotation is significantly smaller than the palaeomagnetic pole such that either recent rates of rotation are not representative of the long-term average value or the small plate is subject to internal deformation. In either case, deformation may be episodic.

The coastal lowlands on both sides of the Red Sea are mostly backed by eroded escarpment uplifted by up to 2–3 km since early Miocene time (e.g. Hötzl, 1984) and for sea level studies it is important to know whether this uplift has continued into the present time or whether it has ceased in recent time as suggested, for example, by Plaziat et al. (1998) for some sectors of the African side of the Red Sea. The geodetic solutions do not yet provide estimates of vertical displacements but evidence for uplift in more recent geological time does occur in the records of Pleistocene-aged marine morphological features occurring at elevations of tens of metres above present sea level. The chronology of these features, particularly the older ones that are often heavily eroded and

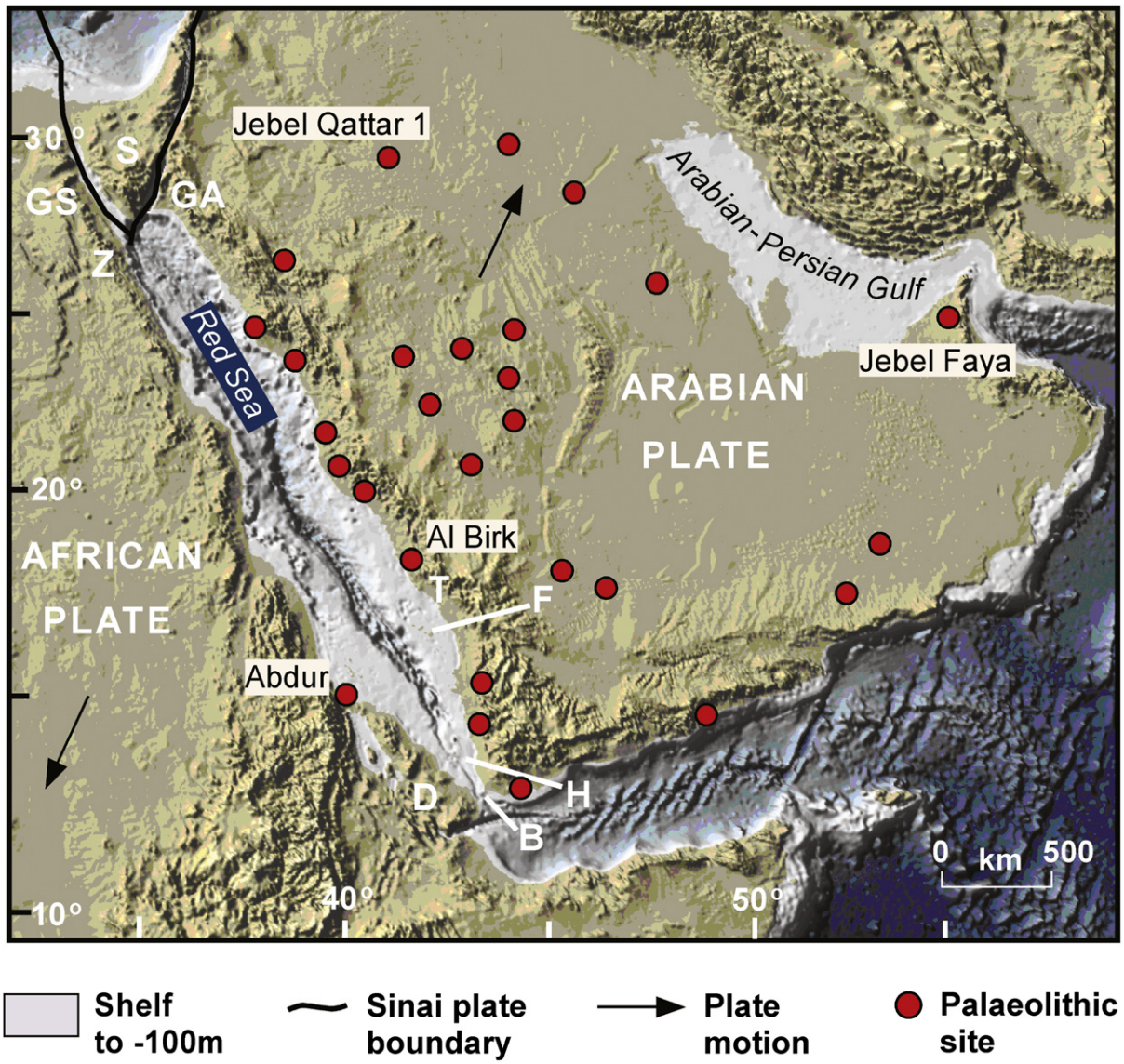

Fig. 2. General map of the Red Sea and adjacent regions, showing major tectonic features. D, Danakil microplate; S, Sinai microplate; GA, Gulf of Aqaba; GS, Gulf of Suez; Z, Gebel el Zeit; F, Farasan Islands; H, Hanish Islands; T, Tihama Plain; B, Bab al Mandab Strait. Also shown (Red dots) is a simplified distribution of Palaeolithic sites in the Arabian Peninsula, together with archaeological sites elsewhere mentioned in the text. (Information from Petraglia, 2003; Petraglia and Alsharekh, 2003; Walter et al., 2000; Bailey, 2009; Armitage et al., 2011; Petraglia et al., 2011.)

chemically altered, is often not well established but generally, in any locality where a step sequence of such features can be identified, their relative ages increase with increasing elevation. Such features, discussed below, occur at different heights along the coasts of the Gulf of Aqaba and Suez and in several locations on both sides of the Red Sea coast with ages up to ~300,000 to 400,000 years, with poorly preserved features sometimes identified at higher elevations.

Evidence for more localised episodic and recent deformation, related to the relative plate motions, can be found at a number of localities where the plate boundaries reach the coast. For example, in the Gulf of Suez, particularly at its southern end in Gebel el Zeit and the Morgan Accommodation Zone as well as further north within the Zaafarana Accommodation Zone, there is evidence for episodic vertical displacements in the form of marine terraces of the same age occurring at different elevations within distances of a few tens of kilometres (Bosworth and Taviani, 1996; see below). Similarly in the southern Red Sea, on the Buri Peninsula, elevated marine terraces have been extensively tilted over a few kilometres as a result of volcanism associated with the Danakil branch of the rift axis (Walter et al., 2000; see below). Offshore, Cochran et al. (1986) identified localised deformations associated with magma intrusions into the stretching continental crust of the northern Red Sea and suggested that this may have occurred as recently as 40,000 years ago. And Vita-Finzi and Spiro (2006) suggested that geochemical evidence for pulsed hydrothermal activity along the Red Sea axis is indicative of episodic rifting and that the locus of major extension events in the southern Red Sea shifted to the Afar area at the latest by ~40,000 years ago.

In addition to these sources of deformation associated with plate tectonics, vertical movements also occur in some parts of the Red Sea due to salt diapirism. This includes the Midyan peninsula immediately to the south of the Gulf of Aqaba, the Farasan islands, the Jizan area and the Dahlak archipelago (Dullo and Montaggioni,

1998). Sometimes quite complex uplift histories are recorded, such as for the Salif salt dome on the Tihama Plain where an older phase of uplift has been followed by submergence before the reefs were uplifted anew to their present elevation of 16–20 m above present sea level (Davison et al., 1996; Bosence et al., 1998).

In summary, the geological, geochemical, geodetic and seismic evidence point to tectonic activity with associated vertical movements across the Red Sea basin throughout the last rifting phase that started in the Miocene, particularly in the Gulfs of Suez and Aqaba and the northern part of the Red Sea and in the south at the latitudes of Eritrea and the Afar triangle. In addition, salt diapirism has resulted in more localised vertical movements in some localities. Thus sea-level change along the entire coast potentially contains tectonic information that will have to be considered along with the changes of sea level associated with the growth and decay of the continental ice sheets.

3. Sea-level change during recent glacial cycles

3.1. Generalities

During glacial cycles the primary control on sea level is the exchange of mass between ice sheets and oceans and over the past 800,000 years the dominant global signal has occurred at an approximately 100,000 year cycle with an amplitude of ~130 m. Before this the dominant period was of shorter duration and of smaller amplitude (Shackleton and Opdyke, 1973; Lambeck et al., 2002). During the successive interglacials the global levels have not exceeded their present positions by more than a few metres (Murray-Wallace, 2002; Waelbroeck et al., 2002). These interglacial and present shoreline positions are representative of only about 10–15% of the 800,000-year period and for about half of this interval sea levels globally were close to the average depth of the continental shelf, at about 75 m below present sea level. Thus for a large part of recent earth history the coastal geometries have been distinctly different from that of today, with nearly 15 million km^2 of shelf exposed globally. Large parts of potential coastal human habitat can therefore be expected to lie below today's sea level, particularly before about 6000–7000 years BP at which time sea levels globally stabilised near present-day levels.

The observed change in sea level is a measure of the shifting disposition of the land and sea surfaces along the coastlines. It therefore reflects land movements, changes in the volume of ocean water and the redistribution of this water in the ocean basins, changes in the shape of these basins, and changes in the planet's gravity field (both from redistribution of mass and from changes in centrifugal force). Even in the absence of tectonic processes, all of these factors contribute during the growth and decay of ice sheets (Lambeck and Johnston, 1998; Peltier, 1998; Mitrovica and Milne, 2003). The globally averaged rise and fall in sea level due to the glacial changes is the ice-volume equivalent sea level (esl) which – as defined in Lambeck et al. (2003) and in the absence of other processes – corresponds to eustatic sea level. The additional effects from the glacial changes are collectively referred to here as the glacio-hydro-isostatic contributions. These contributions result, even in the absence of tectonically-driven land movements, in the sea-level response (i) not being spatially uniform across the world's oceans, and (ii) being time dependent for some thousands of years after the ice loads reached a constant state.

The most significant departures from a globally averaged response occur in the former glaciated regions where the isostatic rebound exceeds the eustatic rise and sea level is actually falling during and after deglaciation. Far from the former ice margins the isostatic departures can still account for 15–20% of the esl signal at times of sea-level lowstands (see e.g., Lambeck and Chappell, 2001). Such departures from globally averaged values are particularly marked across continental shelves due to the asymmetric loading of the sea floor by changing ocean volumes, and their effect on shoreline migrations can become significant across shallow shelves and for determining whether or when these shelves could have been crossed on foot (e.g. for the Persian Gulf (Lambeck, 1996a) or for Northern Australia (Yokoyama et al., 2001)).

The model calculations for past sea-level change in response to changing ice sheets are well established (Cathles, 1975; Farrell and Clark, 1976; Peltier and Andrews, 1976; Peltier, 1998; Mitrovica and Milne, 2003). The formulation used here (the ANU model) has been described in Nakada and Lambeck (1987), Johnston (1993), Lambeck and Johnston (1998) and Lambeck et al. (2003). Comparisons of this theory with that developed by Mitrovica (2003) and Mitrovica and Milne (2003) have shown that this provides an accurate description of the consequences of the exchange of mass between the ice sheets and the oceans. The quantification of the model predictions is dependent on a knowledge of the past ice distributions as well as on the mantle rheology. Both of these are usually partially constrained by the sea-level observations themselves from areas free of vertical tectonic movements or for which the tectonic rates can be independently established. Thus the usual practice is to use the model equations to predict the geometrical structure of the spatial variability in sea level and to use the discrepancies between observations and predictions to infer the rheological response parameters appropriate for the region as well as any improvements to the ice model.

The assumption made in nearly all analysis of rebound data is lateral uniformity of the rheological parameters. This has been made necessary by mathematical and numerical constraints, rather than by a belief that the earth is so simple. But even though considerable progress has been made in refining the response of earth models to variations in lateral viscosity and elastic parameters (e.g. Paulson et al., 2005), observational data is usually inadequate to effect an inversion for lateral heterogeneity, particularly when there are also uncertainties about the ice load that have to be resolved from the same observational data (Lambeck et al., 1998). For the Red Sea, lateral structure may be particularly important because of the spreading zone between the two Precambrian crustal blocks of Nubia and Arabia, as well as the Afar Triple Junction in the south. We return to this point below.

In estimating the earth- and ice-model parameters from the observational evidence, an iterative process has been found useful in which solutions are first attempted for areas away from the former ice margins where the principal isostatic response to glacial melting is from the increasing water loads on the sea floor. At these 'far-field' areas the response is not sensitive to the details of the ice history and, in a first approximation, is a function of the rates and amounts of water added into the oceans. Thus, in a first step the observed far-field relative sea-level data is equated to ice volume and distributed between the major ice sheets using glaciologically based models, such as those of Denton and Hughes (1981). In a second step, inversions of the far-field sea-level data are made, using the rheologically sensitive spatial variability of the sea-level response, to obtain preliminary estimates for the mantle rheology together with new estimates for the esl function (Nakada and Lambeck, 1988). The corresponding new estimate for the total ice mass function is again distributed between the component ice sheets, and a new inversion of the far-field data is carried out for improved earth-model and eustatic parameters. In parallel, regional inversions of sea-level data from the former glaciated regions are conducted to improve the local ice sheet models and mantle rheology estimates, subject to the condition that the change in total ice mass is consistent with the esl estimates from the far-field analyses. The far-field analysis is then repeated using the

new ice models (Lambeck et al., 2002) and the whole process is iterated until convergence occurs.

The most recent iteration, upon which the present results are based, is discussed in Lambeck et al. (2010a). No isostatic rebound analyses have been published for the Red Sea area as part of these iterations (but see Lambeck, 2004) although there have been such studies for adjacent areas in the Persian Gulf (Lambeck, 1996a) and the Mediterranean coast (Lambeck et al., 2004a,b, 2010b; Sivan et al., 2001, 2004). The earth-model parameters found adequate there will be used here as a starting point.

Most glacial rebound studies have been restricted to the glacial history of the last ~20,000 years because most of the geophysical signal is contained in this more recent record and because the observational information on both sea-level change and ice sheets is much more sparse before the Last Glacial Maximum (LGM). Thus data for reconstructing the shorelines during glacial oscillations before the Last Glacial Maximum is limited to discrete observations from a few sites only, and most of the evidence comes from proxy indicators such as oxygen isotope ratios of marine sediments (Shackleton, 1987) calibrated against sparse local sea-level data. The function developed by Waelbroeck et al. (2002) is used here.

Last Interglacial (LIg) shorelines or sea-level indicators have been widely reported both globally and for the Red Sea coast and these are important for establishing the reference surface for measuring long-term rates of vertical tectonic motion. For example, LIg shorelines or sea-level markers from tectonically stable regions have been widely reported at around 5–7 m higher than today during the interval of 130–120 ka BP (e.g. Veeh, 1966; Shackleton, 1987; Stirling et al., 1998) and possibly higher (Kopp et al., 2009) and are usually attributed to there being less ice locked up in the LIg polar ice sheets at some time during this interglacial. Shorelines above or below this nominal level are then taken to reflect tectonic uplift or subsidence.

Glacio-hydro-isostatic signals are also important on these longer time scales, such that sea levels during this interval too will not be spatially uniform (Lambeck and Nakada, 1992; Raymo et al., 2011; Lambeck et al., in press). Observationally this is seen most clearly in areas of former glaciation (e.g. Funder et al., 2002) where LIg[2] marine sediments occur at several tens of metres above present sea level, compared with a few metres above sea level at tectonically stable margins far from the former ice sheets, as in Western Australia (Stirling et al., 1998). This variation becomes particularly important when attempting to estimate LIg ice volumes because the anticipated isostatic contribution – with its spatial variability in amplitude and in the occurrence-time of maximum elevations – will be comparable in amplitude to the differences in ice-volume equivalent sea level between the LIg and present. Thus the relationship between interglacial sea levels and ice volumes will not be simple and its determination will require knowledge of the ice history for both the pre- and post-LIg periods. At continental margins far from former ice margins, for example, today's LIg highstands can be expected to be at a higher elevation when observed at a future time, by an amount equal to the sea-level evolution between today and that future time. Likewise, at sites on the broad bulges around the former ice sheets, the elevations of LIg shorelines will decrease with time into the future (see below).

For the Red Sea region the spatial variability of LIg sea level can be expected to be important primarily because of the hydro-isostatic contributions from the different water bodies. But the glacio-isostatic components will also be significant, in particular from the Eurasian ice sheet which was more important during the penultimate glacial maximum than during the LGM. It cannot, therefore, be assumed *a priori* that Red Sea Last Interglacial sea levels, in the absence of tectonics, will be found at 5–7 m above present sea level, as has been assumed, for example, by Plaziat et al. (1998). Nor can it be assumed that the level of this interglacial highstand was the same for the entire Red Sea region or that the maximum elevation will occur everywhere at the same time. The observational evidence, as discussed below, in fact points to variability, and the challenge will be to establish how much of this is of tectonic origin, how much is the result of the earth's response to past glacial loading, and how much is a consequence of the limitations of the available data set.

In the following analysis the Holocene data is considered first, making the preliminary assessment of vertical tectonics based on the assumption that expected LIG sea levels occur at +5 m everywhere within the Red Sea (Section 3.2). The outcomes are then checked against the limited evidence available for the LGM sea levels (Section 3.3). With the resulting earth-ice parameters and with supplementary material for the pre-LGM ice sheets, a first-order model for the LIg sea-level predictions is then developed (Section 3.4), compared with available observational evidence to estimate new rates of vertical tectonic movement, and the Holocene analysis is repeated with the improved tectonic estimates (Section 3.5).

3.2. Holocene sea-level change in the Red Sea

3.2.1. Model predictions and spatial variability

The Red Sea lies far from the former ice sheets and the spatial variability in the isostatic response is determined largely by the time-dependent water load. This includes contributions from the Indian Ocean, the Mediterranean Sea and the more local Red Sea water load. Thus a complex spatial variability in the sea-level response can be expected along the entirety of the Red Sea coast. This is indeed the case as illustrated in Fig. 3A for predictions at three mid-Holocene epochs corresponding to the time interval when, at continental margins far from former ice sheets, small-amplitude highstands occurred. A section from the Mediterranean (Port Said), along the African side of the Gulf of Suez and Red Sea to Berbera and along the Somali coast to Socotra (Fig. 4), has a water-loading signal that will come variously from the Mediterranean, from the Red Sea itself, from the Gulf of Aden and from the Indian Ocean. The loads of the more distant Indian Ocean and Mediterranean Sea essentially shape the sea-level response at the two ends of the section, whereas the Red Sea and Gulf of Aden loads introduce shorter wavelength oscillations, with the shortest wavelengths resulting from the detailed coastal geometry (Fig. 3B).

Fig. 3C illustrates predictions at 6 ka BP for a range of plausible earth models spanning representative values (Table 1). The patterns for the different earth-model predictions are similar but the relative amplitudes are quite strongly earth model dependent with the strongest dependence determined by the upper mantle viscosity η_{um}. The comparison of models $E1$ and $E3$, for example, indicates that with the lower mantle viscosity η_{lm} the shorter wavelength fluctuations ($E1$), originating from the Red Sea water load, are largely damped out such that the isostatic response is dominated by the distant ice and water loads (c.f. Fig. 3B). This suggests one approximate way of dealing with the lateral variability in mantle response to the loading: introduce different parameters for the Red Sea and Gulf of Aden water load than for the far-field load. But the observational evidence is quite inadequate for any effective inversion for such differences, particularly as trade-offs

[2] For convenience the term Last Interglacial is used loosely in much of the text in the sense of referring to the period when globally averaged sea level was close to present-day sea level, recognising that, like the Holocene, the climatic conditions characterising an interglacial actually started several thousand years before sea levels stabilised.

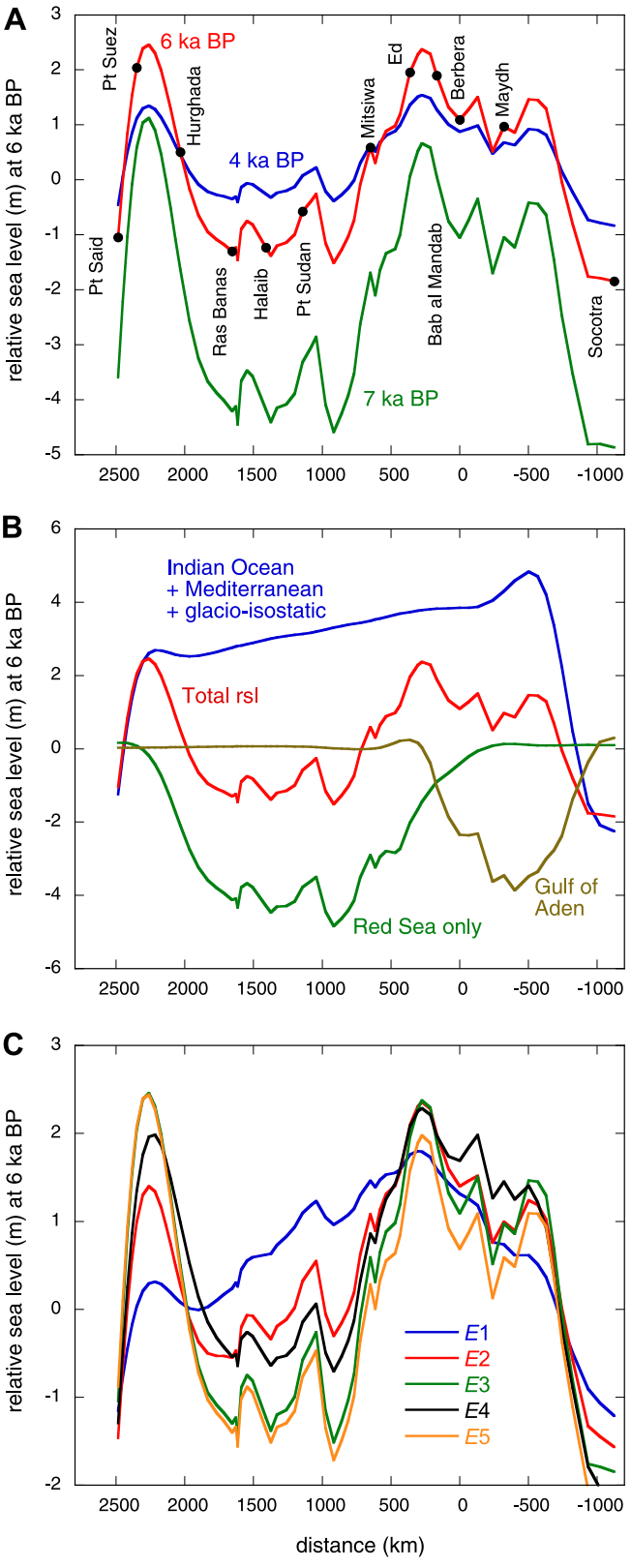

Fig. 3. Representative predictions for mid-Holocene sea-level change along the section illustrated in Fig. 4. The distance on the horizontal axis is measured from Berbera (positive westward). (A) The total relative sea-level change for earth model *E*3 (defined in Table 1) at three epochs. (B) Contributions to the sea-level response for *E*3 from the different load components (the sum of all ice loads and the water loads in the Mediterranean Sea and Indian Ocean, the water loading in the Gulf of Aden only, and the water loading in the Red Sea only) and the total sea-level change. (C) Earth

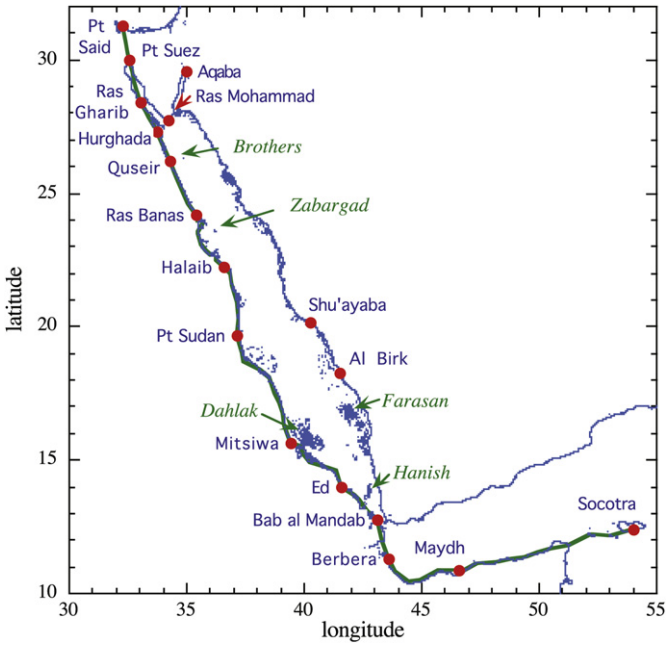

Fig. 4. Location of selected sites mentioned in text and the section corresponding to the profiles in Fig. 3.

between parameters occur: models *E*3 (low lithospheric thickness H_l, high η_{lm}) and *E*5 (high H_l, low η_{lm}) yielding very similar results.

Fig. 5 illustrates the contributions to sea level from the various ice sources at a representative site, Ras Banas, in the Red Sea. The dominant contribution to the departures from eustasy comes from the North American (including Greenland) ice sheet. This, on its own, produces a small-amplitude highstand at 6–7 ka BP, corresponding to the end of melting of this ice sheet and indicating that the hydro-isostatic component dominates thereafter. The nearer European ice sheet contributes a rising sea level during the same time, reflecting the dominance of the glacio-isostatic contribution at the site. The dominant hydro-isostatic contribution from the Antarctic ice sheet would add to this highstand except that in the adopted ice model there is ongoing Late Holocene melting (Nakada and Lambeck, 1988; Lambeck et al., 2010b). The sum of the three ice-sheet contributions, then, results in a small-amplitude highstand that occurs later than is usually found at far-field continental margin sites.

Fig. 6 illustrates the time series for the mid- to Late Holocene period for some representative sites (see Fig. 4 for locations) and for different earth models (see Table 1). The highest and earliest mid-Holocene levels are predicted to occur at the two ends of the Red Sea – within the Gulf of Suez, north of Ras Gharib, or at Aqaba – and at the southern end near Ed and Bab al Mandab, with amplitudes attaining 2 m at ~6000 years BP, depending on which earth model is used. At Hurghada, as well as at Ras Mohammad in southern Sinai, the predicted levels remain nearly constant, close to and just above present sea level for several thousand years after 6000 years BP. South of Hurghada, from Quseir to Ras Banas, the predicted highstands occur later and are of lower amplitude, or may not occur at all for models such as *E*6. The earth model dependence of these predictions is therefore important. If highstands at Ed, for example, are observed to be higher than those at

model dependence of the total predicted sea-level change at 6 ka BP (see Table 1 for the definition of the *E*).

Table 1
Summary of representative 3-layer earth models *E*. H_l is the effective elastic thickness of the lithosphere in km, η_{um} is the effective upper mantle viscosity, from the base of the lithosphere to the 670 km seismic discontinuity, and η_{lm} is the effective depth-averaged viscosity of the mantle below 670 km.

E model	H_l (km)	η_{um} (Pa s)	η_{lm} (Pa s)
*E*1	65	1×10^{20}	10^{22}
*E*2	65	2×10^{20}	10^{22}
*E*3	65	3×10^{20}	10^{22}
*E*4	80	3×10^{20}	10^{22}
*E*5	80	3×10^{20}	0.5×10^{22}
*E*6	65	3×10^{20}	3×10^{22}
*E*7	80	3×10^{20}	10^{22}

Ras Gharib then this would indicate a relatively low upper mantle viscosity (compare *E*2 and *E*3). But if the highstands at Hurghada occur relatively late this would indicate a relatively high lower mantle viscosity (compare *E*3 and *E*6). Thus the Red Sea has the potential to provide a good test of the glacio-hydro-isostatic model and of the earth-model parameters, although this can only be realised if reliable sea-level indicators can be established along the entire length of the coast and if vertical tectonic movements can be separated from the isostatic contributions.

3.2.2. Observational evidence for mid- to Late Holocene

Mid-Holocene sea-level highstands have been reported at a number of locations along the Red Sea coast and Table 2 summarises the evidence collated from the literature and from our own observations. Accurate measurements remain few and most reports do not provide adequate descriptions of sample quality, age reliability and relationship to mean sea level (msl). Thus a number of the observations included are more indicative of whether sea level may have been higher or lower than today, rather than providing an accurate measurement of the change itself. It should also be recognised that in interpreting the observational data our expectation is, in the absence of tectonics, of spatial variability of sea level along the Red Sea and Gulf of Suez shores, whereas most other examinations of the evidence do so with the expectation that sea-level change across the region is a function only of time with the result that any observed spatial variability is attributed only to tectonic movement.

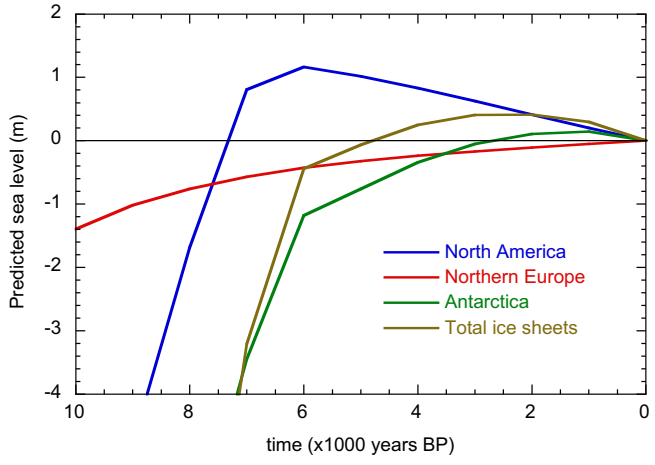

Fig. 5. Predicted contributions to sea level from the three principal ice sheets at Ras Banas for earth model *E*2. Melting of the North American ice sheet ceased by 6 ka BP, that of the Northern European ice sheet ceased before 8 ka BP but a small amount of melting of Antarctica occurred between 6 and 2 ka BP (Lambeck et al., 2010b).

All ages are referred to the calibrated time scale unless otherwise stated. Because many of the radiocarbon ages have standard deviations of 100 years or more, the polynomial approximation of Bard et al. (1993) has been used for this calibration unless calibrated values have been included in the original publications. Where several age determinations are available, the mean age is adopted with the uncertainty estimated from the range of ages and from the uncertainties for the individual measurements if these are available.

Where heights have been extracted from the published figures and uncertainty estimates have not been given, standard deviations of ±0.5 m have been adopted. Tide corrections have been made where necessary using tide information from the UK Admiralty Charts (UKHO, 2000). Tectonic corrections have been applied when the elevation of the Last Interglacial (LIg) sea level is known. Throughout the Red Sea Quaternary literature it is assumed that when the LIg sea levels occur between 5 and 8 m higher than today it indicates a relatively stable tectonic environment. But like Holocene sea levels and as noted above, the LIg levels can also be expected to exhibit some spatial variability and it is not immediately obvious that LIg levels at island or continental margin sites far from the former ice margins are also applicable here. But for the first iteration solution we ignore this possibility and return to this question later.

If h_{LIg} is the observed elevation of the LIg sea level, δh_{LIg} is the difference in esl between the LIg highstand and today, t_{LIg} is the mean age of the LIg and Δt_{LIg} is half the duration of the interstadial, then the tectonic correction $\Delta\zeta^T(t)$ at time t is

$$\Delta\zeta^T(t) = (h_{LIg} - \delta h_{LIg})t/t_{LIg} = u \cdot t \quad (1)$$

with a variance

$$\sigma^2_{\Delta\zeta^T} = \sigma_u^2 t^2 + u^2\sigma_t^2 \quad (2)$$

where u is the average rate of vertical displacement with variance

$$\sigma_u^2 = \left(\sigma_{h_{(LIg)}}/t_{LIg}\right)^2 + \left(\sigma_{\delta h_{(LIg)}}/t_{LIg}\right)^2 + \left((h_{LIg} - \delta h_{LIg})\Delta t_{LIg}/t_{LIg}\right)^2 \quad (3)$$

and $\sigma_{h(LIg)}$ is the uncertainty in δh_{LIg}.

For the present purpose, $\delta h_{LIg} = 5 \pm 5$ m and $t_{LIg} = 125{,}000 \pm 5000$ years BP. Table 2 summarises the data discussed below and includes the site coordinates (see also Fig. 4 for the location of some of the sites).

1. *Ras Abu Bakr (Gulf of Suez, north of Ras Gharib).* The evidence (Plaziat et al., 1998) is a coral fragment within a sandy beach deposit at +4 m at a 'very exposed site'. The elevation of modern beach deposits is not given for this locality but at other more sheltered locations this is reported at ~1 m above msl. Thus the evidence here indicates that msl at 5800 ± 250 BP was <3 m. The age uncertainty has not been given and a value similar to that for other quoted Holocene ages in Plaziat et al. (1998) is used.
2. *Ras Dib (Gulf of Suez, south of Ras Gharib).* Both the Holocene and the Last Interglacial reefs at this site have been described by Plaziat et al. (1998). From their fig. H2.9 the Holocene reef occurs up to 2.5 ± 0.5 m above msl. Tidal amplitudes are given for nearby Ras Gharib (UKHO, 2000) where MLWS is 0.2 m below msl. Thus on the assumption that the upper surface of the reef was at or below MLWS then the change in local level was ≥2.7 m. U/Th ages of corals and calibrated C^{14} ages of molluscs are consistent and give 5650 ± 350 BP. The LIg reef at the same location is at 19 ± 2 m above msl (Plaziat et al., 1998, p. 542) and the first-order average uplift rate is 0.12 ± 0.4 mm/

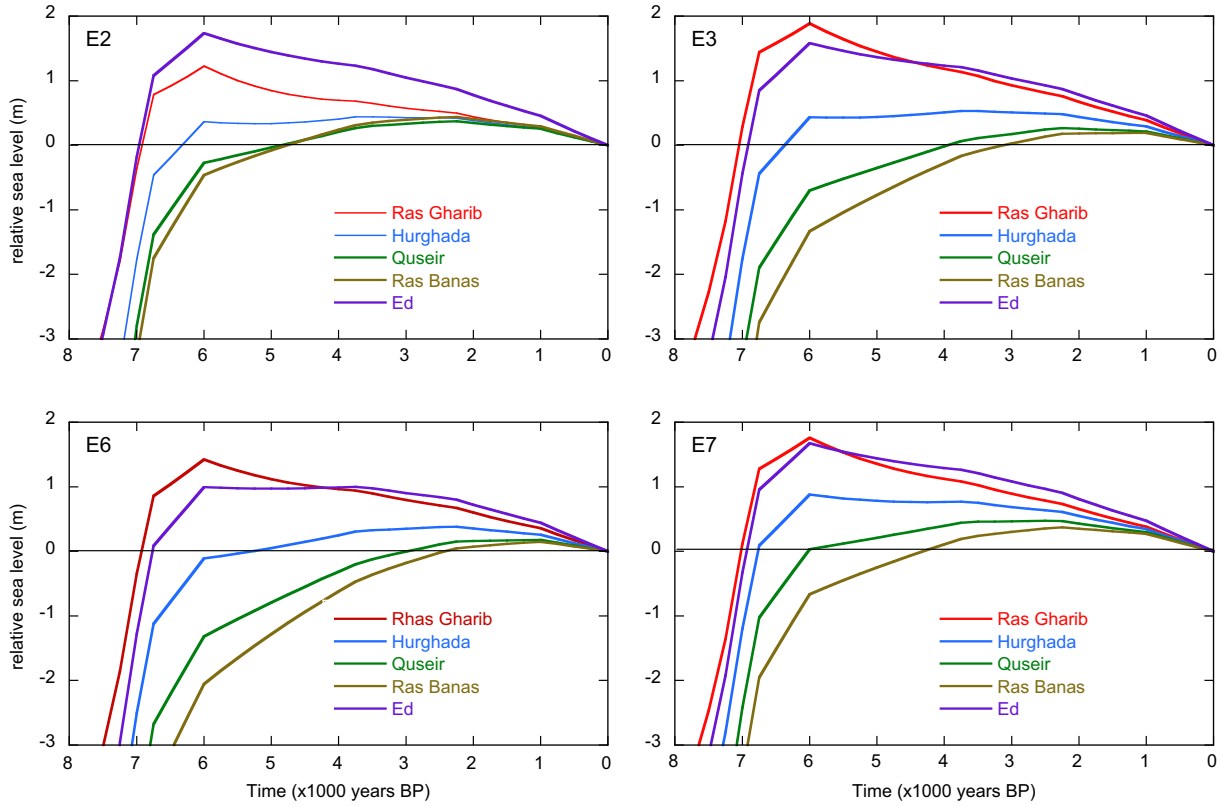

Fig. 6. Mid-late Holocene sea-level predictions at representative sites for different earth models.

year. Hence the tectonic correction for the Mid-Holocene reef flat is 0.65 ± 0.23 m and the observed sea-level change at Ras Dib is 2 ± 0.6 m.

3. *Ras Shukeir (Gulf of Suez, south of Ras Gharib).* This site is north of but near Ras Dib and here the Last Interglacial (LIg) shoreline is only at ~4 m which suggests that the uplift at Ras Dib does not extend far northwards. The evidence (Plaziat et al., 1998, fig. H2.16) is from corals in a 'Holocene upper beach' with an age of 5420 ± 350 at ~1 m above the similar present beach berm. No tide or tectonic correction is required and a value of 1 ± 0.5 m is adopted.
4. *Zeit Bay (about midway between Ras Gharib and Hurghada).* A 'probable Holocene' terrace occurs here at ~1 m – or at ~1.2 m above MLWS – but no quantified data is available

Table 2
Observational Holocene sea-level data. rsl = relative sea level. Accuracies (σ) of the limiting rsl values are given as upper (u.l) and lower (l.l) bounds. The last column gives the corrected rsl estimates (mean or limiting values as appropriate) based on the revised estimates of tectonic uplift at the individual sites (discussed below, Section 3.5).

	Site name	Lat.	Long.	Age (ka)	Mean rsl (m)	σ mean	Upper limit	Lower limit	σ u.l	σ l.l	Revised rsl estimate (m)
1	Ras Abu Bakr	28.77	32.94	5.80			3.0		0.3	1.0	2.7
2	Ras Dib	28.10	33.25	5.65	2.0	0.6					1.8
3	Ras Shukeir	28.23	33.16	5.42	1.0	0.5					0.7
4	Zeit Bay	27.83	33.42	4.00	0.6	0.5					0.5
5	Hurghada	27.28	33.78	5.51	0.3	0.2					0.0
6	Quesir	26.17	34.32	4.00			0.3		0.3	1.0	0.0
7	Sharm el Bahari	25.89	34.45	4.00			0.3		0.3	1.0	0.0
8	Wadi Qalawa	25.61	34.58	4.00	1.0	0.5					0.8
9	Abu Sbikhaia	25.05	34.85	6.10			1.2		0.3	1.0	0.8
10	Wadi Nahari	25.05	34.85	4.00			0.3		0.3	1.0	0.0
11	Wadi Gemal	24.63	35.10	5.80			1.2		0.3	0.5	0.8
12	Wadi Lahami	24.18	35.44	5.50			1.0		0.3	0.5	0.6
13a	Ras Mohammad	27.73	34.25	3.90				−0.3	0.5	0.3	−0.8
13b	Um Seed	27.85	34.32	4.30				−0.3	0.5	0.3	−0.8
13c	El Shara	27.85	34.32	2.70				−0.3	0.5	0.3	−0.9
14a	Aqaba	29.44	34.97	4.17			2.4		0.3	1.5	2.4
14b	Aqaba	29.44	34.97	6.60				0.0	1.9	0.3	0.0
14c	Aqaba	29.44	34.97	5.40	1.4	0.5					1.4
15	Al Birk	18.23	41.55	6.33			4.0		0.3	3.0	3.8
16a	Shu'ayaba	20.14	40.27	3.26			1.8		0.3	1.2	1.7
16b	Shu'ayaba	20.14	40.27	2.11				0.6	1.2	0.3	0.5

(Plaziat et al., 1998, fig. H2.14). This observation is not used by Plaziat et al. (1998) in their summary diagram (fig. H2.35). At this site the LIg is ~20 m above msl and a tectonic correction similar to that for Ras Dib is appropriate. Thus a cautious estimate for sea-level change after ~6000 years BP is ~0.6 m.

5. *Hurghada*. Dullo and Montaggioni (1998) comment on exposed Holocene reef flats between Hurghada and Safaga and on Gifun Island, varying between 0.2 and 0.5 m above present-day reef-flats. C^{14} dates are in the range 3900–5500 BP with a mean calibrated age of ~5500 years. The mean location of the sites that yielded 100% aragonite samples is adopted and the age–height data suggests that sea level was constant in the above interval. Dullo and Montaggioni (1998) suggest that the reef morphology is indicative of tectonic uplift. Hurghada lies to the north of the southern extension of the Aqaba Fault (Plaziat et al., 1998, fig. H2.8) but there is no suggestion in the Dullo and Montaggioni (1998) data of a difference in reef elevation on either side of this fault. North of Hurghada (Zeit), the LIg occurs at similar elevations as at Ras Dib. Plaziat et al. (1995) report the LIg at 6–8 m in Hurghada and conclude that the region was stable during the Late Pleistocene. For the standard assumptions above, the tectonic correction is 0 ± 0.1 and an upper reef elevation of 0.3 m is adopted with an uncertainty of 0.2 m representing the range in observed elevations and the uncertainty of the tectonic correction.
6. *Quseir*. No Holocene corals or other deposits are reported above msl in Plaziat et al. (1998) and the sections in their fig. H2.17 do not show Holocene or modern reefs and deposits. Can the absence of evidence be taken to mean that the highstand did not develop? The LIg reef here occurs between 5 and 10 m and the null hypothesis is that there has been no significant vertical tectonic movement. Predictions for the Late Holocene sea levels indicate that, for certain model parameters, sea level may not occur above present in this region (Fig. 3) and the absence of raised reefs may provide some constraint. From the Admiralty Charts the tidal amplitudes along this part of the African coast are nearly constant with MLWS tides ~0.25 m below msl. A cautious observation is that the Holocene sea level occurred at ~0.25 m or lower relative to the present.
7. *Sharm el Bahari (between Quseir and Ras Banas)*. There is a modern fringing reef but no Holocene highstand has been reported. The LIg here culminates at 7 m above msl (Plaziat et al., 1998) and average vertical tectonic rates are assumed to be small ($>$ 0.02 mm/year). The same interpretation as for Quseir is made that sea level was close to or possibly below present for much of the Late Holocene interval.
8. *Wadi Qalawa – Ras Shagra (between Quseir and Ras Banas)*. Plaziat et al. (1998) describe Holocene reef terraces that are emergent at low tide with coral heads that have been abraded by several tens of centimetres. The highest part is shown at ~1 m above msl in their fig H2.21. No ages are given other than attribution to the Holocene. In their summary diagram, the Holocene highstand is placed at 1 m, and this is adopted with a standard deviation of ± 0.5 m. This places it higher than at the two preceding sites. The LIg here attains 7 m and the nominal tectonic correction is small.
9. *Abu Sbikhaia (between Quseir and Ras Banas)*. The Holocene reef here occurs at $<$1 m above msl and is dated at 6100 ± 270 years (Plaziat et al., 1998). (While not explicitly stated this is assumed to be a U/Th age of coral material.) There is no evidence for or against uplift since the LIg. With a tide correction of ~0.25 m a Holocene sea level <1.25 m ± 0.5 m is adopted for this site.
10. *Wadi Nahari (between Quseir and Ras Banas)*. The evidence here is also one of the absence of Holocene reef above present sea level whereas fringing reefs have developed in more recent times (Plaziat et al., 1998) indicating that locally sea levels reached present sea level late in the Holocene. The LIg reef here is at about 6 m with a beach horizon at ~7.5 m and no tectonic correction has been applied in the first iteration. With a tide correction of 0.25 m the null hypothesis is an upper limit of 0.25 m for mid- to late-Holocene sea level.
11. *Wadi Gemal (between Quseir and Ras Banas)*. The Holocene reef occurs here at 1 m above msl (Plaziat et al., 1998) and corals within it indicate an age of 5800 ± 250 years BP. As for the other sites a tidal correction of 0.25 m is applied. Plaziat et al. (1998) assume that the site is tectonically stable *because* the Holocene reef occurs at ~1 m above sea level. But all model predictions indicate that sea levels here are expected to lie below those at Hurghada or along the Gulf of Suez, in which case there has been some tectonic uplift. Hence the observation is interpreted here as an upper limit of 1.2 ± 0.5 m.
12. *Wadi Lahami (south of Ras Banas)*. In a summary diagram Plaziat et al. (1998) give a number of estimates of ~1 m for mean sea level from Hamata to Abu Ghusun over a distance of ~50 km (see also Plaziat et al., 1995). Coral fragments within the epi-reefal sands at Wadi Lahami provided an age of 4820 ± 220 years but these are not in situ. Other samples from this section of coast yielded ages from 6410 to 5390 years. No tectonic correction is applied and an upper limit to sea level of ~1 m above present between about 6500 and 4500 years BP has been adopted.
13. *South Sinai*. A submerged terrace has been identified by El-Asmar (1997) between 0 and -1 m relative to msl at the locations of Ras Mohammed (13a) and nearby Um Seed (13b) with ages of 3.9 ± 0.4 ka and 4.3 ka respectively. The tidal amplitude in this part of the Red Sea is ~0.25 m and the inferred sea-level change is between $+0.25$ m and -0.75 m. An earlier observation by Gvirtzman (1994) from nearby El Shara (13c) also identified the 'modern' fringing reef at between 0 and 1 m below 'average low tide' with U/Th ages for the aragonite samples of 2.5–2.9 ka. A series of higher reefs have been discussed by both El-Asmar (1997) and Gvirtzman et al. (1992) (see below). Of these the LIg reef is reported at between 3 and 7 m above msl such that any tectonic corrections based on the above assumptions are small ($\pm$0.01 mm/year) and no such corrections have been applied.
14. *Aqaba*. The Gulf of Aqaba, as an extension of the Dead Sea fault, represents a complex tectonic setting (Joffe and Garfunkel, 1987; Girdler, 1990) with significant strike-slip motion having occurred into recent times. Uplifted coral reefs at both ends of the Gulf, including the south Sinai sites, are indicative of a vertical component to the crustal deformation. Several results have been published for the northern end of the Gulf near Aqaba and Elat. The result 14a is from Vita-Finzi (1987) and refers to the age of a terrace at ~2.5 m above high water (his fig. 8). The tidal amplitude is 0.4 at Aqaba and Elat and the inferred relative sea-level change is ~2.9 m assuming terrace formation near msl. A C^{14} age for a Tridacna shell (calibrated age 4150 ± 100 years) indicates that the terrace formed in Late Holocene time and at the same time as reef formation at the southern Sinai sites. Higher carbonate-capped terraces occur along the section of the Gulf from Aqaba to the Saudi border and the area is one of uplift. Vita-Finzi (1987) has identified a terrace at ~18.5 m elevation and shells associated with it gave a C^{14} age of ~30,000 years, near the limit of the conventional dating method used. Thus this upper terrace may be of LIg age, consistent with the typology of a hammer-struck flint found within the deposit. Accepting this, the uplift of the Holocene terrace is approximately 0.4–0.5 m. Because the

relationship of the Holocene terrace to msl is unknown this is considered as an upper limit <2.4 m with the uncertainty in Table 2 reflecting the various assumptions made.

The result 14b is from Dullo and Montaggioni (1998), who place the Holocene reef at 0.5 m above present mean low water. The elevations are for individual corals on exposed reef flats and represent lower limits. The age range of 4 corals is 5600–6200 C^{14} years with a mean calibrated age of ~6500 years. If the same assumptions are made about the tectonics of this section of the coast as for the Vita-Finzi sites, then the lower limit to sea level at ~6500 years BP is at present-day level.

The result 14c is from the western shore of the Gulf where a fossil reef has been reported at ~1 m above sea level with a C^{14} date of 4770 ± 140 years BP (Friedman, 1965; Neev and Friedman, 1978). The sea-level datum is assumed to be msl such that the change since 5485 cal. years BP is ~1.4 m. Shaked et al. (2002) have also identified a buried elevated Holocene reef at this locality, coral samples of which give an age of 4900 years. Precise elevation data is not available but it is reported to be at comparable height to those found elsewhere along the northern part of the Aqaba Gulf.

15. *Al Birk (Saudi Arabia)*. A coral platform 4 m above msl, consisting of coral heads in situ overlain by coral rubble rich in molluscs (including *Tridacna*, with a non-finite ^{14}C age) is surmounted by a shell midden which has yielded a calibrated age of 5885 ± 95 (BETA-191460). This indicates that sea level here did not exceed 4 m during the last 5900 years. The age of the platform itself has not been established but is probably of LIg age (see below).
16. *Shu'ayaba (Saudi Arabia)*. The observation here is of former reef flats (16a) at elevations up to 1.8 m above mean low tide level and Dullo and Montaggioni (1998) estimate formation ages for two overlying beachrock samples of ~3100 C^{14} years. The relation between the beachrock samples and the reefs is not given and this observation is taken as an upper limit estimate. They also provide an age of a coral at 0.60 m above mean low tide (16b) and this constitutes a lower limit for ~ 2140 C^{14} years BP. Thus the two observations bracket relative sea level for this site between ~ 1.8 and 0.6 m during the interval of ~3250 and 2100 years BP, but the age information must be treated with caution as the coral samples appear to have been partly recrystalised.

3.2.3. Comparison of model predictions with observations: mid- to Late Holocene

The above observational data set comprises upper and lower limiting values as well as the estimates for mean sea level, and an optimal set of earth-model parameters will be one for which the predictions lie within the observed limits, to within the uncertainties of these limits, and which yields best agreement with the msl estimates in a least squares sense. Thus the inversion for the 3-layer earth-model parameters has been carried out by a forward prediction through the H_l, η_{um} and η_{lm} parameter space within the limits

$$\begin{aligned} &35 < H < 100 \text{ km} \\ &5\times10^{19} < \eta_{um} < 4\times10^{20} \text{ Pa s} \\ &0.55\times10^{22} < \eta_{lm} < 3\times10^{22} \text{ Pa s} \end{aligned} \tag{4}$$

and searching for the parameters that minimise the solution variance

$$\Psi_k^2 = \frac{1}{M}\sum_{m=1}^{M}\left[\frac{\left(\Delta\zeta_\sigma^w - \Delta\zeta_{k,\text{predicted}}^w\right)w^m}{\sigma^w}\right]^2 \tag{5}$$

In (5) $\Delta\zeta_\sigma^w$ is the observed m^{th} sea-level data point ($m = 1\ldots M$) of standard deviation σ^m and $\Delta\zeta^m{}_{k,predicted}$ is the predicted sea level for earth model k ($k = 1\ldots K$) at the corresponding time and location. w is a weighting factor = 1 for msl estimates and for limiting observations that lie outside, but within one σ^m, of the permissible limit; $=(1/2)^2$ for limiting values that lie between one and two σ^m outside the permissible limit; $=(1/3)^2$ for limiting values between two and three σ^m outside this limit; and so forth for other limiting values.

Solutions meeting these conditions are (Figs. 7 and 8):

$$\begin{aligned} &55 < H < 75 \text{ km} \\ &1.2\times10^{20} < \eta_{um} < 2.5\times10^{20} \text{ Pa s} \\ &0.5\times10^{22} < \eta_{lm} < 2\times10^{22} \text{ Pa s} \end{aligned} \tag{5a}$$

with the overall least variance occurring for parameters

$$\begin{aligned} H &= 72 \text{ km} \\ \eta_{um} &= 2\times10^{20} \text{ Pa s} \\ \eta_{lm} &= 0.7\times10^{22} \text{ Pa s} \end{aligned} \tag{5b}$$

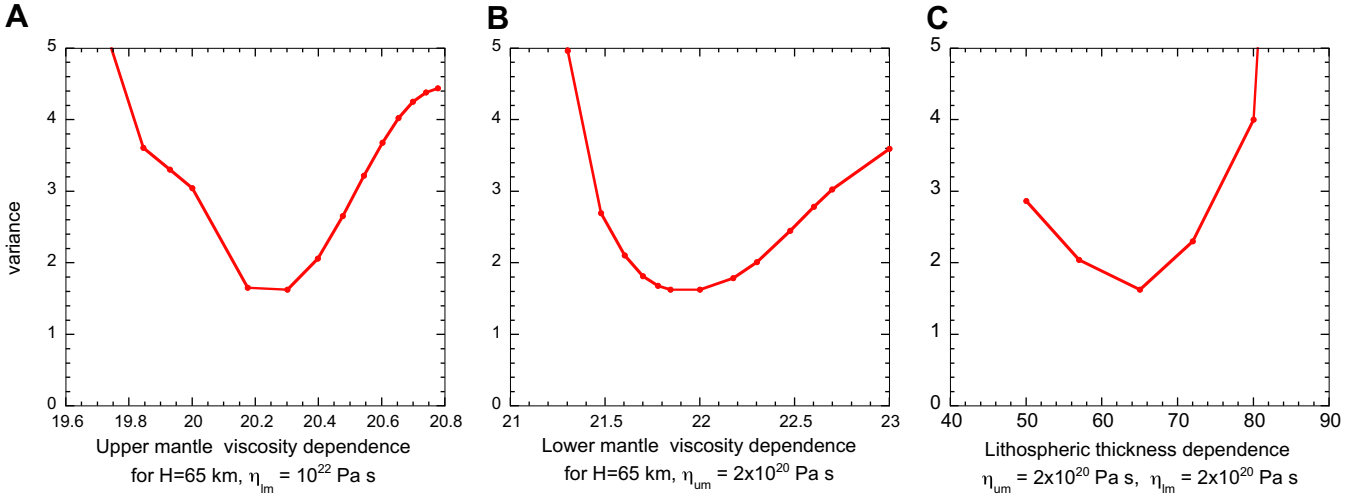

Fig. 7. Variance (as defined in Eq. (5)) dependence on earth rheology for a subspace of the total earth model space defined by (4). (The least variance solution within this subspace does not contain the least variance within the total earth model space explored.)

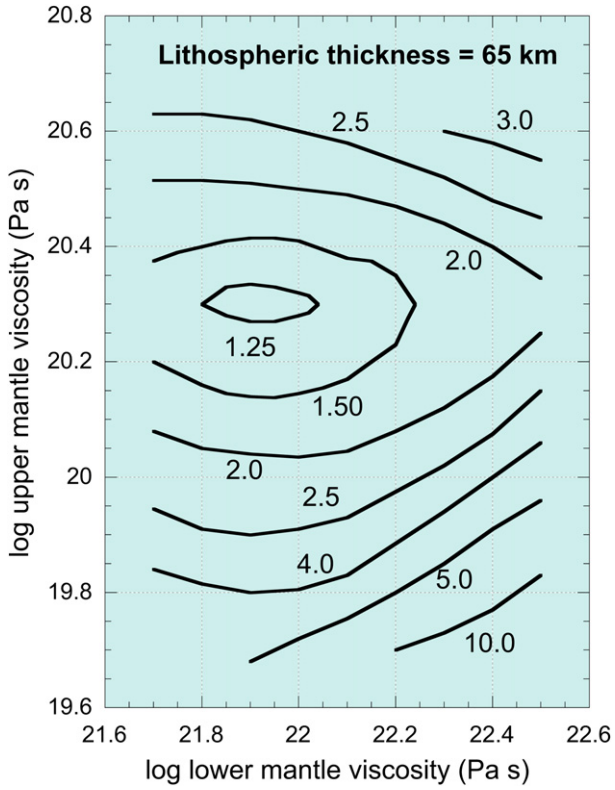

Fig. 8. Variance dependence on upper and lower mantle viscosities for $H = 65$ km. The space within the 2.0 contour represents solutions (5) that satisfy the limiting observation as well as leading to small overall variances.

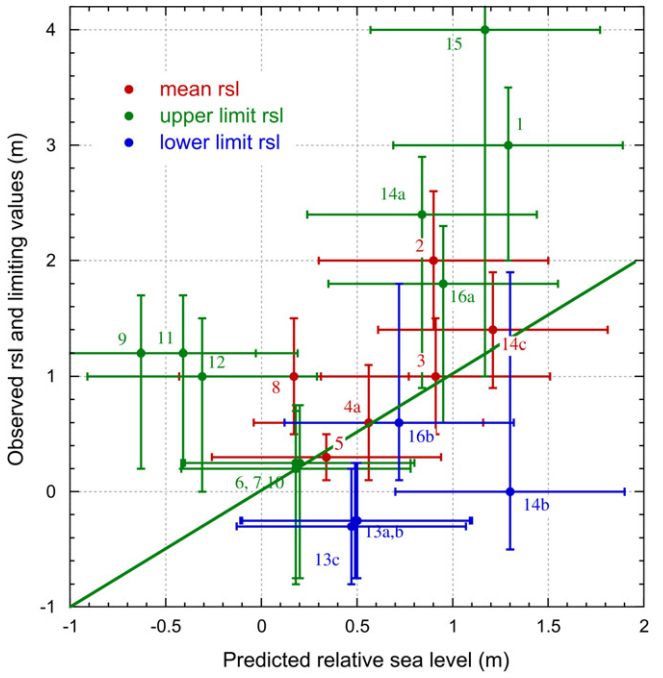

Fig. 9. Comparison of observed and predicted Holocene sea levels for the earth model defined by (5b). The lower limit observations (blue) all lie below their corresponding predictions of mean sea level and the upper limiting observations (green) lie on or above the predicted values.

This solution is largely indistinguishable from predictions based on *E*2 (Table 1).

Fig. 9 illustrates the comparisons of observations and predictions for the earth model defined by (5b). The uncertainty attributed to the predictions includes the departures of the predictions of this model from the models within the range defined by (5a) as well as uncertainties from the choice of ice and esl models (c.f. fig. 2f of Lambeck et al., 2004a). The observational uncertainties include a contribution $d\Delta\zeta/dt \times \sigma_t$ from the uncertainty of the age determination of the observation – where $d\Delta\zeta/dt$ is the temporal gradient of the sea-level change at epoch of observation and σ_t is the standard deviation of the age determination – added in quadrature to the other contributions. At sites where only the age range is given this additional uncertainty is based on the range of predictions for that site within this time interval.

If the observations and predictions are both correct, then, within observational and model uncertainties, the upper limiting values should lie above the 1:1 line and the lower limiting values should lie below this line. This is the case here, as for many other models in the explored *E* space, and the limiting values do not place significant constraints on model parameters because of the relatively large observational uncertainties of these limits (Fig. 9). The mean sea-level estimates should lie on this 1:1 line and agreement between these observations and predictions is reasonable. The data points 2 and 8 lie above the line for all models within the parameter range (5a), and this could be a consequence of errors in the interpretation of the relation between the observed feature and mean sea level, or of unmodelled tectonic contributions. Solutions based on different accuracy assessments, or based on the estimates of mean sea level only, lead to essentially the same solution.

For models with thin lithospheres ($H < 50$ km) and low values for the upper mantle viscosity ($\eta_{um} < 10^{20}$ Pa s) the relaxation is largely complete and all predictions begin to approach a constant value with, for example, upper limiting values occurring below the mean values; such solutions are excluded by the data. Solutions with $\eta_{um} > 2.5 \times 10^{20}$ Pa s are also unsatisfactory, as are solutions with $\eta_{lm} > 1 \times 10^{22}$ Pa s, because the variance estimates become increasingly large (Figs. 7 and 8).

Fig. 10 illustrates the comparisons along the African coast for the earth model (5b) for the observations in the interval 5000–6000 years BP, and separately in the interval 2000–4000 years BP, with the south Sinai and Aqaba sites projected onto this section. Agreement is mostly satisfactory and, in particular, the model is not inconsistent with the northwest–southeast gradient suggested by the observational evidence for the interval 5000–6000 years BP.

The significance of the solution (5b) for the earth-model parameters is discussed below (Section 4.1) and because of its similarity to model *E*2 we adopt the effective earth-model parameters *E*2 in the preliminary analyses for the Last Glacial Maximum and the Last Interglacial.

3.3. Last Glacial Maximum sea level in the Red Sea

3.3.1. Model predictions and spatial variability

Sea levels at the Last Glacial Maximum (LGM), ~20,000 years BP, are also predicted to show considerable geographic variability, with relatively low values for the northern and southern ends of the Red Sea and deeper values for the central part of the Red Sea (Fig. 11). For the preferred earth model *E*2, for example, the predicted LGM levels range from −110 m in south Sinai to −128 m south of Port Sudan. At all locations within the Red Sea the local sea levels lie above the ice-volume equivalent sea level – consistent with the dominant isostatic contribution being from the water loading – and the esl depths are not reached until the Indian Ocean and away from the coast. As for the Holocene, the amplitude of this variation is a function of rheological parameters and – for the model range considered here – this contributes ~4 m to the

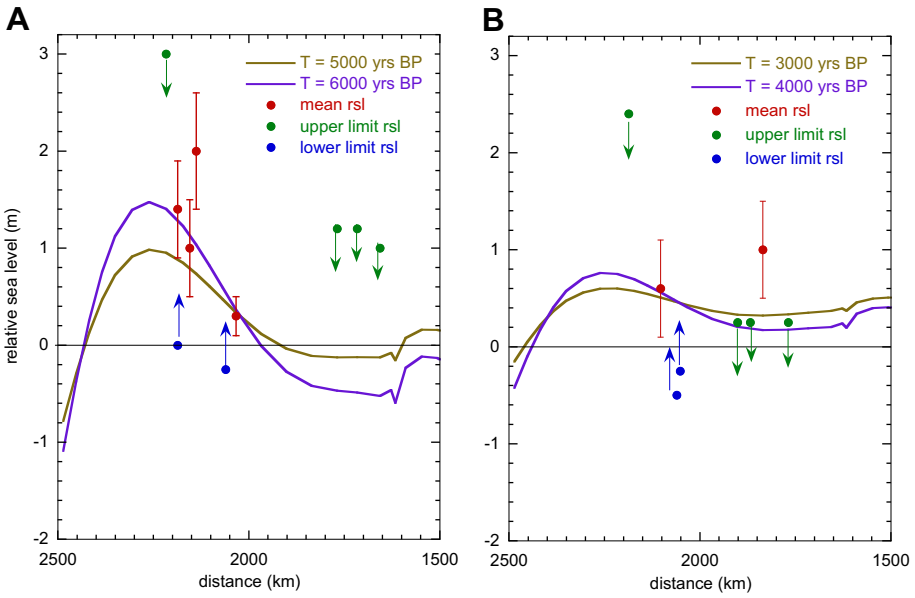

Fig. 10. Comparison of predicted and observed sea levels for the earth model defined by (5b). Upper limit observations in green, lower limits in blue, and mean sea-level estimates, with error bars, in red. (A) Observations between 5 ka and 6 ka BP. (B) Observations between 3 ka and 4 ka BP.

uncertainty of the prediction. Within the Gulf of Suez, present water depths are less than the LGM sea-level fall and the Gulf was isolated from the Red Sea proper until about 13 ka BP (Lambeck, 2004). Records from near the entrance to the Gulf (e.g. Hurghada or South Sinai) would be important because the model predictions here are relatively insensitive to the choice of earth-model parameters (Fig. 11).

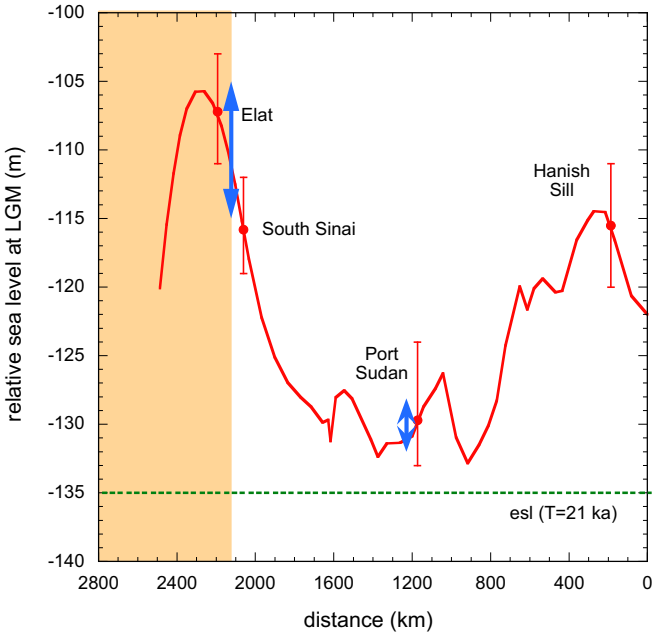

Fig. 11. Predicted LGM sea levels along the section illustrated in Fig. 4 for earth model *E2*. The error bars (red) of the predicted values include a contribution from the esl uncertainty (~4 m at the time of the LGM, Lambeck et al., 2004a) and from the earth-model parameter uncertainty where the latter corresponds to the root-mean-square difference between predictions based on this model and on a range of models within the parameter space defined by Eq. (4). The shaded area corresponds to the Gulf of Suez where water depths are less than the LGM change. The dashed horizontal line denotes the equivalent sea level for the same model at $T = 21$ ka BP.

3.3.2. *Observational evidence for the LGM*

There appear to be no direct observations of sea level for the LGM period within the Red Sea although several authors have identified morphological features that they associated with sea-level stillstands, including submerged terraces sometimes backed by small cliffs (Reches et al., 1987) or nickpoints that identify changes in submarine slope (Emery, 1964; Gvirtzman et al., 1977) (Table 3). Gvirtzman et al. (1977) have attributed a number of 'thalweg nickpoints' at depths between 110 and 130 m to the LGM on the basis that these depths are similar to global estimates. But as Fig. 11 illustrates, considerable regional variation can be expected in this depth within the Red Sea, from about 105 to 130 m. And this may indeed be inferred from some of this observational evidence. Gvirtzman et al. (1977), for example, suggest that the LGM may be at −130 m near Port Sudan, consistent with the model prediction, while Fricke and Landmann (1983) have identified a terrace at ~105 m in southern Sinai. Emery (1964) has suggested approximately −100 m for the northern part of the Gulf of Aqaba although Reches et al. (1987) have identified a fossil reef in the same region at −120 m (reef depths would be greater than the erosional features) and possibly differential vertical tectonic movements are important here (c.f. the Holocene data from location 14). Thus while these inferences on the observed LGM sea levels are not solidly based, they do show a pattern that is consistent with the predicted variations across the region and it is not constructive to (i) describe the change across the region by a single value nor (ii) to assume that Red Sea values are necessarily representative of global values.

3.3.3. *Earlier glacial maxima*

Globally, direct observational evidence for sea levels during the earlier glacial maxima is sparse but the few indicators suggest that during the last three glacial maxima (MIS 2, MIS 6, MIS 8) the peak lowstands reached comparable values. Ferland et al. (1995) examined sedimentary deposits offshore of southeastern Australia and concluded that the last three lowstands locally all occurred at depths of <130 m while Rabineau et al. (2006) concluded that in the Golfe du Lion (Mediterranean) these three maxima occurred at about the same depth of -102 ± 6 m (the difference in depths at the

Table 3
Observationally inferred and predicted estimates for the maximum depths of sea level at three sites and the observed water depth at the Hanish Sill (see below). The predictions are for earth model *E*2 with the uncertainties based on the range of values within the plausible earth model range and for an uncertainty of 4 m for the esl value at the time of the Last Glacial Maximum, with the two contributions added in quadrature.

Site	*E*2	Observed
Ras Mohammad	-110 ± 4.5	~ -105 m (Fricke and Landmann, 1983)
Elat	-102 ± 4.5	~ -100 m (Emery, 1964). ~ -120 m (Reches et al., 1987)
Port Sudan	-125 ± 4.7	~ -130 m (Gvirtzman et al., 1977)
Hanish Sill	-113 ± 4.8	-137 ± 3 (see below)

two locations is the consequence of the different amplitudes of the isostatic corrections as shown by Lambeck and Bard, 2000 for the Golfe du Lion area and by Lambeck and Nakada, 1990 for south-eastern Australia). Rabineau et al. (2006) also noted that the two earlier maxima (MIS 10 and MIS 12) were considerably deeper, with MIS 12 possibly at -150 ± 10 m. The occurrence of deeper low-stands during these two glacial periods, particularly the latter, is generally consistent with the isotopic evidence (Shackleton, 1987; Waelbroeck et al., 2002) and with the salinity evidence from the Red Sea (Rohling et al., 1998; Siddall et al., 2004) except that the lowstand during MIS 10 may not have been as deep as suggested by the Golfe du Lyon data.

3.4. Last and earlier interglacial sea levels

3.4.1. Model predictions

As noted earlier, there is no *a priori* reason for assuming that LIg sea levels in the Red Sea occurred at a constant elevation across the region or that this elevation corresponds to the often-assumed global values of 5–7 m above present sea level. Instead, from the analogy with the Holocene pattern, considerable spatial variation can be expected in the amplitude and chronology of the sea levels during this interval that will be a function of the ice history from before the Last Interglacial up to the present as well as of the earth's rheological response to loading. To model this variability requires (i) appropriate ice models for the past two glacial cycles, including differences in ice volumes between today and the Last Interglacial, and (ii) an earth rheology that defines the earth response over this extended period.

Being far from the margins of the former ice sheets, the Red Sea is not sensitive to the details of the earlier ice sheets and LIg sea-level estimates are influenced primarily by the global changes in ice volumes. The principal source for estimating these changes for the interval between the last two glacial maxima remains the local sea-level curve inferred from the Huon Peninsula coral record (Chappell, 1974; Chappell et al., 1996) and a conversion of this local sea-level curve to the ice-volume-equivalent sea-level function using the same iterative process outlined above for the post-LGM interval (Lambeck and Chappell, 2001). For the earlier cycle, the ice-volume is constrained by the function developed by Waelbroeck et al. (2002) and the distribution of ice between the component ice sheets is from Lambeck et al. (2010a).

In the absence of adequate sea-level data to allow an inversion for mantle rheological parameters corresponding to the longer time period, the earth is assumed to have a linear rheology such that the parameters estimated from the analysis of the last deglaciation are also valid on the longer time scale. This is in fact a most plausible assumption because the interglacial sea levels are primarily a function of the ice history immediately preceding that interglacial and of the residual response to the last deglaciation (see below), both of which operate on similar time scales. Finally, information is required on the esl function during the LIg (esl_{LIg}). In a first iteration, ice volumes during the LIg are assumed to have been constant, reaching present-day values at 129 ka BP and remaining there until 118 ka BP at which time renewed ice growth occurred. Differences between observed and predicted LIg sea levels for the Red Sea sites, in the absence of observational errors, are then attributed to the sum of tectonic and esl_{LIg} contributions where the latter are independently estimated from sea-level information from stable continental margins far from the former ice margins (Stirling et al., 1998).

Fig. 12A illustrates the predictions for earth model *E*2 at a number of representative sites from Port Said on the Mediterranean coast to the Socotra Islands in the Indian Ocean and along the African side of the Red Sea. Of immediate note is that nowhere are the relative highstands predicted to occur above present sea level if the first-order assumption $esl_{LIg} = 0$ is valid. At the northern end (Port Said) sea levels continued to rise, as a consequence of the glacio-isostatic contribution, up to the onset of renewed glaciation at 118 ka BP. At the southern end of the section (e.g. Maydh on the Somalian coast) the relative sea-level curve is similar in shape (but not in magnitude) to what occurs at continental margins far from the ice margins, a consequence primarily of the hydro-isostatic component. At the Socotra site the signal resembles that of a typical mid-Holocene island located in a far-field ocean environment, with the relative highstand occurring later than at the continental margin sites because of the ongoing viscous deformation of the sea floor after deglaciation is complete.

The interpretation of the LIg signal is more complex than its Holocene counterpart because it reflects the response to the differences in ice loads from those that exist today and that existed before, during and after the interglacial period. Fig. 13 gives the sea-level response at the Ras Banas location separately for the pre- and post-LIg ice components of the two principal ice sheets with the assumption $esl_{LIg} = 0$. For the North American ice sheet, for which the Red Sea is sufficiently distant for the hydro-isostatic response to dominate, a highstand is produced at the termination of melting of the MIS 6 ice (Fig. 13A) but the subsequent relaxation occurs over the next 60 ka or so and any shorelines that formed during the LIg interval would be seen at approximately 3–3.5 m above sea level once relaxation is complete. This highstand would be a measure of the relaxation process and not indicative of a departure of global LIg ice volume from $esl_{LIg} = 0$. For the post-LIg ice load, a similar highstand is predicted at the time of the cessation of melting of the last ice sheet. But this occurred at about 6–7 ka BP; the present elevation of the Holocene highstand reflects only the initial relaxation and it will be several tens of thousands of years into the future before the earth returns to its original equilibrium state – assuming no further change in ice load. Hence any shorelines formed before the onset of this post-LIg ice will today be seen below sea level by an amount equal to the residual relaxation of the last ice load (Lambeck et al., in press). The shape of the LIg sea-level response to the totality of the distant ice sheets (North America and also Antarctica), with $esl_{LIg} = 0$, is then determined by the pre-LIg ice while the amplitude is determined by this ice and by the residual post-LGM relaxation.

The response to the Eurasian ice sheets is similar (Fig. 13B) but now the Red Sea sites lie within the sphere of direct influence of the ice, with the result that sea levels continue to rise after deglaciation and, from this ice sheet alone, highstands do not develop. From the pre-LIg Eurasian ice alone, relaxation is not complete by the end of the LIg and, if no further changes occurred in this ice sheet, sea levels would continue to rise a further ~ 4 m at the Ras Banas site until equilibrium was reached. Similarly the

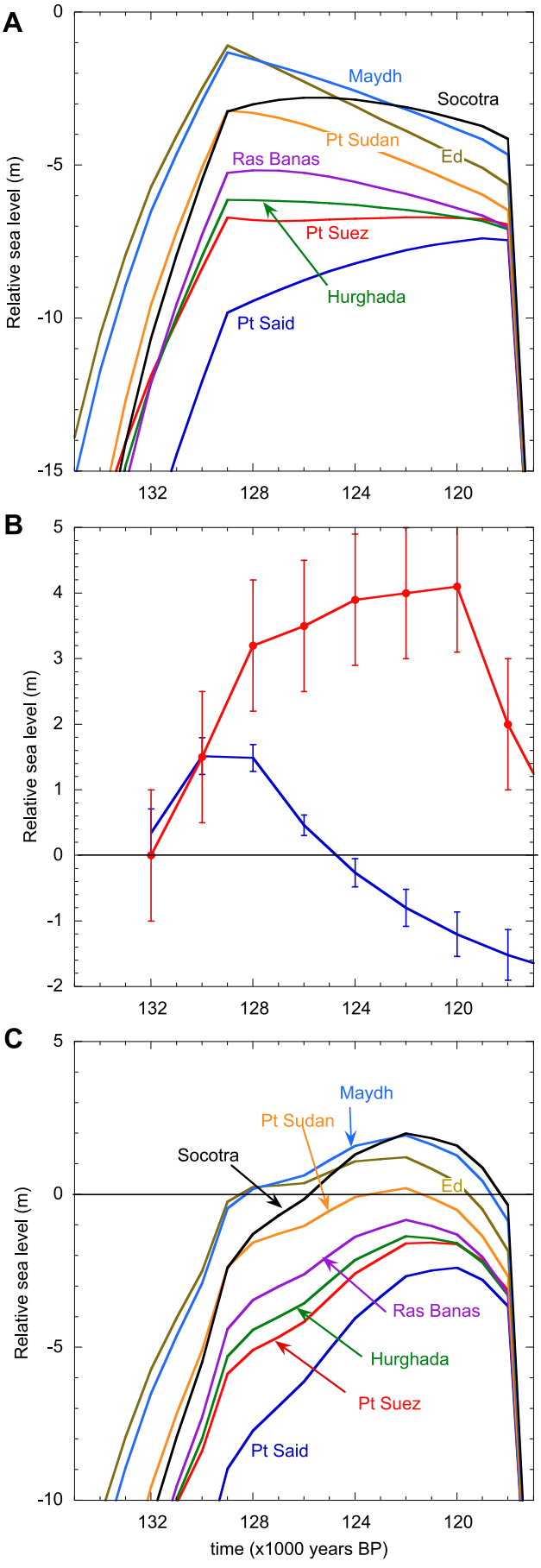

post-LGM relaxation is not complete at present, and sea level from this contribution will continue to rise with the consequence that, in the absence of pre-LIg ice, any LIg shorelines would today occur above sea level by the amount equal to the residual relaxation, or ~1.5 m (the MIS 6 Eurasian ice sheet is considerably larger than the MIS 2 ice sheet).

The total Last Interglacial signal (always with $esl_{LIg} = 0$) is therefore made up of the responses to the principal individual ice sheets for the periods both before and after the interglacial period, contributions that are of similar amplitudes but that are also as likely to be positive as negative depending on location relative to the ice sheets. For the Red Sea sites the residual relaxation for the total ice load is ~3.5 m, the amount by which the presently observed LIg shorelines lie below their equilibrium levels: come back in approximately 50–60 ka and these shorelines will be higher by this amount. A value of 3.5 ± 1.0 is adopted here, the uncertainty reflecting the uncertainties in both the earth-model parameters and in the LGM ice volumes and the predicted spatial variability of this term for the locations in question.

Like the Holocene predictions, the Last Interglacial sea-level predictions are sensitive to the choice of earth-model parameters, more so than for most far-field continental margin sites that do not have the complicated water load of the Red Sea configuration. This dependence is illustrated in Fig. 14 for the Ras Banas location. Lithospheric thickness (H) dependence becomes important only for low values, with thin lithospheres leading to higher LIg elevations, the other parameters being the same. The mantle viscosity (η) dependence is of greater importance, particularly for the lower mantle, where decreasing the viscosity leads to higher LIg levels (Fig. 14C).

Only for combinations of thin lithosphere, relatively high upper-mantle (η_{um}) viscosity and relatively low lower-mantle viscosity do the predictions reach present sea levels. Such combinations are excluded by the Holocene analysis but are also physically implausible since thinner than 'normal' lithospheres imply higher than normal upper mantle temperatures and hence lower values for mantle viscosity. Elevated Last Interglacial sea levels therefore require either a persistent pattern of uplift or significantly less ice during the LIg than today.

The above trade-off between H and η_{um} is not the same for all global sites but for the Red Sea area it is an advantage since the sea-level response to an earth model with low H, η_{um} values (the central part of the Red Sea) will be similar to that for an earth model with high H, η_{um} values (the continental shelves and interior shields).

Fig. 12B illustrates comparable predictions for a site along the coast of Western Australia for an earth model that gives a good description of the Holocene sea-level variation around the Australian coast (models $E3$, $E4$, $E6$) where a small highstand develops at the time when the global ocean volume first reached its present value. The envelope of the observed sea-level change is also illustrated (Stirling et al., 1998; McCulloch and Mortimer, 2008), using the platform elevations as a measure of low tide at ~1 m

Fig. 12. A. Model predictions for Last Interglacial sea level for $E2$ on the assumption that ice volumes have been constant and at today's values ($esl_{LIg} = 0$) from 129 to 118 ka BP. B. Model predictions for Last Interglacial sea levels for the Western Australian coast (blue) compared with observed LIg sea levels (red). The difference between the two represents the difference in esl between the LIg and present. The predicted sea levels are for the mean location of the five sites (Margaret River, Rottnest, Leander Point, Ningaloo, NW Cape) that have contributed to the Western Australian result. The earth-model parameters used for this location are consistent with Holocene sea-level analysis for the Australian region. The observations have been corrected for the differential isostatic signal between this mean reference site and the individual observation sites. The observed reef platforms are assumed to have formed at low water at ~1 m below mean sea level. C. Predicted sea levels for the Red Sea and Gulf of Aden corrected for the LIg esl function. The error bars shown for Ras Banas are representative of those for the other sites.

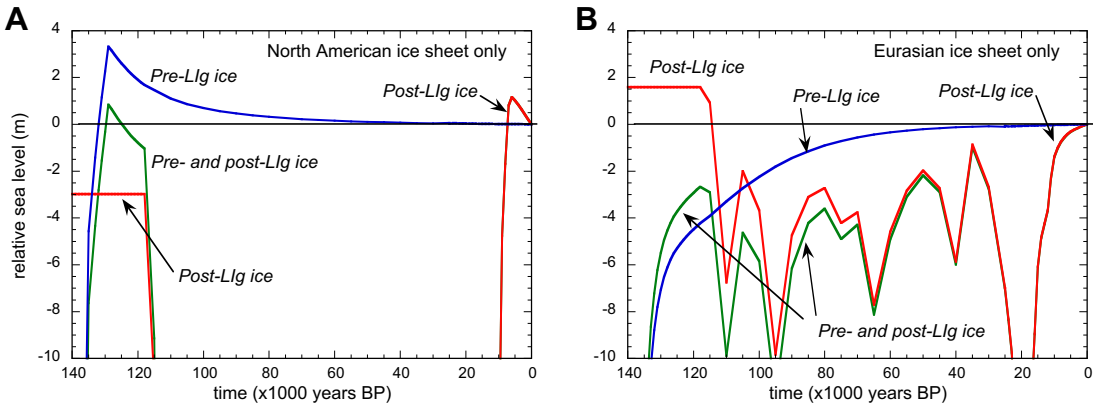

Fig. 13. Contributions to relative sea level at Ras Banas from the North American (A) and Eurasian (B) ice sheets for the pre-LIg and post-LIg periods separately and for the total ice model from MIS 7 to present.

below mean sea level. The coast of Western Australia is considered stable over this time scale and the difference between the observed and predicted functions, within observational and model uncertainties, provides a first-order estimate of the reduced amount of ice during the interglacial compared with today and reaches about 5 m in the latter part of the interglacial. The addition of this esl correction to the predictions of Fig. 12A then produces the LIg predictions for the Red Sea sites illustrated in Fig. 12C. The uncertainty of these predictions includes contributions from (i) the estimated esl function for the LIg interval, including the contributions from the sea-level predictions for the Western Australia reference site and the observational uncertainties, and (ii) the earth- and ice-model parameter assumptions for both the Red Sea and the Western Australian reference site.

3.4.2. Last Interglacial and earlier interglacial observational evidence

The raised reefs of the Red Sea margin have been widely commented on and a considerable amount of information on their age-height relationships has been published (Fig. 15). With some notable exceptions, the field evidence indicates that the LIg reefs in the northern and central part of the Red Sea lie mostly between 5 and 8 m above present sea level and it has usually been argued that this indicates an absence of vertical tectonics (e.g. Hoang and Taviani, 1991; Hoang et al., 1996; Bosworth and Taviani, 1996; Plaziat et al., 2008). The occurrence of higher and older reefs is then taken as evidence that uplift ceased sometime before the Last Interglacial (e.g. Plaziat et al., 1998). In the south, again with exceptions, the LIg levels tend to be at or only a few metres above present sea level (e.g. Faure et al., 1980).

The most complete survey of the LIg and older interglacial reefs remains that of Plaziat et al. (1995, 1998, 2008) for the western side of the Gulf of Suez and the northern Red Sea. Age control is provided by U–Th α counting and most ages cluster around 123 ka BP with error estimates of ~6 ka. (Many of the other results from the Red Sea also rely on conventional U–Th dates.) Thus in most cases the precise time of formation within the LIG interval cannot be established. Plaziat et al. (2008) have identified both 'reef-and-beach' outcrops (their 5.53 sub-stage) and the top of a 'subaqueous gypsum layer' (their 5.51 sub-stage) as indicators of LIg sea levels, and conclude that the former are both the higher and older of the two with an elevation difference of ~3 m. But because of the limited time resolution of the U–Th α dates, which yield effectively the same ages for both the 5.53 and 5.51 formations within large error bars, we use only the reef data as estimates of the highest sea level during the LIg interval.

The highest elevations of the coral surface have been adopted as indicators of mean low water at the time of reef growth (from figures in Plaziat et al., 1998, and from figures 4.1–4.4 in Plaziat et al., 2008). The present Red Sea reef flats are typically between 0.5 and 1.0 m below present sea level (Dullo, 1990; Dullo and Montaggioni, 1998) and a reference height level at 0.5 m below mean sea level is adopted. The possibility that erosion of the reef flats may have occurred is ignored since in several instances the overlying beach deposits are of similar age. Thus the estimates can be construed as lower limits. The top of overlying beach deposits of MIS 5.5 age can be interpreted as marking the storm limits and typically they occur 2–4 m above the reef flats and provide estimates of upper limits.

Table 4 summarises the LIg elevations inferred from Plaziat et al. (1998, 2008) (see also Reyss et al., 1993). Where comparisons can be made, the elevations are consistent with those inferred earlier by Andres and Radtke (1988) and Bosworth and Taviani (1996), considering that (i) the localities sampled by the different groups may not be the same and that some variation occurs along this section of coast (e.g. Bosworth and Taviani, 1996) and that (ii) height measurement methods of different accuracies have been used. Between the Zaafarana and Morgan Accommodation Zones in the Gulf of Suez, Zone 1 in Table 4 from Ras Gharib to Ras Shukeir, the data is internally consistent, with an average maximum reef elevation at ~6 m above the present-day reference level, although Plaziat et al. (1998) suggested that, on the basis of Holocene evidence, rejuvenation of Miocene faults may have occurred. The Zone 2 sites lie within the highly faulted Gebel el Zeit complex and the LIg reefs here lie at significantly higher elevations than elsewhere. The significance of these sites is that higher elevation reefs are also recorded here and results from four locations from Ras Dib to southern Zeit are included. The Zone 3 sites correspond to the southern part of this deformation zone down to the Aqaba Fault and the Zone 4 sites are from the coast further south between Quseir and north of Ras Banas.

With the exception of the Group 2 sites the maximum elevations of the MIS 5.5 reefs lie between 5 and 9 m with a mean of 7 ± 1.5, as previously noted by Plaziat et al. (1995), and – if the Zone 2 data is excluded – there is no discernible trend in elevation from north to south within uncertainty estimates (Fig. 16). Nor do the predictions of the maximum elevation of sea level during the LIg interval show a major gradient along the Egyptian coast of the Gulf of Suez and the Red Sea but they do lie systematically below the observed levels by 5 ± 2.5 m (Fig. 16).

According to Plaziat et al. (2008) the MIS 5.5 reefs have grown over older Pleistocene reefs at a number of sites with ages that are

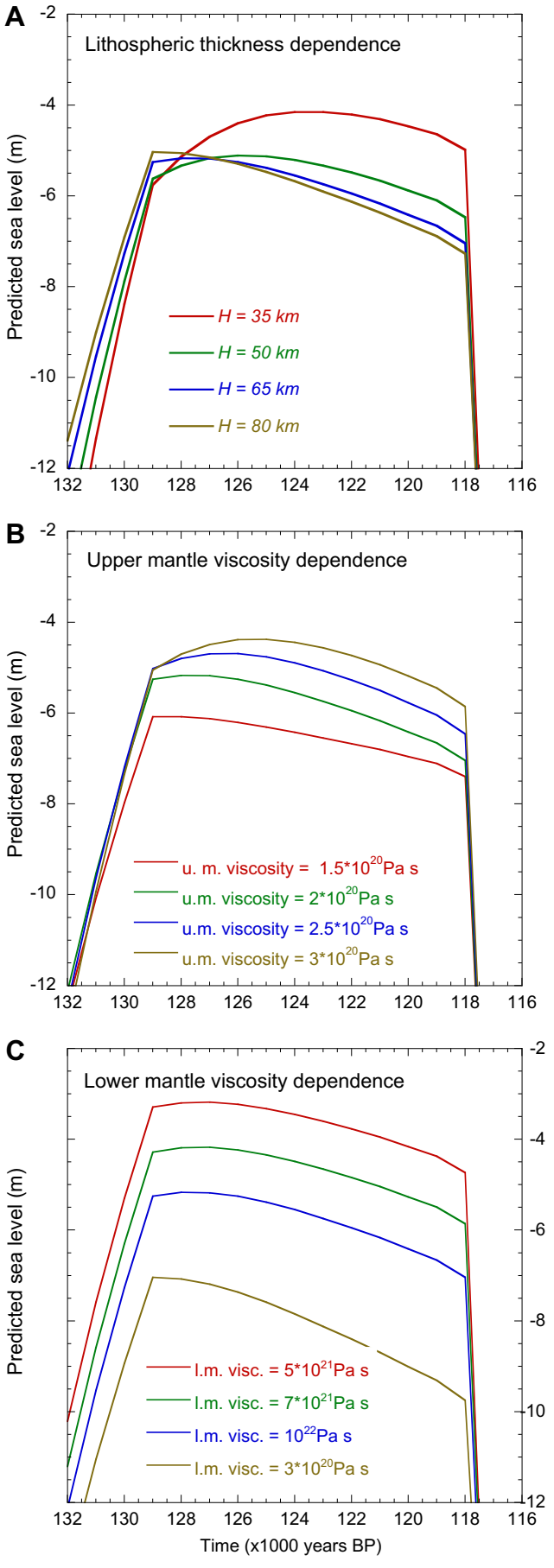

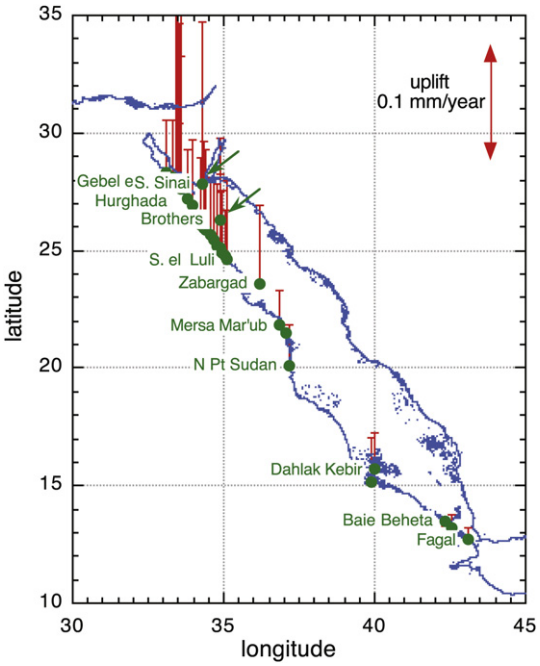

Fig. 15. Location of the Last Interglacial shoreline sites in Table 4. The vertical bars indicate the estimated rates of uplift at each site (see discussion below).

consistent with formation during MIS 9 but the upper elevation limits of reef development usually cannot be established. Also, the profiles illustrated in Plaziat et al. (2008) indicate that these older reefs have often been extensively eroded. At central Zeit, terraces have been reported at a number of higher elevations. Thus Andres and Radtke (1988) identified a terrace ~45–50 m with a U/Th age > 400 ka although Plaziat et al. (1998) place it at ~36 m near the same locality. Bosworth and Taviani (1996) have identified a terrace at ~42 m with an age of 426 ± 17 ka and we adopt an elevation of 42 ± 6 for the MIS 11 shoreline for this locality (Table 4). Undated higher terraces have been reported at ~65 m (Andres and Radtke, 1988, northern Zeit) and at ~90 m (Bosworth and Taviani, 1996, central Zeit). At the southern end of Gebel el Zeit a MIS 7 reef has been identified at ~16 m above the reference height, just below the highest MIS 5.5 reef (Plaziat et al., 1998, 2008). At Sharm el Naga an older reef, extending up to at least 35 m, is consistent with an MIS 9 formation with ages of 340–345 ka BP although the error bars are large (~80 ka) and the reef could equally be of MIS 11 age (Plaziat et al., 1998, their fig. H2.6). Plaziat et al. (2008) place the LIg reef here at either ~7 m or ~12 m but suggest that the 12 m reef could also be of MIS 7 age. This possibility has been kept here (Table 4).

At Wadi Egla the corals underlying the LIg reef are dated at 310–350 ka with one age of 191 ka (Plaziat et al., 2008). This underlying unit appears to correspond to the reef units R5 and R7 of Plaziat et al. (1998) at ~6 m, which they attribute to either MIS 7 or MIS 9. An older reef unit, attributed to the early-middle Pleistocene, occurs up to 42 m. At Wadi Nahari and Wadi Khalilat el Bahari such early-middle Pleistocene reefs occur at elevations from 30 to 42 m (Plaziat et al., 1998). While much of this information cannot be used for quantitative dating it does suggest that uplift occurred at many

Fig. 14. Last Interglacial sea-level predictions for Ras Banas with $esl_{LIg} = 0$ from 130 to 118 ka BP and for different combinations of earth-model parameters. (A) Upper and lower mantle viscosities of 2×10^{20} and 10^{22} Pa s respectively and variable effective lithospheric thickness. (B) Lower mantle viscosity of 10^{22} Pa s, lithospheric thickness of 65 km, and variable upper mantle viscosity. (C) Upper mantle viscosity of 2×10^{20} Pa s, lithospheric thickness of 65 km, and variable lower mantle viscosity.

Table 4
Summary of observed (obs) and predicted (pred) interglacial sea levels (m), the corresponding accuracy estimates (sigma obs, sigma pred) and vertical tectonic rates (mm/year) based on the Last Interglacial data. Observed elevations denoted with an * refer to reefs that are stated to be of early-middle Pleistocene age. (1) Plaziat et al. (1998); (2) Plaziat et al. (2008); (3) Bosworth and Taviani (1996) (4) Andres and Radtke (1988); (5) Gvirtzman et al. (1992); (6) El-Asmar (1997); (7) Hoang and Taviani (1991); (8) Hoang et al. (1996); (9) Conforto et al. (1976); (10) Walter et al. (2000); (11) Faure et al. (1980). For (7) and (8) the reef crests are assumed to lie below coeval mean sea level by the palaeo-depths indicated and the range of elevations given mostly lie within this palaeo-depth range. Where there is only a single sample, or where no palaeo-depth has been reported, uncertainties similar to those for the other sites in (7) and (8) have been adopted. In (10) the elevations correspond to the elevation of the upper reef which slopes steeply inland and along the coast. The LIg predictions are based on zero tectonic uplift. See Section 3.4.4 for discussion of the predicted elevations of the pre-LIg marine levels. Italicised numbers are direct comparisons that can be made between the observed and predicted elevations of pre-LIg shoreline elevations.

Site (reference)	Lat	Long	Obs. LIg	Sigma obs.	Pred. LIg	Sigma pred.	Tect rate	Sigma rate	Obs. MIS 7	Pred. MIS 7	Sigma pred	Obs. MIS 9	Pred. MIS 9	Sigma pred.	Obs. MIS 11	Pred. MIS 11	Sigma pred.
Ras Gharib (2)	28.35	33.10	5.5	1.5	−0.01	1.02	0.044	0.015		1.1	6.0		11.3	7.0		19.9	7.9
Ras Shukeir (2)	28.10	33.30	6.0	1.5	−0.04	1.03	0.048	0.015		1.9	6.0		12.7	7.0		21.6	7.9
Ras Dib (2)	28.03	33.42	19.0	1.5	−0.07	1.03	0.153	0.016		23.8	6.3		47.1	7.3		64.3	8.4
Gebel el Zeit (north) (2,4)	27.97	33.48	19.0	1.5	−0.09	1.04	0.153	0.016		23.9	6.2		47.2	7.3	*65**	*64.4*	*8.3*
Gebel el Zeit (central) (1−4)	27.90	33.57	19.0	1.5	−0.09	1.04	0.153	0.016		23.9	6.3	*42 ± 6*	*47.2*	*7.3*	*90**	*64.4*	*8.3*
Gebel el Zeit (south) (1,2)	27.83	33.55	17.0	1.5	−0.09	1.04	0.137	0.016	*≥16*	*20.5*	*6.3*		41.9	7.3		57.9	8.3
Ras el Bahar (2)	27.80	33.54	6.5	1.5	−0.10	1.04	0.053	0.015		2.9	6.0		14.2	7.1		23.4	7.9
Ras Jemsah (2)	27.65	33.58	14.0	1.5	−0.11	1.04	0.113	0.015		15.5	6.1		34.1	7.2		48.1	8.2
Hurghada (2)	27.20	33.80	5.0	1.5	−0.16	1.05	0.041	0.015		0.5	6.0		10.4	7.1		18.7	7.9
Sharm el Naga (1,2)	26.90	33.97	7.0	1.5	−0.11	1.05	0.057	0.015	*12*	*3.7*	*6.0*	*35*	*15.6*	*7.1*		25.1	8.0
			12.0	1.5	−0.11	1.05	0.097	0.015	*12*	*12.1*	*6.1*	*35*	*28.8*	*7.2*		41.5	8.1
Qseir el Qadim (2)	26.12	34.22	7.0	1.5	−0.12	1.04	0.057	0.015		3.8	6.0		15.6	7.1		25.2	7.9
Sharm el Bahari (2)	25.97	34.35	9.0	1.5	−0.12	1.05	0.073	0.015		7.1	6.0		20.9	7.1		31.7	8.0
Sharm el Qibli (2)	25.87	34.42	8.5	1.5	−0.10	1.04	0.069	0.015		6.2	6.0		19.5	7.1		30.0	8.0
Wadi Nakara (2)	25.66	34.55	6.0	1.5	−0.10	1.04	0.049	0.015		2.0	6.0		12.9	7.1		21.8	7.9
Ras Shagra (2)	25.48	34.69	6.5	1.5	−0.07	1.04	0.053	0.015		2.8	6.0		14.1	7.1		23.3	7.9
Wadi Egla (1,2)	25.20	34.76	6.5	1.5	−0.06	1.03	0.052	0.015	*≥6*	*2.8*	*6.0*		14.1	7.0	*42**	*23.3*	*7.9*
Mersa Alam (2)	25.09	34.87	6.0	1.5	−0.05	1.03	0.048	0.015		2.0	6.0		12.8	7.0		21.6	7.9
Wadi Abu Sbikhaia (2)	25.01	34.90	8.0	1.5	−0.05	1.03	0.064	0.015		5.3	6.0		18.1	7.1		28.2	7.9
Wadi Nahari (1,2)	24.93	34.97	6.5	1.5	−0.03	1.03	0.052	0.015		2.8	6.0		14.0	7.0	*30**	*23.2*	*7.9*
Wadi K.el Bahari (1,2)	24.75	35.03	5.0	1.5	0.00	1.02	0.040	0.015		0.2	6.0		10.0	7.0	*30−42**	*18.2*	*7.9*
Sharm el Luli (2)	24.60	35.10	8.5	1.5	0.04	1.01	0.068	0.015		6.0	6.0		19.1	7.1		29.5	7.9
Sinai (5)	27.85	34.32	17.0	1.5	−0.19	1.06	0.138	0.016	*15*	*20.7*	*6.2*	*31*	*42.2*	*7.3*		58.2	8.3
Sinai (6)	27.73	34.25	4.5	1.5	−0.19	1.06	0.038	0.015	*10−12*	*−0.3*	*6.0*	*15−20*	*9.2*	*7.1*	*25−30*	*17.2*	*7.9*
El Akhawein (7)	26.32	34.87	8.5	1.5	−0.23	1.07	0.070	0.015	*∼8*	*6.5*	*6.0*		19.8	7.1		30.4	8.0
Zabargad (7)	23.61	36.20	8.0	1.5	−0.25	1.01	0.066	0.015	*≥17*	*5.7*	*6.0*	*16.5 ± 2*	*18.6*	*7.0*		28.9	7.9
Mersa Mar'ub (8)	21.83	36.85	4.0	2.0	0.33	0.93	0.029	0.018		−2.0	6.3	*9.5 ± 2*	*6.5*	*7.8*		13.8	8.9
Mersa Halaka (8)	21.47	37.08			0.49	0.92											
N Pt Sudan (8)	20.10	37.17	5.0	2.0	0.60	0.86	0.035	0.017		−0.8	6.3		8.4	7.7		16.2	8.8
Dahlak Kebir (9)	15.68	40.02	5.0	2.0	1.15	0.74	0.031	0.017		−1.7	6.2		7.0	7.6		14.4	8.7
Abdur (10)	15.15	39.87	6.0		1.32	0.70	0.037			−0.3			9.2			17.2	
Baie Beheta (11)	13.49	42.32	1.0	2.0	1.51	0.64	−0.004	0.017		−9.1	6.2		−4.5	7.5		0.1	8.6
Kalla'assa (11)	13.21	42.53	3.0	2.0	1.62	0.63	0.011	0.017		−5.9	6.2		0.4	7.5		6.3	8.6
Fagal (11)	12.70	43.11	3.0	2.0	1.74	0.62	0.010	0.017		−6.1	6.2		0.1	7.5		5.9	8.6

locations along this section of the Red Sea coast during the Pleistocene, including sites where the LIg levels are now near the mean value of 6–8 m.

A second source of significant information on LIg and older interglacial sea levels comes from southern Sinai, including the Gulf of Aqaba (Gvirtzman et al., 1992; Gvirtzman, 1994; El-Asmar, 1997). In particular, for southern Sinai, along a 30 km section north of Ras Mohammed, three raised reef units and a number of morphological terraces have been identified with ages that correspond to the interglacials MIS 5.5, 7 and 9. As emphasised by Gvirtzman et al. (1992), there may not always be a direct relationship between the ages of reef growth and terrace formation and younger terraces may have been eroded into older reef. For example, their Terrace III at 5–8 m above sea level is cut into the LIg reef complex that extends up to 18 m above sea level. Gvirtzman et al. (1992) have examined evidence from a number of sites from within the Gulf of Suez to the Gulf of Aqaba and, because the predicted spatial variability of the LIg signals for these locations is significantly less than the observational uncertainties, their results are taken as representative of the mean location of their sites 3–8 (Sinai, Table 4). El-Asmar (1997) has examined the reefs at Ras Mohammad and Um Seed (Table 4) (see also Strasser et al., 1992). The Um Seed site has also been examined by Gvirtzman et al. (1992) but, because elevations for individual reefs are not given in either paper, a direct comparison cannot be made. The comparison does indicate that the identification of the terraces in the two papers is largely consistent in terms of their elevations but that these terraces may not always correspond to the maximum elevation of reef development during a particular interglacial.

A third group of results is from Hoang and Taviani (1991) for islands off the Egypt coast and Hoang et al. (1996) for the Sudan coast (Table 4). For El Akhawein island (Northern Brothers) the fossil reef crest of the Last Interglacial formed in shallow waters with a palaeo-depth of 1.5 ± 1 m and now occurs at 6–8 m above sea level (Hoang and Taviani, 1991). Within the same reef complex one sample yielded an older date of 204 ± 25 ka but the authors provide no stratigraphic information to suggest that, apart from the age, it is a fragment of a different reef complex. It is included here only to test the hypothesis that MIS 7 sea levels may have reached similar heights as MIS 5.5 levels. Reef crest elevations from Zabargad Island, at a number of sites with MIS 5.5 ages and palaeo-water depths of 1 ± 1 m also range between 6 and 8 m (Hoang and Taviani, 1991). Reef ages from samples with palaeo-depths of 3 ± 1 m of 200 ± 30 ka (1 sample) occur at ~17 m and >300 ka years (4 samples from two localities) at 12–15 m.

For the coast of Sudan, Hoang et al. (1996) provide results from several locations a few tens of kilometres north of Port Sudan and these are grouped together as a single site in Table 4. The ages are consistent with MIS 5.5 and the sample elevations range mostly from 2 to 4 m above present sea level (or approximately 3–5 m above the floor of the modern lagoon), attaining 6 m at one site that is taken here to represent an upper limit estimate of the LIg levels. At Mersa Halaka and Mersa Mar'ub, approximately 80–100 km north of this first group, reefs occur with ages of 253 ± 50 and >300 ka at elevations of 5 and 8.5 m respectively. These elevations correspond to the sample position and are therefore lower limits. Hoang et al. (1996), on the basis of correlation with Egyptian coast results, suggest that these reefs may correspond to MIS 7.

The fourth set of observational evidence on earlier sea-level highstands is from the coast of Eritrea and Djibouti, north from Bab al Mandab, and has most recently been summarised by Walter et al. (2000) (Table 4). A raised terrace occurs along much of this entire section of coast and its age has been widely attributed to MIS 5.5 on the basis of its similarity in morphology and elevation to the raised reefs further north. Local tectonics do appear to play an important role at Abdur (Buri Peninsula) where the reef elevations at the coast slope upwards from ~6 m in the south to ~14 m in the north, over a distance of less than 10 km, and also slope upwards inland from the coast to ~20 m where they are in contact with basaltic lavas whose youngest ages are ~0.44 Ma (Bruggemann et al., 2004).

For Dahlak Kebir, Conforto et al. (1976) have provided only the sample elevations, and the dated materials have high calcite content (3–5%) such that this observation yields only a lower limit of sea level at a time (117–170 ka) that is not inconsistent with LIg formation at or above 5 m. Faure et al. (1980) have identified a discontinuous outcrop of corals in association with palaeo-shorelines at elevations near present sea level from Baie Béhéta to ~3 m near Fagal with ages that are clearly Last Interglacial. These sites border the Bab al Mandab, with Baie Béhéta located on about the same latitude as the Red Sea sill (see below). Further south the tectonics become dominated by the progressive opening of the Gulf of Tadjoura, and at Obock, for example, these same stratigraphic units occur at up to 40 m and remain high around the shores of the Gulf of Tadjoura. Thus we consider the results only as far south as Bab al Mandab.

For the Saudi coast of the Red Sea, raised reefs and marine terraces have frequently been commented on (see for example, the illustration of the raised shoreline sequence near Umm Lajj (~25.0°N, 37.2°E) in Vincent, 2008) but quantitative information on their age-height relationship is sparse (Al Sayari and Zötl, 1978; Jado and Hötzl, 1984; Dullo, 1990; Jado et al., 1990). For both the Saudi coast along the Gulf of Aqaba and the Red Sea between about 28° and 24°N, Dullo (1990) has identified three reef units in addition to the Holocene reef that he attributes to MIS 5.5, MIS 7 and MIS 9, respectively, based on U/Th ages for the lower and middle units at a few locations only (but no details provided) and on correlation with similar sequences, primarily in Sinai. He notes that they occur at increasing elevation with age but the descriptions generally are insufficient to extract height-age relationships. Within the Gulf of Aqaba, these reefs have been identified at elevations up to 98 m and there is abundant evidence of tectonic uplift but without more specific information we cannot use this data. Along the Red Sea coast the least ambiguous record is from Sharm al Harr, north of Dhuba, where the three reef elevations are at ~6 m, 15–20 m and ~30 m respectively. Of note is that for several locations Dullo (1990) also describes erosional surfaces within the lower reef unit at between 1 and 3 m above msl, but there is no information to suggest that they may be of mid- to Late Holocene age.

Hötzl (1984) describe similar series of reefs and terraces for a site near Jabal al Jarra (24.7°N, 37.3°E) with a mid-Holocene surface identified at ~2.5 m with higher erosional terraces, some containing reef-edge fauna, up to 32 m above sea level and with further terraces with 'reef-top development' and 'back-reef formations' up to 90 m above sea level. Further south again, near Jeddah, 'terraces of coral rocks' occur at ~20 m (Chapman, 1978), and at Al Birk (see Table 1) the coral platform at 4 m above sea level is probably of LIg age. For the Yemen coast the information is even less satisfactory with only occasional references in passing to elevated coral reefs, notably between latitudes approximately 15–16°N.

3.4.3. Discussion of the earlier interglacial sea levels

The observationally inferred sea levels for the LIg lie consistently higher than the predicted levels, from a few metres to tens of metres, with a predominance of values between 5 and 9 m above present sea level, whereas the model predictions are closer to present sea level as well as being confined within a much narrower elevation range (Fig. 16 and 17). Within the observational and

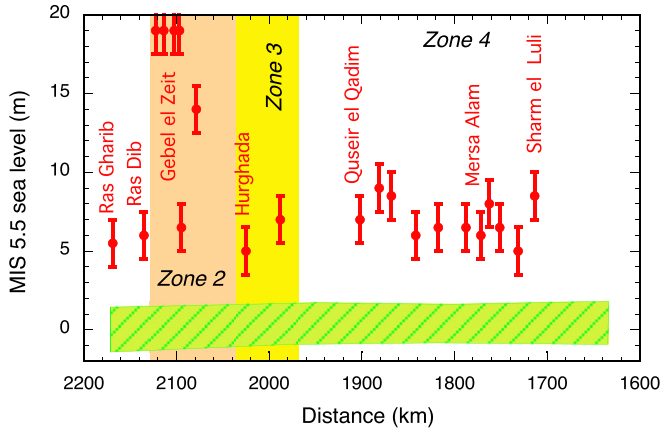

Fig. 16. Comparison of observed (solid circles with error bars) and predicted (box with diagonal shading) estimates of the highest level of sea level during the Last Interglacial and along the Egyptian coast of the Gulf of Suez and the Red Sea. The horizontal scale is distance from same reference site as in Fig. 3. Zone 2 corresponds to the Morgan Accommodation Zone and Gebel el Zeit complex. The spread of predictions corresponds to the range of earth models (5a) that are consistent with the inversion of the Holocene sea-level evidence.

model uncertainties these differences are significant and could be attributed to one or a combination of three factors: (i) the model predictions underestimate the isostatic signal, (ii) the esl has been underestimated for the LIg interval – that is, the ice volumes during this interval have been overestimated – or, (iii) widespread tectonic uplift occurs along the flanks of the Red Sea.

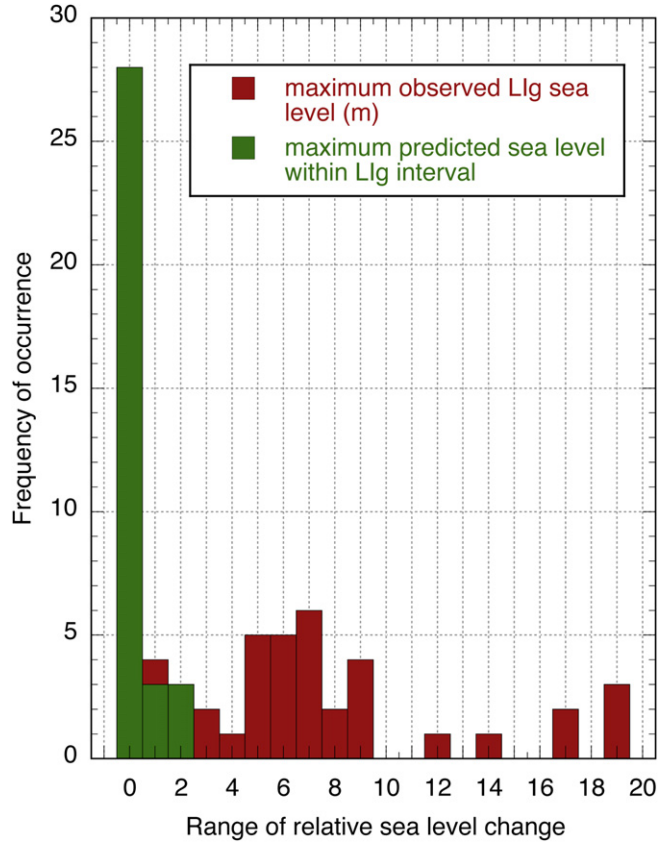

Fig. 17. Histogram of observed (red) and predicted (green) Red Sea Last Interglacial elevations with the latter based on the assumption of an absence of vertical tectonics.

The principal reason why, with the assumption of $LIg_{esl} = 0$, the predicted Red Sea LIg levels occur below present sea level is the contribution of 2–3 m from the incomplete relaxation of the Earth's mantle following the last deglaciation, and a comparable amount from the mantle response to the Eurasian MIS 6 ice sheet during the LIg (Fig. 13). Thus the only way to produce elevated sea levels (without modifying the LIg esl function) is to assume that the relaxation occurs at a higher rate than assumed. But all parameters that are consistent with the Holocene analysis for the same region do not lead to much higher levels (Fig. 14). Alternatively, a reduction of the MIS 6 ice sheet can raise levels by a few metres but this is inconsistent with the rebound analysis (Lambeck et al., 2006) and with most field evidence from the Eurasian region (Svendsen et al., 1999).

A second possibility is that LIg_{esl} has been underestimated. This is discussed further in Section 4.1 and for the present the above hypothesis for the LIg esl function is maintained. The third possibility is that the flanks of the Red Sea and Gulf of Suez have been systematically uplifted since the LIg and this can be tested against the evidence for the older interglacial reefs (Table 4). Wadi Egla, Wadi Nahari and Wadi Khalilat el Bahari, are examples where the LIg levels occur at the 'expected' atectonic levels of 5–8 m, yet higher and older, but undated, reefs have been identified which would require a cessation of tectonics sometime between MIS 7 and 5.5. Alternatively, if the assumed reference level for tectonic instability is incorrect then it may be possible solutions can be found in which all Late Pleistocene data from a given site is consistent with long-term uniform uplift rates.

The average uplift rate u with its variance σ_u^2 is based on the LIg data using expressions analogous to Eqs. (1)–(3), and the predicted elevations of earlier interglacials are determined from this site-specific uplift rate, from the residual relaxation for the LGM ice unloading, and from an interglacial esl function assumed for each of the earlier interglacials. Table 5 summarises the parameters used. The timing, duration and interglacial elevations are from Waelbroeck et al. (2002, their fig. 4). The last of these is expressed with respect to present-day ice volumes such that the MIS 7 ice volumes, for example, are assumed to be the same as today, which results in reefs of this age being below present sea level at tectonically stable far-field locations.

Table 4 includes the predictions for the elevations of these higher shorelines and Fig. 18 compares the observed elevations with the predicted values for both the MIS 7 and MIS 9 epochs. Agreement between the two is satisfactory and while improved correlations may be established by adjusting some of the variables (such as the assumed values for the LIg and earlier interglacial maximum esl values) this is not warranted for the current data set. For the sites within the Gebel el Zeit deformation zone (zone 2, Fig 16) the observations and model predictions are consistent, within the uncertainties of both, for all three earlier interglacials, and consistent with the assumption of uniform uplift rates over periods of tens of thousands of years. The comparison also suggests that the undated 65 m terrace noted by Andres and Radtke (1988) may have

Table 5
Parameters for estimating tectonic uplift (and accuracy) of interglacial shorelines. σ_{age} is half the duration of the interglacial. esl refers to the maximum ice-volume equivalent sea level during the interglacial. The unrelaxed part of the response to the LGM load is taken as 3.5 ± 1.0 m and constant across the region (Section 3.4.1).

MIS	Mean Age (ka)	σ_{age} (ka)	esl (m)	σ_{esl} (m)
5	125	5	5	2
7	210	10	−5	5
9	330	10	0	5
11	410	10	5	5

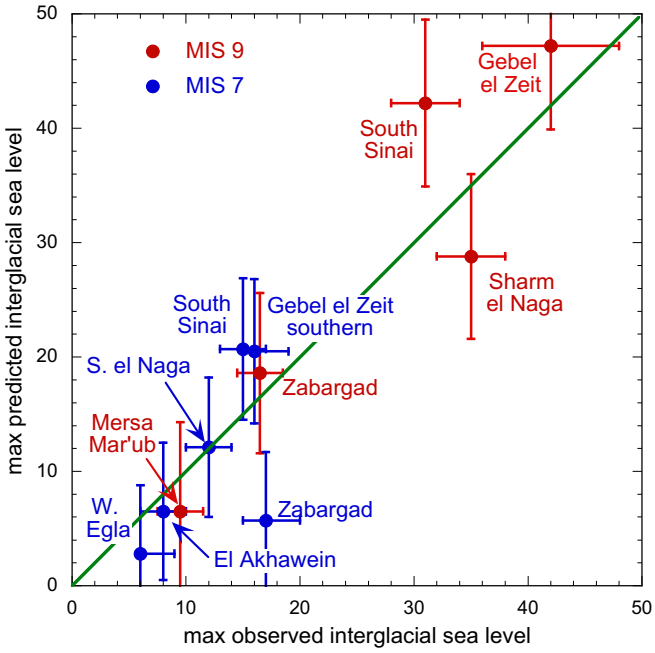

Fig. 18. Comparison of the observed and predicted maximum elevations for shorelines corresponding to the MIS 7 and MIS 9 interglacials with uplift rates for the former inferred from the MIS 5.5 shoreline elevations (Table 4).

formed during MIS 11 and that the 90 m terrace noted by Bosworth and Taviani (1996) is older than this. At these sites the uplift is sufficiently rapid (>0.1 mm/year) for the MIS 7 shorelines to occur at elevations above the LIg and the prediction is consistent with the observed elevation at the southern Gebel el Zeit location. At Sharm el Naga, the three shorelines are consistent with the assumption of uniform uplift only if the upper of the two reefs (at ~7 and 12 m) identified by Plaziat et al. (2008) is of LIg age as is indicated by the age data given in Plaziat et al. (1998).

The two results for southern Sinai lead to conflicting interpretations. If the Gvirtzman et al. (1992) interpretation of the LIg level is adopted then the uplift rate is sufficiently rapid for MIS 7 and MIS 9 shorelines to be elevated to a higher level although the predictions for both are higher than observed. This suggests that the inferred tectonic uplift rate may be approximately 15–20% too high although this is within the range of realistic accuracy estimates for the various parameter values used. For the El-Asmar (1997) interpretation the uplift rates are too low to yield MIS 7 levels above the LIg reef and the predictions for the older interglacials lie below the observed range. It would be desirable to be able to analyse the results for the individual sections to understand the differences in the two field results.

At El Akhawein the prediction is that MIS 5.5 and MIS 7 shorelines occurred at about the same elevation and this is consistent with the one sample dated at ~200 ka within a reef complex that also yielded LIg ages. At Zagarab the higher than LIG level suggested for MIS 7 by Hoang and Taviani (1991) (again from a single sample) is not supported by the model predictions, although the MIS 9 data does lead to better agreement. Finally the Mersa Mar'ub prediction is in good agreement with the observed values from Hoang et al. (1996).

Further south, the observed interglacials occur at lower elevations than in the north, reaching only the present-day sea level from Baie Béhéta to Bab al Mandab (Faure et al., 1980). This is in agreement with the model predictions in the absence of tectonics for Baie Béhéta, and implies low rates of vertical uplift at Kalla'assa and Fagal, such that at these latter sites any MIS 7 shorelines would only be found below present sea level.

3.5. A second iteration solution

Considering the large uncertainties of some of the observational evidence, the model predictions for the entire length of the western side of the Gulf of Suez and the Red Sea as far south as Bab al Mandab provide a plausible explanation of the interglacial high-stands as a combination of isostatic, eustatic and tectonic processes with the assumption of near-uniform long-term rates of tectonic uplift at any site. In realising this outcome the isostatic signals are based on models whose earth- parameters have been estimated from the Holocene sea-level data corrected with the zero-order assumption that LIg shorelines at 5–8 m above present sea levels are indicative of vertical tectonic stability. On the basis of the new first-iteration estimates of tectonic rates (Table 4), this zero-order assumption can lead to errors in the Holocene sea level estimates of up to ~0.5 m and, while this is mostly less than the individual error estimates of the data, the effect will be systematic and could introduce a bias into the solution for the earth parameters. Therefore, the Holocene analysis has been repeated with the Holocene observational evidence now corrected for the first-iteration tectonic rates from Table 4.

Table 2 includes the revised Holocene data after correction for tectonic uplift according to the estimates from Table 4 (where appropriate, corrections initially applied for uplift with respect to the 5–8 m reference level have been removed). For the Aqaba sites the previously discussed LIg information from Vita-Finzi (1987) is used. For Al Birk and Shu'ayaba the tectonic corrections are based on the assumption that the elevated coral terraces in this region are of LIg age. For those Holocene sites for which there are no corresponding LIg data the tectonic corrections have been interpolated between the nearest LIg sites.

The inversion for the 3-layer earth-model parameters has been carried out in the same parameter space as (4) using the criterion (5) and the requirement that the predictions must lie within the bounds specified by the limiting data. The resulting least variance occurs for

$$H = 65 \text{ km}$$
$$\eta_{\text{um}} = 1.5 \times 10^{20} \text{ Pa s}$$
$$\eta_{\text{lm}} = 0.6 \times 10^{22}$$

This solution is not statistically different from (5b) although all three effective mantle parameters are marginally lower than for the first iteration solution with the consequence of increasing the LIg predictions (c.f. Fig. 14) but by an amount that is less than the other uncertainties, and here we do not pursue further this second-iteration solution.

4. Discussion and conclusions

4.1. Model outcomes

Observations of relative sea-level change reflect the combined response of the earth–ocean system to a number of different processes. Changing ice volumes during glacial cycles are the most important and include the eustatic and the spatially variable isostatic components. These components are global phenomena that are observed to varying degrees of completeness at many sites and which, through models for the earth's response to the changing ice and water loads, can be predicted with some certainty and tested against observations from tectonically stable sites. Vertical

land movements driven by active tectonic processes can also make an important contribution to the relative sea levels. These contributions are usually more regional or even local and their quantitative modelling is much more complex and less well developed than for the isostatic processes. In the case of the Red Sea the isostatic and active tectonic processes both operate to produce a spatially variable sea-level response for any time epoch. Separation of these contributions cannot be achieved from the observational evidence alone. But if one or other of the processes is sufficiently well understood so that predictive models can be developed that depend on a minimum number of parameters, and information from outside of the Red Sea region can be imported to constrain the global fluctuations in sea level (e.g. corrective terms to the esl function), then some separation becomes possible. In the case of the Red Sea region we have effectively extracted the characteristic wavelength structure of the isostatic process from the observational evidence to determine the regional earth rheology parameters, and used data from stable tectonic sites elsewhere to estimate the esl function. Hence any differences between model predictions and observations have been attributed to tectonic movement. We then used the additional information contained in the records of pre-LIg sea levels to test whether these estimates of tectonic uplift or subsidence are representative of movement on longer time scales.

In developing these models a number of assumptions have had to be made for reasons of computational ease or because of the limited quality of the available observational data set. For the earth's rheology, considerable simplifications have been made in describing the rheological zonation of the mantle and lithosphere but the radial description in terms of 'effective' viscosities and effective lithospheric thickness has worked well in other areas where the observational data is of considerably higher quality, both for areas of former glaciation and for areas far from the former ice sheets. In the approach developed here no *a priori* assumptions about these parameters are made other than that they fall within a very broad range of values that encompasses most proposed values. The actual values are determined from the inversion of the data itself and are assumed to be representative of the region of the mantle that is most deformed by the surface loads. A second assumption made is that the mantle response is linear and its acceptability again rests on the experience with rebound analyses in other regions: that linear models provide a very satisfactory description of the observed rebound such that these models can be used to interpolate between poorly time-space distributed observations of sea level to provide global, regional and local descriptions of sea-level change. In this study, where both Last Interglacial and Holocene observational evidence is examined, the assumption continues to work well because the observed LIg signals reflect mainly the relaxation within two epochs of approximately the same duration, the period of deglaciation leading into the LIg and the period coming out of the Last Glacial Maximum.

A third rheological assumption made is that the lateral variations in earth structure do not result in significant lateral variation in the effective rheological parameters. Differences in mantle structure from one region to another are allowed because the analysis is limited to a region, but within a region we have no operational method for including complex lateral variations in rheology, in large part because the observational data is too limited in its accuracy and distribution in time and space to constrain any such three-dimensional mantle models. Within the Red Sea Basin, however, the rifted sea floor is relatively narrow and that part of the upper mantle with anomalously high heat flow is also confined to a narrow axial zone whereas most of the observational sites are from the broad shelves overlying continental mantle. Also, as shown by some of the above model results for the sea-level response to loading, some trade-offs occur between viscosities and lithospheric thickness such that, in this region at least, models with low upper-mantle viscosity (η_{um}) and low lithospheric thickness (H) describe the response about equally well as models with higher values for both η_{um} and H (see also Lambeck, 1993).

The solution (5b) for the earth-model parameters is similar to that established from Mediterranean sea-level analyses although for the latter the preferred viscosities were somewhat higher, up to 3×10^{20} Pa s for the upper mantle and $\sim 2 \times 10^{22}$ Pa s for the lower mantle (Lambeck et al., 2004a,b; Anzidei et al., in press). It appears, therefore, that the consequence of rifting within the Red Sea is unimportant for these effective parameters and is partly compensated for by the more normal lithosphere and mantle conditions beneath the adjacent continental crust.

The ice models themselves used to define the load have been developed from analyses of sea level and shoreline data from areas of former glaciation combined with the constraint that the sum of the ice-volume functions of the individual ice sheets must equal the ice-volume function established from the far-field analyses. Of importance for the present analysis is the ice-volume function during the earlier interglacials compared with the present-day ice volume. Only for the Last Interglacial is this function observationally constrained (e.g., Stirling et al., 1998) and for the earlier interglacials it is inferred from the oxygen isotope record of marine sediments (Waelbroeck et al., 2002). A more recent analysis (Kopp et al., 2009) has suggested that the equivalent sea level during the LIg may have peaked by as much as 8–9 m above present-day levels although the higher values are primarily derived from poorly constrained datasets. Thus the lower value of ~5 m, based on one of the most complete records from tectonically stable sites in Western Australia (see Fig. 12) far from the former ice sheets has been adopted here. If this value is too conservative then our predictions for the LIg shoreline elevations in the Red Sea will be too low by about 3–4 m. But it would also mean that the coral reefs of Western Australia have not tracked sea level well and that they define lower limits by at least this amount (we have assumed that the maximum preserved upper reef elevations are no more than 1 m below the low-tide level).

4.2. The behaviour of past sea level in the Red Sea and tectonics

The analysis for the Red Sea clearly indicates that the spatial variability of sea level at any time is complex because of the geometry of the ocean and sea basins and because of the different distances from the main ice sheets. This variability is significant for all epochs (see Figs. 3, 11 and 12) and a function of time only cannot provide an adequate description for the entire Red Sea Basin. The analysis also shows that the magnitude of sea level at key periods, such as for the mid-Holocene, for the LGM or for the LIG, cannot be directly compared with that from other localities around the globe without considering the differences in the isostatic responses between the sites. For example, it cannot be assumed that the timing of maxima or minima in Red Sea interglacial sea levels will occur at the same time across the region (Fig. 12). Moreover, if the mid-Holocene highstand at some location in the Red Sea occurs at 1–2 m above present sea level, the same as at some far-field tectonically stable continental margin sites, it cannot be assumed that the Red Sea site is also tectonically stable without first evaluating the isostatic components. Nor can it be assumed that the LIg sea levels within the Red Sea Basin will occur at the same elevation or at the same time as in, for example, Western Australia. As a result of these isostatic processes the commonly used sea-level reference for vertical tectonic stability will not be appropriate for the Red Sea region.

For the models developed here – consistent with the far-field LIg_{esl} evidence from Western Australia – the Red Sea LIg levels at the sites for which there is observational data are predicted to occur barely above present sea level, primarily because of the influence of the Eurasian ice sheets during MIS 6 and MIS 2. Thus if LIg sea levels are observed at 5–7 m, we reject the null hypothesis of tectonic stability and accept the alternative hypothesis of tectonic uplift. This occurs for much of the coast on both sides of the Red Sea with the exception of the coast of southern Eritrea (Fig. 15). At many sites where the LIg occurs at 5–7 m elevations, higher and older reefs have also been identified, and for the null hypothesis this would signify that tectonics ceased before MIS 5.5. The alternative inference of site-specific near-uniform, long-term uplift rates is consistent with the observational evidence, within observational and model uncertainties (Fig. 18, Table 4) and in so far as long-term average vertical motions are driven mostly by geophysical processes that have long time constants, we consider this hypothesis to be the more likely.

4.3. Palaeo reconstructions of shorelines and bathymetry

If the isostatic rebound parameters and the tectonic contributions can be established from the regional sea level information then it also becomes possible to predict the palaeo-topography $h(t)$ at any epoch t, as expressed relative to sea level at t, as

$$h(t) = h(t_p) - \Delta\zeta(t) \quad (6)$$

where $h(t_p)$ is the present bathymetry and $\Delta\zeta(t)$ is the sea-level change at t compared with the present, including both the isostatic and tectonic contributions.

The area of greatest interest for developing palaeo-shorelines and palaeo-water-depths is across the Bab al Mandab and the southern end of the Red Sea, where present water depths are relatively shallow; a sill controlling the flow into the Red Sea has been reported at −137 m by Werner and Lange (1975) at approximately 42°32′E, 13°44°N in the vicinity of Hanish and Zuqar islands.

4.3.1. The Hanish Sill bathymetry

The original 1972 R/V Valdivia survey (Werner and Lange, 1975) was conducted over a restricted area, and several questions have remained about this sill. Is it certain that there is no shallower sill within the complex braided topography of submerged banks and channels to the south of Hanish Island? If the limiting sill is in the area identified by Werner and Lange (1975), is the bathymetry sufficiently well defined to guarantee that there is no previously undetected deeper channel or shallower ridge within that region? Are there modern soundings that require modification of the Werner and Lange (1975) conclusion, and since the salinity and temperature of the stratified water column in the area is complex, have the soundings been adequately corrected for variations in sound velocity?

The most complete publicly available bathymetric dataset is the GEBCO_08 30″ (900 m) grid dataset (GEBCO, 2008) that we use below for the regional reconstruction. But with this relatively low resolution it is not immediately clear whether the above questions have been resolved. Therefore the raw data held at the UK Hydrographic Office (UKHO) has been re-examined, with sound velocity and other corrections applied (Appendix 1). Fig. 19 illustrates the results for the area in the immediate neighbourhood of the sill. This is based on the data available for compiling the General Bathymetric Chart of the Ocean (GEBCO, 2008) and, to the south of Hanish Island, the PERSGA commercial survey data (See Appendix 1), plotted over the Admiralty chart as background.

A continuous channel can be identified cutting across the broad topographic high from off the Hanish Islands to the Haycock group of islands, with the shallowest depth of 137 ± 3 m at the same location as originally found by Werner and Lange (1975) (see Appendix 1 for further details). In the sill area the topography appears to be smooth with a number of deeps and highs within the major channels, suggesting that neither sedimentation nor erosion is a major issue here. Thus a controlling sill at a depth of 137 ± 3 m is adopted, wholly consistent with the original Werner and Lange value.

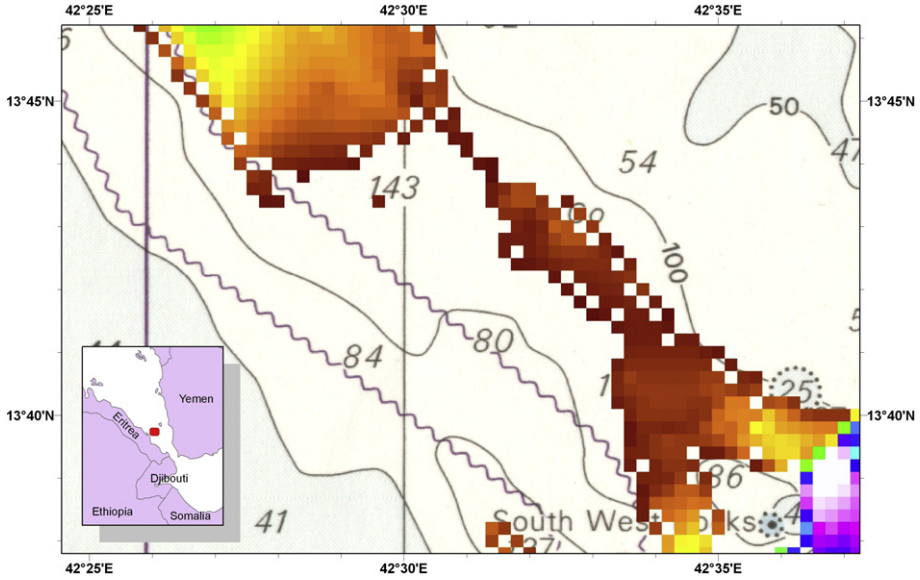

Fig. 19. The position of the deepest channel in the neighbourhood of the Hanish Sill, plotted over the soundings of Admiralty Chart 453. The pixel size arises from the gridding of the available soundings. The total dataset has been filtered at a depth of 134 m (uncorrected depth), with darkest brown representing the shallowest channel below that depth, grading into yellow and green in deeper water. The purple-blue tints in the southeast corner represent the deep channel surveyed by PERSGA. When the soundings are corrected for the local velocity of sound in seawater (See Appendix 1) the corrected depth at the sill is 137 ± 3 m. The narrowest constriction of the channel is not closely constrained by the new soundings, but the close presence of the 100 m isobath to the east indicates that the correct positon is unlikely to occur much further in that direction.

4.3.2. Bathymetry of Southern Red Sea and Bab al Mandab during glacial maxima

Fig. 20 illustrates the predicted shoreline configuration for the southern Red Sea at the time of the lowest sea level during the Last Glacial Maximum using the GEBCO_08 bathymetry. Reconstructions for other post-LGM epochs are given at http://rses.anu.edu/geodynamics/Red_Sea. (Reconstructions for the Gulf of Suez, updated from Lambeck (2004) can also be found there.) In these reconstructions, sedimentation on, or erosion of, the sill has been assumed to be minimal, consistent with the nature of the topography across the area. Tectonic uplift or subsidence has also been ignored for the southern Red Sea, consistent with a general absence of seismicity in this area (Ambraseys et al., 1995; Bosworth et al., 2005) and with the smooth topography of the actual sill area. Also, as noted by Faure (1975), the LIg reef flats on the western side of the Red Sea at the latitude of the Hanish sill and Bab al Mandab are at low elevation and indicative of vertical tectonic stability (Table 4). The predicted Holocene highstands for this section of the coast are at ~1–2 m (see Figs 3 and 6 for the site of Ed) and are consistent with the qualitative observation by Faure (1975) of 'a maximum Holocene sea level undoubtedly lower than +2 m'. Thus, on a time scale of ~6000 years as well as of ~120,000 years, the coastal zone west of the Hanish Sill appears to have been stable.

In the deeper waters immediately to the south of the Hanish Sill the topography is more rugged and there the role of tectonics in shaping the seafloor topography may have been more important as is also suggested by the occurrence of Holocene volcanism and mid Pleistocene lava flows onshore and offshore at about the latitude of Fagal (Table 4) and the Sawabi islands (Boucarut et al., 1985), although the LIg reef at Fagal is indicative of vertical stability of the coast.

With these caveats, the reconstruction indicates that the Red Sea remained in contact with the Gulf of Aden throughout the LGM with a maximum water depth of 25 ± 4 m and an average depth of $\sim 13 \pm 4$ m over a channel width of ~8.3 km, giving a cross sectional area of ~110,000 m^2 or about 2 % of the present cross sectional area (Fig. 21). Likewise, during the two earlier glacial maxima (MIS 6 and MIS 8), the flow between the Red Sea and the Indian Ocean would have been similarly restricted. If, as suggested by Rabineau et al. (2006), the MIS 10 and MIS 12 sea levels were some 40–50 m lower than during MIS 2 then the Red Sea would have been isolated from the Gulf of Aden but this is inconsistent with the conclusions drawn from sediment core analyses that the Red Sea remained open to the Indian Ocean throughout the past 500,000 years (Rohling et al., 1998, 2009; Siddall et al., 2004). Tectonic uplift of the sill in its current position probably cannot be excluded on this time scale but this would imply that rates of uplift have been lower after the LIg than for the earlier period. Additional direct evidence for MIS 10 and MIS 12 sea levels is highly desirable but for the present we adopt the inferences drawn by Rohling et al. (1998).

The reconstruction for the LGM (Fig. 20) indicates that while the sill controlling the flow into the Red Sea occurs at the latitude of Hanish Island, the narrowest channels connecting the Red Sea to the Gulf of Aden occur further south, at the latitude of SW Haycock Island, in an area where the channel from the Gulf of Aden widens

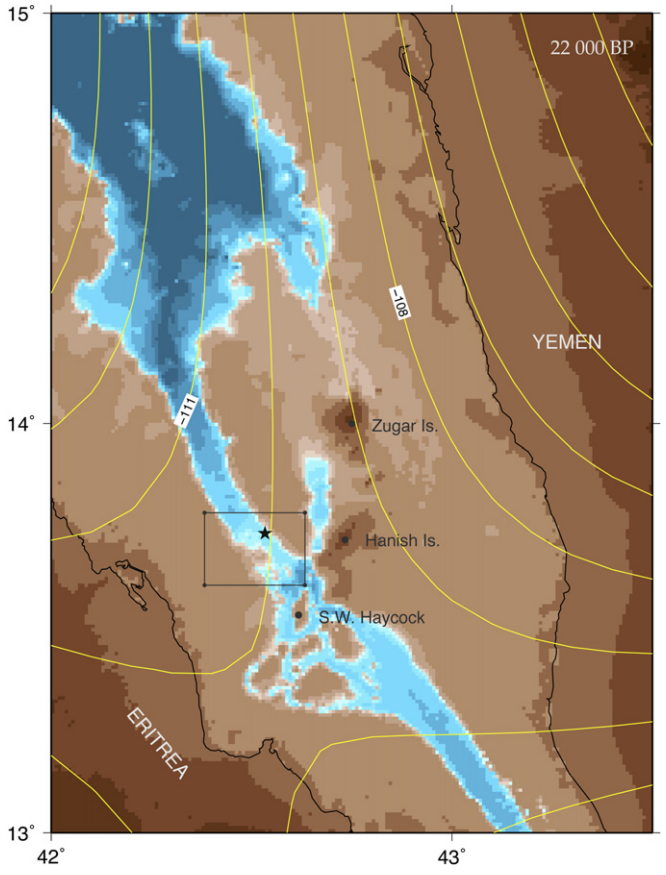

Fig. 20. Palaeo reconstructions of Last Glacial Maximum shorelines and topography for the southern end of the Red Sea. The star locates the Hanish Sill location and the small rectangle corresponds to the area shown in Fig. 19. The yellow lines correspond to contours of equal relative sea-level change at 21,000 years BP compared to present (c.f. Fig. 11).

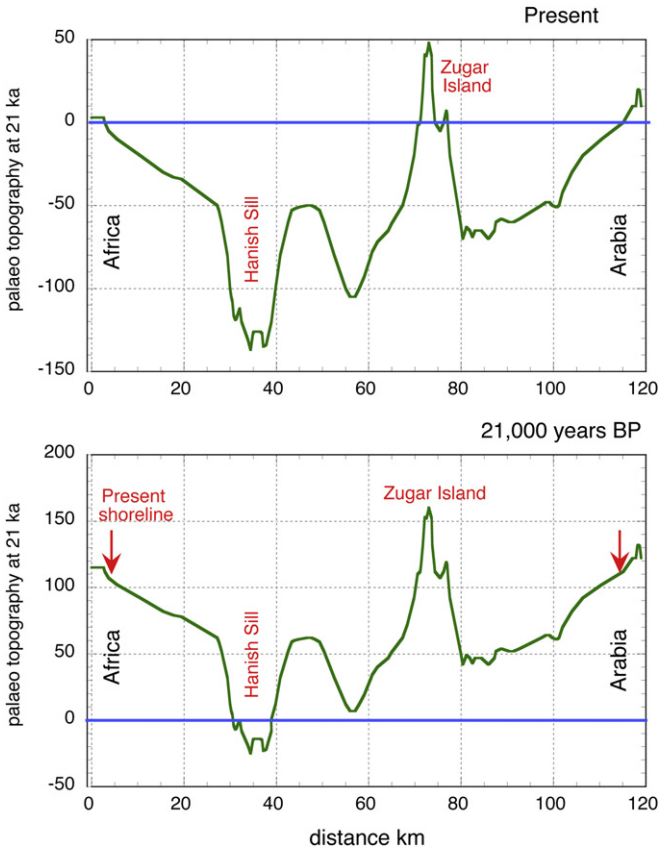

Fig. 21. Elevation profiles along a section across the Hanish Sill (top) for the present and (bottom) for the maximum lowstand during the Last Glacial Maximum. The arrows in the latter indicate the position of today's shorelines relative to the LGM sea level.

and branches into several narrow channels (Fig. 22). Fig. 23 illustrates the cross-section from Africa to Arabia that minimises the sea-crossing distance for this epoch. The minimum channel width is now <3 km although the average water depth is almost 100 m such that the cross sectional area is ~2.5 times greater than for the Hanish sill; current velocities, assuming no energy dissipation between the two sections, will be correspondingly greater at the sill location. Of potential significance are the steep slopes of both sides

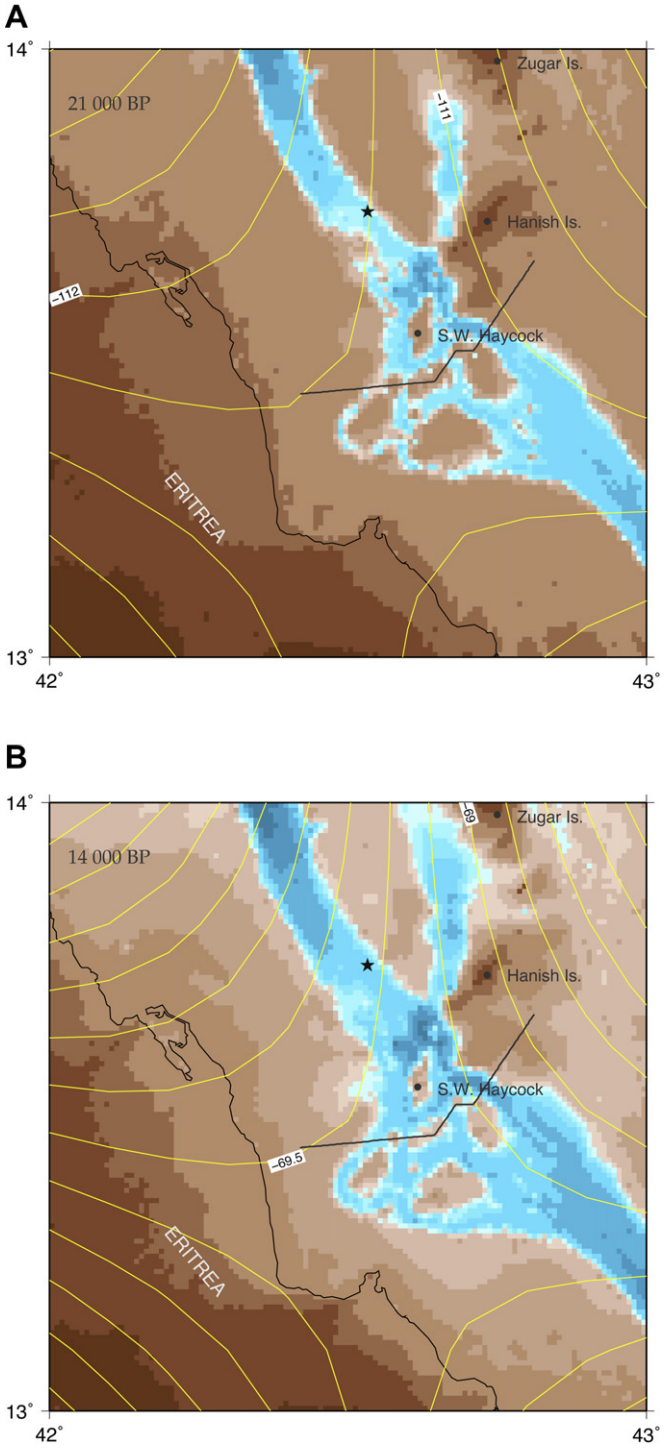

Fig. 22. (A) Palaeo reconstruction of the topography for the Bab al Mandab at the Haycock and Hanish Islands. The black line denotes the location of the section illustrated in Fig. 23. (B) Same as (A) but at 14,000 years BP.

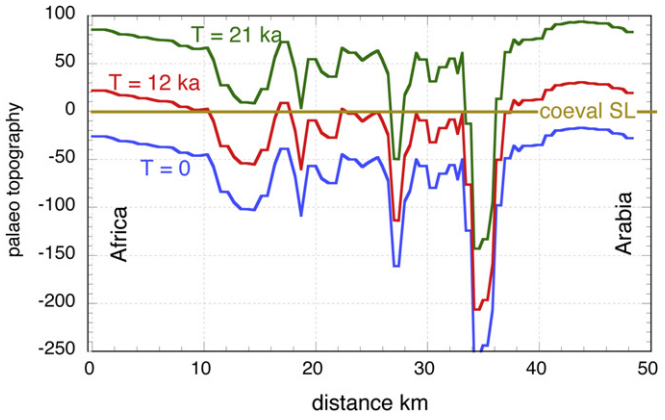

Fig. 23. Topographic cross-sections south of the Hanish sill along the section identified in Fig. 22 today ($T = 0$) and at 12,000 and 21,000 years before present. All profiles are with respect to sea level for that epoch.

of the principal 'Haycock-section' channel and, as sea level rises, the width of the channel initially increases only slowly, although other channels develop and the location of the minimum sea crossing distance migrates with time. At 14,000 years ago, for example, local sea level was some 70 m lower than today but the main eastern channel width has increased to only 3.5 km. The location of the minimum crossing distance of the western channel at this time has shifted southwards but the crossing distance remains less than for the eastern channel (Fig. 22B). By 12,000 years ago there has been a rapid expansion of the channel widths to more than 25 km, apart from some very low-lying islands.

Fig. 24A illustrates the evolution of the minimum channel crossing width throughout the Last Glacial cycle; at any epoch for which there are several channels, the minimum crossing is taken as the widest of the individual channels that collectively define the shortest pathway between the African and the Arabian shorelines. Throughout the past 120,000 years there are a number of, sometimes prolonged, intervals when the crossing width is less than 4–5 km, and for which at all times both sides of the crossing are visible from sea level at any point of the crossing (Fig. 24A). The imposition of this latter condition excludes some of the low islands being used as stepping-stones when their elevations are too low for them to appear above the horizon from a raft, as occurs, for example, during the interval 30–35 ka or at 46 ka.

Further back in time sea level models are less accurate, but the reconstructions indicate that there are again numerous extended intervals during which the local sea level fell below −50 m and the crossing distance was less than 4–5 km (Fig. 24B).

5. Archaeological implications and human migrations out of Africa

In the past decade there has been renewed interest in coastal environments and marine resources as potentially significant factors in human evolution and dispersal (Stringer, 2000; Walter et al., 2000; Erlandson, 2001; Bailey and Milner, 2002; Mannino and Thomas, 2002; Flemming et al., 2003; Bailey, 2004a,b). In part, this reflects the recognition that many coastal regions offer productive and diverse resources for human settlement and attractive corridors for population dispersal and colonisation of new territory, even without advanced cognitive abilities or technical skills. Also, sea-level reconstructions that have been applied with growing frequency to archaeological problems over the past three decades (Bailey, 1978; Van Andel and Shackleton, 1982; Lambeck, 1996a,b; Bailey and Flemming, 2008) have made it

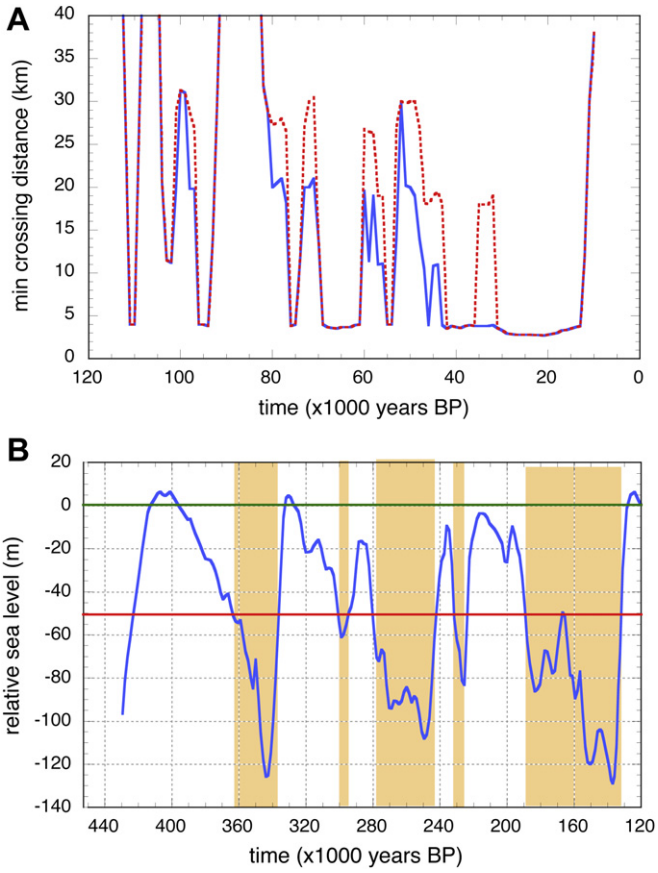

Fig. 24. (A) Minimum crossing distance between Africa and Arabia during the Last Glacial cycle. The blue function is the minimum crossing distance without intervisibility requirements and the red function is the minimum distance with the requirement that there is two-way visibility for all channel crossings. (B) Periods (shaded areas) when sea levels at Bab al Mandab were lower than −50 m and when minimum channel widths were less than 5 km.

increasingly obvious that the scarcity of archaeological evidence for the exploitation of marine resources before the mid-Holocene is most likely due to submergence of coastal archaeological sites by sea-level change rather than to a lack of interest in coastal and marine resources by earlier human populations.

With this sharpened archaeological focus comes a demand for more accurate and detailed reconstructions of the palaeogeography and environment of ancient coastlines. Traditionally, archaeological interpretations have relied on global eustatic curves applied to modern navigational bathymetry. For many archaeological purposes such a broad-brush approach may be adequate, but where the estimation of relative sea level and the reconstruction of palaeo-shorelines are sensitive to errors introduced by low-resolution bathymetric data, or by localised crustal movements, a more detailed approach is required. Shoreline reconstructions at the southern end of the Red Sea are especially sensitive to both sources of uncertainty, since the reported depth of the shallowest sill is similar to the eustatic lowering of sea level at glacial maxima. In circumstances such as these, more detailed local and regional field data are required as well as a more sophisticated approach to interpretation using modelling techniques that have been pioneered in a number of ocean basins of archaeological interest such as the Persian Gulf and the Mediterranean (Lambeck, 1996a,b).

Palaeogeographical shoreline reconstructions in this region have been presented by us in earlier papers (Bailey et al., 2007a,b; Bailey, 2009), and interpreted in terms of their significance for potential human movement and contact across the southern Red Sea. These used earlier iteration ice models and nominal earth-model parameters. The results reported in this paper considerably refine and in some respects significantly modify understanding of these changes and their human implications. Two key factors emphasised in the new model results are (a) the extent to which shoreline elevations and reconstructions of relative sea level can be affected by isostatic effects, even in regions far from the continental ice sheets, and (b) the importance of separating isostatic and tectonic movements through isostatic modelling in conjunction with field data.

The most important outcomes are: (i) the demonstration of ongoing tectonic deformation as a potentially significant variable in palaeo-shoreline reconstruction in many parts of the Red Sea, becoming especially important further back in time beyond the Last Glacial–Interglacial cycle; (ii) a re-evaluation of the bathymetry in the shallowest part of the southern channel; (iii) a more detailed reconstruction of changes in palaeoshoreline configuration in this region during the Last Glacial; and (iv) a clearer though still incomplete understanding of palaeoshoreline positions during earlier glacial periods.

In considering the human implications of these results, palaeogeographical conditions have been reconstructed over the last sea-level cycle (MIS 5 to MIS 1) for which the most detailed evidence is available. The principles used in this reconstruction can be extended back through the previous glacial cycle, MIS 9 to MIS 6, to ~200 ka with reasonable confidence, thus encompassing the full range of time within which the expansion out of Africa of anatomically modern humans is believed to have taken place. For earlier periods of the Pleistocene beyond ~200 ka, the uncertainties increase because of incomplete knowledge about earlier variations in global ice volumes and local or regional tectonic and volcanic effects, and it is not possible to extrapolate the results to these earlier periods except in general terms.

The likelihood of sea crossings at different periods of the sea level cycle is considered in the light of these reconstructions of shoreline positions and sea channels. First, and in agreement with the earlier reconstructions, the new results demonstrate that the southern channel would have remained open during the maximum lowering of sea level in MIS 2, with a continuing marine connection between the Red Sea and the Gulf of Aden, providing independent corroboration of the Red Sea isotope record (Rohling et al., 1998; Siddall et al., 2003), with a minimum channel width across the Hanish Sill of ~8 km and a water depth averaging ~13 m.

Second, and more importantly for archaeological purposes, the modelling of palaeoshoreline positions brings into sharper focus the issue of where and during which periods sea crossings would have been easiest at different stages of the sea-level cycle. Previous discussions of sea-level change have concentrated on establishing whether or not there could have been a land crossing during periods of low sea level, and have therefore focussed either on the narrowest part of the present-day channel at the Bab al Mandab Strait, or the shallowest part of the seabed in the vicinity of the Hanish Sill and the volume of water required to explain the deep-sea isotope record within the Red Sea Basin.

All sources of evidence reject the possible existence of a land connection and the discussion can now be focussed on the distance and feasibility of sea crossings and the regions that would have offered optimum opportunities for such crossings. Here, the key variables are the width of sea barriers, current flows, and the target angle and degree of inter-visibility of opposing shorelines. As the above results have shown, the optimum for these variables is not necessarily in the same part of the channel as the shallowest depth of the seabed or the narrowest crossing at modern sea level.

In fact, at times of minimum sea level, the narrowest crossings occur to the south of the Hanish Sill, where the channel branches

into several narrow and shallow channels. The islands that appear at this time, referred to here collectively as the Haycock Islands, are well elevated (~50 m) above the contemporaneous sea level and afford shorter sea crossings than either the Hanish region to the north or the Bab al Mandab Strait to the south (Figs. 20 and 22). The steep slopes of the islands indicate that they are the result of tectonics or marine erosion of the bedrock rather than more ephemeral sandbanks. These islands would have afforded a series of short crossings, approximately 1–3 km wide at minimum sea level, and sufficiently narrow for both sides of the channel to have been visible at all times.

As sea level rises, additional channel crossings are required in the western section and the location of the narrowest crossings for each of these channels shifts. But for the most part they remain narrower than the principal channel in the east until the rise in post LGM sea level approaches ~50 m. This occurs shortly before 12 ka, and from this point on the crossing exceeds ~30 km, ignoring occasional small, low islands (Fig. 22). The evolution of this width is illustrated in Fig. 24 for the two cases, with and without intervisibility constraints. In practice there is little difference between these results and what they confirm in either case is that there are a number of periods during the glacial cycle when the sea crossings were narrow – no more than 4 km for the longest crossing in the sequence – with very ample 'banks' on both sides and intervisibility of land at every crossing. The LGM itself is not particularly special in this regard. During the cold stages of MIS 5.4 and MIS 5.2 for example, there are short periods (~1000 years) when the crossings would not have been very different from the LGM, thanks to the steep topography of the channels. In effect, there are two alternating states for the Red Sea crossing in this region, with few intermediate conditions. Either the crossing requires a sea journey greater than about ~30 km with no inter-visibility, close to the distance of the present-day crossing at the narrowest point of the Bab al Mandab Strait (~30 km including Perim Island), or the crossing requires two or more short sea journeys, none greater than 4 km. Over the past 120 ka, the short-distance crossings were available for about one third of the time, with the longest period of availability occurring between 12 and 32 ka, shorter periods between 61–68 ka and 94–96 ka, and brief periods of availability lasting no more than ~1 ka at 55 ka, 75 ka and 110 ka. Likewise, for the earlier glacial cycles, there were extended periods when the maximum crossing distances were less than 4–5 km (Fig. 24B). As previously noted, only during the glacial Stage MIS 12 (before ~440,000 years BP) is there a possibility that the Red Sea may have been isolated from the Gulf of Aden if the low sea levels identified in the Golfe du Lyon (Rabineau et al., 2006) are of global significance.

How far do these results constrain the likelihood and timing of human movement across the southern end of the Red Sea? Three considerations set the terms of debate. The first is that the concept of 'seafaring' when applied to the earliest evidence of sea travel is often used in an ill-defined way and may encompass a very wide range of possibilities from organised seafaring in carefully constructed boats requiring considerable investment of social capital and cognitive, technical and navigational skills at one extreme, to casual sea crossings involving swimming, drifting, or use of floats or simple rafts at the other (Anderson et al., 2010). The presence of a sea channel, especially if it is relatively narrow – at the shorter end of the distance range considered here (at ≤4 km) – is not in itself sufficient to impose a permanent barrier to human crossing, regardless of the presumed abilities and motivations of the human populations in question. Conversely, evidence that a sea channel, especially a relatively narrow one, has been crossed, for example human presence on an offshore island, is not in itself evidence of organised seafaring involving the use of boats.

The second consideration is that a land passage, especially with plentiful food resources and water supplies en route, is the ideal reference standard against which any sea crossing should be measured. From that point of view any sea crossing, however short, must set some constraint on the frequency of movement or the number of people moving, especially if encumbered with material possessions or young children, and must therefore impose to some degree a bottleneck on contact between adjacent land masses. At the same time, it is axiomatic that the likelihood of sea-crossing becomes greater as the sea distances involved become shorter, and the length of time (as measured in centuries or millennia) during which such crossings are possible becomes greater.

Thirdly, none of the independent evidence that has been cited in relation to early crossings of the southern Red Sea decisively supports or rejects the possibility of such crossings, as opposed to movement between Northeast Africa and the Arabian Peninsula via the northern end of the Red Sea, whether it is variability in stone tool assemblages (Marks, 2009; Armitage et al., 2011), deductions from modern genetic variation (Macaulay et al., 2005; Cabrera et al., 2009; Rídl et al., 2009), or the biogeographical distributions of other mammals (Fernandes et al., 2006; Fernandes, 2009). The stone tool assemblages are separated by thousands of kilometres, the genetic data, whatever they may say about the relationship between populations in Africa and southern Asia, cannot specify the route that connected them, and the behaviour of other mammals is not an exact proxy for humans.

Given all the above considerations, the palaeogeographic reconstructions presented here cannot provide decisive evidence for or against sea crossings. But they can define the possibilities at different sea-level positions. During the periods of short sea-crossings in the southern Red Sea (~4 km), the possibility of human movement between Africa and Arabia can be regarded as high, especially given the many thousands of years during which such short sea crossings were available. The distances involved could be crossed relatively easily by drifting or with the use of simple rafts. Current speeds might pose a deterrent, but are difficult to determine at lower sea levels and need to be further investigated. Stronger currents might have flowed between the Red Sea and the Gulf of Aden when the main channel was longer and narrower than today, but equally these flows might have been moderated by the presence of islands such as the Haycock group, or at certain seasons of the year. In any case, any risk of being swept off course by strong currents would have been offset by the very wide target angles of opposing shorelines.

The fact that sea crossings were feasible at these times with minimal skills and technology does not of course mean that sea crossings actually took place, let alone that they engaged sufficient numbers of people to sustain a successful founding population on the other side of the sea barrier. The distance in question, approximately the distance to a ship visible on the far horizon visible to an observer standing on the seashore, might be a strong barrier for some populations, but not for others. Additional factors are the pressure or motivation to leave the pre-existing homeland, and the attractions of the resources available on the other side. Recent discussions emphasise the aridity of the Arabian Peninsula as a major deterrent to human entry and the importance of periods of wetter climate as an attractor, with conditions regularly alternating between these two states during the Pleistocene (Parker, 2009). Generally speaking, wetter conditions are associated with periods of higher sea level, but there is some overlap between wetter climates and lower sea levels. Armitage et al. (2011), for example, have explained the close similarities of the stone tool assemblages dated at 125 ka at Jebel Faya with those in East Africa in terms of an expansion by modern humans across the southern Red Sea when lower sea levels coincided with wetter conditions,

a conjunction they identify with the transition from MIS 6 to MIS 5.5. The timing of the global sea-level rise during this transition remains poorly constrained but levels below −50 m would have occurred before about 135 ka BP such that sea crossings not involving long distances could have occurred up to about this time. Jebel Qattar 1 dated at 75 ka (Petraglia et al., 2011) also coincides with a narrow sea crossing in the south (Fig. 24B). Parker identifies wetter episodes in MIS 7, MIS 6 and MIS 3, periods before and after the postulated expansion out of Africa of modern humans. The last two coincide with intervals when short sea crossings were possible, but the fragmentary records for MIS 7 reefs indicate that sea levels were close to present (Section 3.4). However, identifying these conjunctions between favourable sea crossings and climate is complicated by uncertainties over the dating of climate variation in the Arabian Peninsula particularly beyond MIS 5 (Parker, 2009, p. 42), and also by the claim that improved flow of groundwater onto the emerged shelf at periods of maximum sea level lowering would have created well-watered conditions in coastal areas regardless of climatic aridity in the Arabian hinterland (Faure et al., 2002).

Irrespective of any uncertainties in timing and because the channel widths are insensitive to sea levels whenever the latter locally are more than 50 m below present, the palaeoshoreline reconstructions indicate that (i) there are a number of periods over the past 150 ka when short sea crossings were possible, (ii) similar periods most probably occurred further back in time as well, and (iii) some of these coincided with favourable environmental conditions on the Arabian side. Furthermore, because the crossings are short, with intervisibility assured at all times and because currents are unlikely to be fast, there is no reason to invoke sophisticated seafaring technologies for the crossings and to confine the possibility of sea travel to anatomically modern humans only. In so far as analogies for sea travel by archaic humans from other parts of the world are valid, there is evidence of Middle Palaeolithic finds on the island of Kephallinia, western Greece, demonstrably separated from the Greek mainland by a sea channel ~5 km wide (Ferentinos, pers. comm. 2009), perhaps earlier evidence on Crete (Strasser et al., 2010) – though the early dates here have yet to be verified – and human occupation on the island of Flores at ~900 ka involving a sea crossing of 25 km, though the skill involved in such a crossing is disputed given the apparent subsequent isolation of this island population and the failure to undertake the longer sea journeys required to reach eastwards to the islands of Wallacea and beyond until much later (Morwood et al., 1999; Bednarik, 2003; Morwood and Jungers, 2009; Brumm et al., 2010).

For the longer sea crossings across the southern Red Sea of ~30 km, the considerations are different. Sea crossings over this distance by swimming, accidental drifting or simple rafts and floats, though not impossible, are less likely, and the longer crossings during these periods would most likely require purposeful sea journeys using seaworthy rafts or boats. Such capabilities are generally considered to require the cognitive skills of modern humans, and analogies from other parts of the world show that modern humans undertook sea journeys over comparable or greater distances at least as early as 50 ka from South-east Asia to Australia and New Guinea (O'Connell et al., 2010; O'Connor, 2010), 30 ka in the Japanese archipelago (Habu, 2010), and 12 ka in the eastern Mediterranean (Lambeck, 1996b; Ammerman, 2010), although opinion is divided as to how frequent, systematic, planned or technically sophisticated such early sea journeys were. Australia is frequently taken as the limiting case for earliest sea journeys over extended distances, the coincidence of modern humans and seafaring in the earliest colonisation being taken as evidence that more archaic hominins lacked the cognitive and linguistic skills to undertake such journeys (Noble and Davidson, 1996). However, the evidence that archaic humans did not voyage to New Guinea or Australia does not mean that they lacked the abilities to do so, or could not have made sea journeys over distances of ~30 km or more in other parts of the world, and the assumption that archaic humans lacked the ability or motivation to practise extended sea journeys or exploitation of marine resources assumes the very matters that need to be investigated.

Equally, the fact that modern humans supposedly originating in Africa ultimately reached Australia and New Guinea by lengthy sea crossings does not mean that their initial departure from Africa required equivalent skills and equipment. Growing familiarity with sea travel might be predictable in the context of offshore fishing activity, which could then provide a pathway to longer sea journeys. However, early evidence for this, at least in the Red Sea region, is currently lacking. Claims of marine resources at the 130 ka site of Abdur refer only to shell gathering on the seashore (Walter et al., 2000), and even here the shells in question appear to represent a natural death assemblage rather than food remains (Bruggemann et al., 2004). Given the limited extent of archaeological exploration and evidence in the southern Red Sea region, none of these possibilities can be ruled out, but the shoreline reconstructions also show that there is no need to invoke them, since there are many periods when the southern Red Sea could have been traversed by short sea crossings with only the most rudimentary technology and technical skill.

Finally, we should not lose sight of the fact that an alternative dry-land pathway, around the Red Sea from Africa into the Arabian Peninsula, albeit a relatively narrow one, persisted throughout the Pleistocene in the north via the Sinai Peninsula, with relatively little physical impediment to human movement (Bailey and King, 2011). The possibility of a southern pathway nevertheless remains important in that it would have multiplied the opportunities for movement and contact between Africa and Asia.

In summary, we emphasise three broad conclusions.

- The pathways of movement between Africa and Arabia have always been constrained to limited exit points at the northern and southern ends of the Red Sea, reinforced in some periods by climatic aridity over much of the Arabian Peninsula, and a generally patchy distribution and periodic contraction of resources in the core of the Peninsula. These potential pathways have been further constrained by sea-level change, particularly in the south. Here, a land crossing is ruled out for any period back to at least MIS 12 (440,000 ka) and probably beyond that, with the easiest potential sea crossings occurring when channel widths reduced to about 4 km or less. These opportunities occurred periodically throughout the Pleistocene, and would most likely have opened up the southern crossing to some degree of population movement even in the absence of rafts or boats. But this southern pathway would also have remained closed for long periods, creating the potential for genetic and cultural bottlenecks and the development of human populations in the Arabian Peninsula with distinctive biological and cultural characteristics. If anatomically modern human populations did use the southern corridor across the Red Sea, as claimed by the most recent comparison of stone tool assemblages between southern Arabia and Northeast Africa (Armitage et al., 2011), they could have done so without the seaworthy boats or seafaring skills necessary for regular journeys over distances of 30 km or more.
- Although the palaeo-shoreline reconstructions must necessarily be open to increasing uncertainty further back into the Pleistocene, it is likely that similar opportunities for short sea crossings were periodically available in earlier periods, at least during the Middle Pleistocene, and perhaps earlier too – even with the lower amplitude of sea-level oscillations in the Lower Pleistocene, our palaeo-shoreline reconstructions show that a drop in relative sea level of −50 m is sufficient to create short

sea-crossings comparable to those available at −130 m. There is no obvious reason to restrict the ability to exploit these opportunities to anatomically modern humans.

- The sea-level reconstructions underline the need for new field investigations aimed at giving greater precision to the pattern of environmental and climatic change in the Arabian Peninsula, and providing more substantial archaeological evidence for the human response to changing conditions in the broader region, especially on the submerged landscapes that would have been exposed for long periods, and which all current indicators suggest were extensive and potentially attractive regions for human settlement on both sides of the southern Red Sea.

Acknowledgements

This research was funded by the Australian Research Council and the Australian National University, and by the NERC, UK (grant NE/A516937/1), through its EFCHED (Environmental Factors in Human Evolution and Dispersal) thematic programme. We also acknowledge funding support to G.B. and C.V-F. from the British Academy (grants LRG-35406 and LRG-45481) and the Leverhulme Trust (grant F/00 224/AB), and the cooperation and support of HRH Prince Sultan bin Salman and Prof. Ali Ghabban of the General Commission for Tourism and Antiquities of Saudi Arabia. K.L. was partly funded by the Chaire Internationale de Recherche Blaise Pascal financée par l'Etat et la Région Ile-de-France. We are grateful to Geoffrey King (IPGP) for discussion of Red Sea tectonics and to Graeme Potter, UKHO, for access to unpublished track data, the ability to inspect commercially confidential data, and the provision of analytic plots (errors or misjudgements that remain are ours) Figs. 19 and A1 have been redrawn by Peter Hunter of the National Oceanography Centre. We thank the Programme for the Environment of the Red Sea and Gulf of Aden for given us access to their high-resolution bathymetric data within Bab al Mandab. Constructive discussions with Jean-Claude Plaziat and Jean-Louis Reyss about the observational evidence for sea-level change in the Red Sea are gratefully acknowledged.

Appendix 1

Hanish Sill bathymetry

Is there a possibility of a limiting sill south of Hanish?

The bathymetry between Hanish and Bab al Mandab shows a narrow meandering central channel deeper than 200 m for much of its length, bordered on each side by a broad shelf approximately 50 m deep. The Hanish Islands are volcanic, and the submerged topography south west of the main Hanish Island (al Kubra) shows precipitate slopes, submerged banks or pinnacles of rock, and multiple braided channels between 100 m and 200 m deep. The soundings on published charts, such as the UK Admiralty Chart 453 (1:100,000, 2003) or 1925 (1:200,000, 1985), are not sufficiently close spaced to give confidence that there is no volcanic ridge or earthquake-driven slump that may restrict the channels locally and create a sill shallower than 137 m. The grid spacing on the General Bathymetric Chart of the Ocean (GEBCO) chart is 900 m, leaving the same ambiguity.

In the 1990s the International Maritime Organization (IMO) approved a Traffic Separation Zone in the southern Red Sea requiring the traffic lanes from directly west of Hanish al Kubra (Fig. A1) to Bab al Mandab to be surveyed to full Hydrographic Survey standards. This was conducted by PERSGA (Programme for the Environment of the Red Sea and Gulf of Aden), and the contractor was Gardline Surveys. For reasons of commercial confidentiality, the survey cannot be reproduced but an examination of the raw data at the UK Hydrographic Office (UKHO) showed that the mean spacing between plotted soundings is 108 m (Graeme Potter, UKHO, personal communication) and that the survey covered all the shoals and multiple channels south of Hanish with a vertical depth accuracy of the order of 0.5–1.0 m. If the contoured gridded data are cut off at a depth of 137 m, showing only areas deeper than that value, a continuous channel is shown and confirms that it is highly unlikely that there remains an undiscovered limiting sill shallower than 137 m south of Hanish.

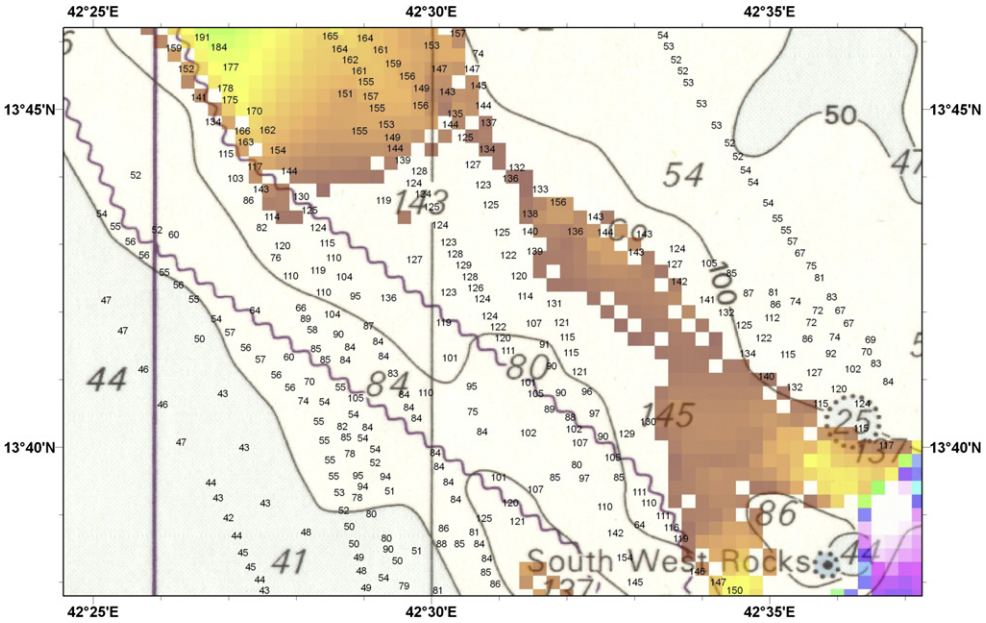

Fig. A1. The position of the deepest channel in the neighbourhood of the Hanish Sill, plotted over the soundings of Admiralty Chart 453, together with the most recent soundings obtained from ships in passage. The pixel size arises from the gridding of the available soundings. The total data set has been filtered at a depth of 134 m (uncorrected depth), with darkest brown representing the shallowest channel below that depth, grading into yellow and green in deeper water. The purple-blue tints in the south-east corner represent the deep channel surveyed by PERSGA. Note that there is a single sounding of 134 m at the shallowest and narrowest point of the sill. When this is corrected for the local velocity of sound in seawater the sill is 137 ± 3 m.

Could there be deeper channels or shallower sills in the region of the Werner and Lange (1975) sill?

The topography mapped by Werner and Lange (1975) suggests an undulating seabed in the neighbourhood of the sill, sloping gradually to 200 m within 10 km to both the northwest and the southeast. The tracks of the survey by Werner and Lange (1975) were 1–2 km apart, and the soundings are recorded and published at a spacing of 1–2 km along track. Thus unexpectedly deep narrow channels, or abrupt ridge-like obstructions of a channel, cannot be resolved at a resolution of less than about 1 km. However, as the work was conducted as a research survey, with the specific objective of locating the sill, instruments would presumably have been under continuous observation even if outlier values were not recorded automatically. The navigation was based on visual range and bearing to Hanish al Kubra and radar bearings from temporary buoys. Absolute errors of position could have been of the order of 100 m. However, topographic gradients are low in the area, of the order of 0.5°, such that positioning errors will not introduce depth errors exceeding 1 m. Thus, on this evidence, the shallowest depth located on the channel axis both by echo sounder and wire sounding is 137 m at the location identified by Werner and Lange.

Modern soundings since 1975 and errors and corrections of modern measurements

The UKHO maintains both international charts and the compilation of the GEBCO chart data for the Red Sea. Fig. A1 corresponds to the chart from 2008, superimposed on which is the PERSGA data in the southeast corner and *Tracks on Passage* data not included in the chart. These latter are records accepted by the UKHO as reliable and are usually taken by a Ministry of Defence Royal Navy vessel operating a single-beam echo sounder and assuming that the sound velocity in sea water is always 1500 m/s. The corrections carried out for a *Full Accuracy Hydrographic Survey* are not made in these measurements and thus errors from tide, sound velocity, etc., have to be accepted. Sound velocity in the southern Red Sea, with a salinity of 37–38 ppm, is of the order of 1550 m/s so that depths of the order of 100 m will be under-estimated by about 3.0 m. The Carter Tables (Carter, 1980), which correct for the typical median sea water salinity in different ocean areas and depths, are only applied by the IMO and GEBCO in water depths greater than 200 m and GEBCO data points in the southern Red Sea have not been corrected for the salinity effect on sound velocity.

With the assistance of UKHO all available data have been merged, including the data in the GEBCO compilation, the PERSGA data and the Tracks on Passage data. The data has been gridded with a grid spacing of 300 m (including a correction for shoal bias[3]) and contoured and filtered to indicate only depths equal or below −134 m to check the most probable location of the limiting sill. The resulting image (Fig. 19 in main text) confirms the existence of the continuous channel and the unique constriction close to the point identified by Werner and Lange (1975) at a depth of 134 m which, when corrected for sound velocity using the formula of Coppens (1981) and reduced from lowest astronomical tide to mean sea level, yields a sill at 137.5 ± 2.5 m below mean sea level.

[3] For reasons of safety, the gridded bathymetry from which the navigational charts are produced is 'shoal biased' with the result that the shallowest sounding is used in every grid square such that the chart depths are biased towards shallower values

References

Al Sayari, S.S., Zötl, J.G. (Eds.), 1978, Quaternary Period in Saudi Arabia, vol. 1. Springer Verlag, Vienna, 334 pp.

Ambraseys, N.N., Melville, C.P., Adams, R.D., 1995. The Seismicity of Egypt, Arabia and the Red Sea: a Historical Review. Cambridge University Press, Cambridge, 181 pp.

Ammerman, A., 2010. The first Argonauts: towards the study of the earliest seafaring in the Mediterranean. In: Anderson, A., Barrett, J.H., Boyle, K.V. (Eds.), The Global Origins and Development of Seafaring. McDonald Institute for Archaeological Research, Cambridge, pp. 81–92.

Anderson, A., Barrett, J.H., Boyle, K.V. (Eds.), 2010. The Global Origins and Development of Seafaring. McDonald Institute for Archaeological Research, Cambridge, p. 320.

Andres, W., Radtke, U., 1988. Quartäre strandterrassen an der küste des Gebel Zeit (Golf von Suez/Ägypten. Erdkunde 42, 7–16.

Anzidei, M., Antonioli, F., Benini, A., Lambeck, K., Sivan, D., Serpelloni, E., Stocchi, P., 2011. Sea-level change and vertical land movements since the last two millennia along the coasts of southwestern Turkey and Israel. Quaternary International 13–20.

Armitage, S.J., Jasim, S.A., Marks, A.E., Parker, A.G., Usik, V.I., Uerpmann, H.-P., 2011. The southern route "Out of Africa": evidence for an early expansion of modern humans into Arabia. Science 331, 453–456.

ArRajehi, A., McClusky, S., Reilinger, R., Daoud, M., Alchalbi, A., Ergintav, S., Gomez, F., Sholan, J., Bou-Rabee, F., Ogubazghi, G., Haileab, B., Fisseha, S., Asfaw, L., Mahmoud, S., Rayan, A., Bendik, R., Kogan, L., 2010. Geodetic constraints on present-day motion of the Arabian Plate: implications for Red Sea and Gulf of Aden rifting. Tectonics 29, TC3011.

Bailey, G.N., 1978. Shell middens as indicators of postglacial economies: a territorial perspective. In: Mellars, P.A. (Ed.), The Early Postglacial Settlement of Northern Europe. Duckworth, London, pp. 37–63.

Bailey, G.N., 2004a. The wider significance of submerged archaeological sites and their relevance to world prehistory. In: Flemming, N.C. (Ed.), Submarine Prehistoric Archaeology of the North Sea: Research Priorities and Collaboration with Industry. CBA Research Report 141. English Heritage and Council for British Archaeology, York, pp. 3–10.

Bailey, G.N., 2004b. World prehistory from the margins: the role of coastlines in human evolution. Journal of Interdisciplinary Studies in History and Archaeology 1, 39–50.

Bailey, G.N., 2009. The Red Sea, coastal landscapes, and hominin dispersals. In: Petraglia, M.D., Rose, J.I. (Eds.), The Evolution of Human Populations in Arabia. Springer, Dordrecht, Netherlands, pp. 15–37.

Bailey, G.N., Milner, N.J., 2002. Coastal hunters and gatherers and social evolution: marginal or central? Before Farming: the Archaeology of Old World Hunter–Gatherers 3 (4), 1–15.

Bailey, G.N., Flemming, N.C., 2008. Archaeology of the continental shelf: marine resources, submerged landscapes and underwater archaeology. Quaternary Science Reviews 27, 2153–2166.

Bailey, G.N., King, G.C.P., 2011. Dynamic landscapes and human dispersal patterns: tectonics, coastlines, and the reconstruction of human habitats. Quaternary Science Reviews 30, 1533–1553.

Bailey, G.N., King, G.C.P., Flemming, N.C., Lambeck, K., Momber, G., Moran, L.J., Al-Sharekh, A., Vita-Finzi, C., 2007a. Coastlines, submerged landscapes and human evolution: the Red Sea Basin and the Farasan Islands. Journal of Island and Coastal Archaeology 2, 127–160.

Bailey, G., Al-Sharekh, A., Flemming, N.C., Lambeck, K., Momber, M., Sinclair, A., Vita-Finzi, C., 2007b. Coastal prehistory in the southern Red Sea Basin, underwater archaeology and the Farasan islands. Proceedings of the Seminar for Arabian Studies 37, 1–16.

Bard, E., Arnold, M., Fairbanks, R.G., Hamelin, B., 1993. ^{230}Th–^{234}U and ^{14}C ages obtained by mass spectrometry on corals. Radiocarbon 35, 191–199.

Bednarik, R.G., 2003. Seafaring in the Pleistocene. Cambridge Archaeological Journal 13, 41–66.

Beyin, A., 2006. The Bab-al-Mandab vs the Nile-Sinai-Levant: an appraisal of the two dispersal routes for early modern humans out of Africa. African Archaeological Review 23, 5–30.

Bohannon, R.G., Naeser, C.W., Schmidt, D.L., Zimmermann, R.A., 1989. The timing of uplift, volcanism, and rifting peripheral to the Red Sea: a case for passive rifting. Journal of Geophysical Research 94, 1683–1701.

Bosence, D., AlAawah, M.H., Davison, I., Rosen, B., Vita-Finzi, C., Whittaker, L., 1998. Salt domes and their control on basin margin sedimentation; a case study from the Tihama Plain, Yemen. In: Purser, B., Bosence, D. (Eds.), Sedimentation and Tectonics of Rift Basins: Red Sea–Gulf of Aden. Chapman and Hall, London, pp. 448–464.

Bosworth, W., Taviani, M., 1996. Late Quaternary reorientation of stress field and extension direction in the southern Gulf of Suez, Egypt: evidence from uplifted coral terraces, mesoscopic fault arrays, and borehole breakouts. Tectonics 15, 791–802.

Bosworth, W., Huchon, P., McClay, K., Abbate, E., 2005. The Red Sea and Gulf of Aden Basins. Journal of African Earth Sciences 43, 334–378.

Boucarut, M., Clin, M., Poucham, P., Thibault, C., 1985. Impact des événements tectono-volcaniques plio-pléistocènes sur la sédimentation en République de Djibouti (Afar Central). Geologishe Rundschau 71, 123–137.

Bruggemann, J.H., Buffler, R.T., Guillaume, M.M.M., Walter, R.C., von Cosel, R., Ghebretensae, B.N., Berhe, S.M., 2004. Stratigraphy, palaeoenvironments and

model for the deposition of the Abdur Reef Limestone: context for an important archaeological site from the last interglacial on the Red Sea coast of Eritrea. Palaeogeography, Palaeoclimatology, Palaeoecology 20, 179–206.
Brumm, A., Jensen, G.M., van den Bergh, G.D., Morwood, M.J., Kurniawan, I., Aziz, F., Storey, M., 2010. Hominins on Flores, Indonesia, by one million years ago. Nature 464, 748–752.
Cabrera, V.M., Abu-Amero, K., Larruga, J.M., González, A.M., 2009. The Arabian Peninsula: gate for human migrations out of Africa or cul-de-sac? A mitochondrial DNA phylogeographic perspective. In: Petraglia, M.D., Rose, J.I. (Eds.), The Evolution of Human Populations in Arabia. Springer, Dordrecht, Netherlands, pp. 79–87.
Carter, D.J.T., 1980. In: Echo-Sounding Correction Tables, third ed. Hydrographic Department, Ministry of Defence, United Kingdom.
Cathles, L.M., 1975. The Viscosity of the Earth's Mantle. Princeton University Press, Princeton, NJ, 386 pp.
Chapman, R.W., 1978. Geomorphology. In: Al-Sayari, S.S., Zötl, J.G. (Eds.), Quaternary Period in Saudi Arabia, vol. 1. Springer Verlag, Vienna, pp. 19–25.
Chappell, J., 1974. Geology of coral terraces, Huon Peninsula, New Guinea: a study of Quaternary tectonic movements and sea-level changes. Geological Society of America Bulletin 85, 553–570.
Chappell, J., Omura, A., Esat, T., McCulloch, M., Pandolfi, J., Ota, Y., Pillans, B., 1996. Reconciliation of late Quaternary sea levels derived from coral terraces at Huon Peninsula with deep sea oxygen isotope records. Earth and Planetary Science Letters 141, 227–236.
Chu, D., Gordon, R.G., 1998. Current plate motions across the Red Sea. Geophysical Journal International 135, 313–328.
Cochran, J.R., 1983. A model for the development of the Red Sea. Bulletin of the American Association of Petroleum Geologists 67. doi:10.1306/03B5ACBE-16D1-11D7-8645000102C1865D.
Cochran, J.R., Martinez, F., Steckler, M.S., Hobart, M., 1986. Conrad Deep: a new northern Red Sea Deep: origin and implications for continental rifting. Earth and Planetary Science Letters 78, 18–32.
Conforto, L., Delitala, M.C., Taddeucci, A., 1976. Datazioni col ^{230}Th di alcune formazioni coralligene delle Isole Dahlak (Mar Rosso). Rivista Italiana di Mineralogia e Petrologia 32, 153–158.
Coppens, A.B., 1981. Simple equations for the speed of sound in Neptunian waters. Journal of the Acoustical Society of America 69, 862–863. http://resource.npl.co.uk/acoustics/techguides/soundseawater/.
Darwin, C.R., 1842. The Structure and Distribution of Coral Reefs. Smith, Elder and Co., London.
Davison, I., Bosence, D., Alsop, G.I., Al-Aawah, M., 1996. Deformation and sedimentation around active Miocene salt diapirs on the Tihama Plain, northwest Yemen. In: Geological Society, London, Special Publications, vol. 100, 23–39 pp.
Denton, G.H., Hughes, T.H., 1981. The Last Great Ice Sheets. Wiley, New York, 484 pp.
Drury, S.A., Kelley, S.P., Berhe, S.M., Collier, R.E.Ll., Abraha, M., 1994. Structures related to Red Sea evolution in northern Eritrea. Tectonics 13, 1371–1380.
Dullo, W.-C., 1990. Facies, fossil record, and age of Pleistocene reefs from the Red Sea – Saudi Arabia. Facies 81, 175–192.
Dullo, W.-C., Montaggioni, L., 1998. Modern Red Sea coral reefs: a review of morphologies and zonation. In: Purser, B.H., Bosence, D.W.J. (Eds.), Sedimentation and Tectonics of Rift Basins: Red Sea–Gulf of Aden. Chapman and Hall, London, pp. 583–594.
El-Asmar, H.M., 1997. Quaternary isotope stratigraphy and paleoclimate of coral reef terraces, Gulf of Aqaba, south Sinai, Egypt. Quaternary Science Reviews 16, 911–924.
Emery, K.O., 1964. Sediments of Gulf of Aqaba (Elat). In: Miller, R.L. (Ed.), Papers in Marine Geology. Macmillan, New York, pp. 257–273.
Erlandson, J.M., 2001. The archaeology of aquatic adaptations: paradigms for a new millennium. Journal of Archaeological Research 9, 287–350.
Farrell, W.E., Clark, J.A., 1976. On postglacial sea level. Geophysical Journal of the Royal Astronomical Society 46, 647–667.
Faure, H., 1975. Recent crustal movements along the Red Sea and Gulf of Aden in AFAR (Ethiopia and T.F.A.I). Tectonophysics 29, 479–486.
Faure, H., Hoang, C.T., Lalou, C., 1980. Datations ^{230}Th/^{234}U de calcaires corallines et mouvements verticaux à Djibouti. Bulletin de la Societé Géologique de France 22, 959–962.
Faure, H., Walter, R.C., Grant, D.R., 2002. The coastal oasis: ice age springs on emerged continental shelves. Global and Planetary Change 33, 47–56.
Ferland, M.A., Roy, P.S., Murray-Wallace, C.V., 1995. Glacial lowstand deposits on the outer continental shelf of southeastern Australia. Quaternary Research 44, 294–299.
Fernandes, C.A., 2009. Bayesian coalescent inference from mitochondrial DNA variation of the colonization time of Arabia by the Hamadryas baboon (*Papio hamadryas hamadryas*). In: Petraglia, M.D., Rose, J.I. (Eds.), The Evolution of Human Populations in Arabia. Springer, Dordrecht, Netherlands, pp. 89–100.
Fernandes, C.A., Rohling, E.J., Siddall, M., 2006. Absence of post-Miocene Red Sea land bridges: biogeographic implications. Journal of Biogeography 33, 961–966.
Flemming, N.C., Bailey, G.N., Courtillot, V., King, G., Lambeck, K., Ryerson, F., Vita Finzi, C., 2003. Coastal and marine palaeo-environments and human dispersal points across the Africa-Eurasia boundary. In: Brebbia, C.A., Gambin, T. (Eds.), The Maritime and Underwater Heritage. Wessex Institute of Technology Press, Southampton, pp. 61–74.
Fricke, H.W., Landmann, G., 1983. On the origin of Red Sea submarine canyons. Naturwissenschaften 70, 195–196.
Friedman, G.M., 1965. A fossil shoreline reef in the Gulf of Elat (Aqaba). Israel Journal of Earth Sciences 14, 86–90.
Funder, S., Demoidov, I.N., Yelovicheva, Y., 2002. Hydrography and mollusc faunas of the Baltic and the White Sea-North Sea seaway in the Eemian. Palaeogeography, Palaeoclimatology, Palaeoecology 184, 275–304.
GEBCO (General Bathymetric Chart of the Oceans), 2008. GEBCO_08 Grid. At: www.gebco.net/.
Girdler, R.W., 1990. The Dead Sea transform fault system. Tectonophysics 180, 1–13.
Girdler, R.W., Styles, P., 1974. Two stage Red Sea floor spreading. Nature 247, 7–11.
Gvirtzman, G., 1994. Fluctuations of sea level during the past 400,000 years: the record of Sinai, Egypt (northern Red Sea). Coral Reefs 13, 203–214.
Gvirtzman, G., Buchbinder, B., Sneh, A., Nir, Y., Friedman, G.M., 1977. Morphology of the Red Sea fringing reefs: a result of the erosional pattern of the last glacial low-stand sea-level and the following Holocene recolonization. Memoir BRGM 89, 480–491.
Gvirtzman, G., Kronfeld, J., Buchbinder, B., 1992. Dated coral reefs of southern Sinai (Red Sea) and their implication to late Quaternary sea levels. Marine Geology 108, 29–37.
Habu, J., 2010. Seafaring and the development of cultural complexity in Northeast Asia: evidence from the Japanese archipelago. In: Anderson, A., Barrett, J.H., Boyle, K.V. (Eds.), The Global Origins and Development of Seafaring. McDonald Institute for Archaeological Research, Cambridge, pp. 159–170.
Hempton, M.R., 1987. Constraints on Arabian plate motion and extensional history of the Red Sea. Tectonics 6, 687–705.
Hoang, C.T., Taviani, M., 1991. Stratigraphic and tectonic implications of Uranium-series-dated coral reefs from uplifted Red Sea islands. Quaternary Research 35, 264–273.
Hoang, C.T., Dalongeville, R., Sanlaville, P., 1996. Stratigraphy, tectonics and palaeoclimatic implications of uranium-series-dated coral reefs from the Sudanese coast of the Red Sea. Quaternary International 31, 47–51.
Hötzl, J.G., 1984. The Red Sea. In: Jado, A.R., Hötzl, J.G. (Eds.), Quaternary Period in Saudi Arabia, vol. 2. Springer, Vienna, pp. 13–25.
Jado, A.R., Hötzl, J.G. (Eds.), 1984, Quaternary Period in Saudi Arabia, vol. 2. Springer, Vienna, 360 pp.
Jado, A.R., Hötzl, J.G., Roscher, B., 1990. Development of sedimentation along the Saudi Arabian Red Sea coast. Journal of King Abdul Aziz University, Earth Science 3, 47–62.
Joffe, S., Garfunkel, Z., 1987. Plate kinematics of the circum Red Sea – a re-evaluation. Tectonophysics 141, 5–22.
Johnston, P., 1993. The effect of spatially non-uniform water loads on predictions of sea-level change. Geophysical Journal International 114, 615–634.
Kopp, R.E., Simons, F.J., Mitrovica, J.X., Maloof, A.C., Oppenheimer, M., 2009. Probabilistic assessment of sea level during the last interglacial stage. Nature 462, 863–867.
Lahr, M.M., Foley, R., 1994. Multiple dispersals and modern human origins. Evolutionary Anthropology 3, 48–60.
Lambeck, K., 1993. Glacial rebound and sea-level change: an example of a relationship between mantle and surface processes. Tectonophysics 223, 15–37.
Lambeck, K., 1996a. Shoreline reconstructions for the Persian Gulf since the last glacial maximum. Earth and Planetary Science Letters 142, 43–57.
Lambeck, K., 1996b. Sea-level change and shore-line evolution in Aegean Greece since Upper Palaeolithic time. Antiquity 70, 588–611.
Lambeck, K., 2004. Sea-level change through the last glacial cycle: geophysical, glaciological and palaeogeographic consequences. Comptes Rendus Geoscience 336, 677–689.
Lambeck, K., Nakada, M., 1990. Late Pleistocene and Holocene sea-level change along the Australian Coast. Palaeogeography, Palaeoclimatology, Palaeoecology (Global and Planetary Change Section) 89, 143–176.
Lambeck, K., Nakada, M., 1992. Constraints on the age and duration of the last interglacial period and on sea-level variations. Nature 357, 125–128.
Lambeck, K., Johnston, P., 1998. The viscosity of the mantle: evidence from analyses of glacial rebound phenomena. In: Jackson, I. (Ed.), The Earth's Mantle: Composition, Structure, and Evolution. Cambridge University Press, Cambridge, pp. 461–502.
Lambeck, K., Bard, E., 2000. Sea-level change along the French Mediterranean coast since the time of the Last Glacial Maximum. Earth and Planetary Science Letters 175, 203–222.
Lambeck, K., Chappell, J., 2001. Sea-level change through the last Glacial Cycle. Science 292, 679–686.
Lambeck, K., Smither, C., Johnston, P., 1998. Sea-level change, glacial rebound and mantle viscosity for northern Europe. Geophysical Journal International 134, 102–144.
Lambeck, K., Esat, T.M., Potter, E.-K., 2002. Links between climate and sea levels for the past three million years. Nature 419, 199–206.
Lambeck, K., Purcell, A., Johnston, P., Nakada, M., Yokoyama, Y., 2003. Water-load definition in the glacio-hydro-isostatic sea-level equation. Quaternary Science Reviews 22, 309–318.
Lambeck, K., Antonioli, F., Purcell, A., Silenzi, S., 2004a. Sea-level change along the Italian coast for the past 10,000 yr. Quaternary Science Reviews 23, 1567–1598.
Lambeck, K., Anzidei, M., Antonioli, F., Benini, A., Esposito, A., 2004b. Sea level in Roman time in the Central Mediterranean and implications for recent change. Earth and Planetary Science Letters 224, 563–575.
Lambeck, K., Purcell, A., Funder, S., Kjær, K., Larsen, E., Möller, P., 2006. Constraints on the Late Saalian to early Middle Weichselian ice sheet of Eurasia from field data and rebound modelling. Boreas 35, 539–575.

Lambeck, K., Purcell, A., Zhao, J., Svensson, N.-O., 2010a. The Scandinavian Ice Sheet: from MIS 4 to the end of the Last Glacial Maximum. Boreas 39 (2), 410–435.
Lambeck, K., Woodroffe, C.D., Antonioli, F., Anzidei, M., Gehrels, W.R., Laborel, J., Wright, A.J., 2010b. Palaeoenvironmental records, geophysical modelling and reconstruction of sea-level trends and variability on centennial and longer time scales. In: Church, J.A., Woodworth, P.L., Aarup, T., Wilson, W.S. (Eds.), Understanding Sea-level Rise and Variability. Blackwell Publishing, London, pp. 61–121.
Lambeck, K., Purcell, A., Dutton, A. The anatomy of interglacial sea levels: the relationship between sea level and ice volume during past interglacials. Earth and Planetary Science Letters, in press.
Macaulay, V., Hill, C., Achilli, A., et al., 2005. Single, rapid coastal settlement of Asia revealed by analysis of complete mitochondrial genomes. Science 308, 1034–1036.
McClusky, S., Reilinger, R., Mahmoud, S., Ben Sari, D., Tealeb, A., 2003. GPS constraints on Africa (Nubia) and Arabia plate motions. Geophysical Journal International 155, 126–138.
McClusky, S., Reilinger, R., Obugazghi, G., Amleson, A., Healeb, B., Vernant, P., Sholan, J., Fisseha, S., Asfaw, L., Bendick, R., Kogan, L., 2010. Kinematics of the southern Red Sea–Afar Triple Junction and implications for plate dynamics. Geophysical Research Letters 37, L05301.
McCulloch, M.T., Mortimer, G.E., 2008. Applications of the $^{238}U/^{230}Th$ decay series to dating of fossil and modern corals using MCICPMS. Australian Journal of Earth Science 55, 955–965.
Mannino, M.A., Thomas, K.D., 2002. Depletion of a resource? The impact of prehistoric human foraging on intertidal communities and its significance for human settlement, mobility and dispersal. World Archaeology 33, 452–474.
Marks, A.E., 2009. The Paleolithic of Arabia in an inter-regional context. In: Petraglia, M.D., Rose, J.I. (Eds.), The Evolution of Human Populations in Arabia. Springer, Dordrecht, Netherlands, pp. 295–308.
Mitrovica, J.X., 2003. Recent controversies in predicting post-glacial sea-level change: a viewpoint. Quaternary Science Reviews 22, 127–133.
Mitrovica, J.X., Milne, G.A., 2003. On post-glacial sea level: I. General theory. Geophysical Journal International 154, 253–267.
Morwood, M.J., Jungers, W.L., 2009. Conclusions: implications of the Liang Bua excavations for hominin evolution and biogeography. Journal of Human Evolution 57 (5), 640–648.
Morwood, M.J., Aziz, F., O'Sullivan, P., NasruddinHobbs, D.R., Raza, A., 1999. Archaeological and palaeontological research in central Flores, east Indonesia: results of fieldwork 1997–98. Antiquity 73, 273–286.
Murray-Wallace, C.V., 2002. Pleistocene coastal stratigraphy, sea-level highstands and neotectonism of the southern Australian passive continental margin – a review. Journal of Quaternary Science 17, 469–489.
Nakada, M., Lambeck, K., 1987. Glacial rebound and relative sea-level variations: a new appraisal. Geophysical Journal of the Royal Astronomical Society 90, 171–224.
Nakada, M., Lambeck, K., 1988. The melting history of the late Pleistocene Antarctic ice sheet. Nature 333, 36–40.
Neev, D., Friedman, G.M., 1978. Late Holocene tectonic activity along the margins of the Sinai subplate. Science 202, 427–429.
Noble, W., Davidson, I., 1996. Human Evolution, Language and Mind. Cambridge University Press, Cambridge.
O'Connell, J.F., Allen, J., Hawkes, K., 2010. Pleistocene Sahul and the origins of seafaring. In: Anderson, A., Barrett, J.H., Boyle, K.V. (Eds.), The Global Origins and Development of Seafaring. McDonald Institute for Archaeological Research, Cambridge, pp. 57–68.
O'Connor, S., 2010. Pleistocene migrations and colonization in the Indo-Pacific region. In: Anderson, A., Barrett, J.H., Boyle, K.V. (Eds.), The Global Origins and Development of Seafaring. McDonald Institute for Archaeological Research, Cambridge, pp. 41–55.
Parker, A.G., 2009. Pleistocene climate change in Arabia: developing a framework for hominin dispersal over the last 350 ka. In: Petraglia, M.D., Rose, J.I. (Eds.), The Evolution of Human Populations in Arabia. Springer, Dordrecht, Netherlands, pp. 39–49.
Paulson, A., Zhong, S., Wahr, J., 2005. Modelling post-glacial rebound with lateral viscosity variations. Geophysical Journal International 163, 357–371.
Peltier, W.R., 1998. Postglacial variations in the level of the sea: implications for climate dynamics and solid-Earth geophysics. Reviews of Geophysics 36, 603–689.
Peltier, W.R., Andrews, J.T., 1976. Glacial-isostatic adjustment – I: the forward problem. Geophysical Journal of the Royal Astronomical Society 46, 669–705.
Petraglia, M.D., 2003. The Lower Palaeolithic of the Arabian Peninsula: occupations, adaptations, and dispersals. Journal of World Prehistory 17, 141–179.
Petraglia, M.D., Rose, J.I. (Eds.), 2009. The Evolution of Human Populations in Arabia. Springer, Dordrecht, Netherlands.
Petraglia, M., Alsharekh, A., 2003. The Middle Palaeolithic of Arabia: implications for modern human origins, behaviour and dispersals. Antiquity 77 (298), 671–684.
Petraglia, M.D., Alsharekh, A.M., Crassard, E., Drake, N.A., Groucutt, H., Parker, A.G., Roberts, R.G., 2011. Middle Paleolithic occupation on a Marine Isotope Stage 5 lakeshore in the Nefud Desert, Saudi Arabia. Quaternary Science Reviews 30 (13–4), 1555–1559.
Plaziat, J.-C., Baltzer, F., Choukri, A., Conchon, O., Freytet, P., Orszag-Sperber, F., Purser, B.H., Raguideau, A., Reyss, J.-L., 1995. Quaternary changes in the Egyptian shoreline of the northwestern Red Sea and Gulf of Suez. Quaternary International 29–30, 11–22.
Plaziat, J.-C., Baltzer, F., Choukri, A., Conchon, O., Freytet, P., Orszag-Sperber, F., Raguideau, A., Reyss, J.-L., 1998. Quaternary marine and continental sedimentation in the northern Red Sea and Gulf of Suez (Egyptian coast): influences of rift tectonics, climatic changes and sea-level fluctuations. In: Purser, B.H., Bosence, D.W.J. (Eds.), Sedimentation and Tectonics of Rift Basins: Red Sea – Gulf of Aden. Chapman & Hall, London, pp. 537–573.
Plaziat, J.-C., Reyss, J.-L., Choukri, A., Cazala, C., 2008. Diagenetic rejuvenation of raised coral reefs and precision of dating. The contribution of the Red Sea reefs to the question of reliability of the Uranium-series datings of middle to late Pleistocene key reef-terraces of the world. Carnets de Géologie 4, 1–40.
Purser, B.H., Bosence, D.W.J. (Eds.), 1998. Sedimentation and Tectonics of Rift Basins: Red Sea–Gulf of Aden. Chapman and Hall, London.
Rabineau, M., Berné, S., Olivet, J.-L., Aslanian, D., Guillocheau, F., Joseph, P., 2006. Paleo sea levels reconsidered from direct observation of paleoshoreline position during Glacial Maxima (for the last 500,000 years). Earth and Planetary Science Letters 252, 119–137.
Raymo, M.E., Mitrovica, J.X., O'Leary, M.J., DeConto, R.M., Hearty, P.J., 2011. Departures from eustasy in Pliocene sea-level records. Nature Geoscience 4, 328–332.
Reches, Z., Erez, J., Garfunkel, Z., 1987. Sedimentary and tectonic features in the northwestern Gulf of Elat, Israel. Tectonophysics 141, 169–180.
Reyss, J.-L., Choukri, A., Plaziat, J.-C., Purser, B.H., 1993. Datations radiochimiques des récifs coralliens de la rive occidentale du Nord de la Mer Rouge, premières implications stratigraphiques et tectoniques. Comptes Rendus de l'Académie des Sciences 317, 487–492.
Rídl, J., Edens, C.M., Černý, V., 2009. Mitochondrial DNA structure of Yemeni population: regional differences and the implications for different migratory contributions. In: Petraglia, M.D., Rose, J.I. (Eds.), The Evolution of Human Populations in Arabia. Springer, Dordrecht, Netherlands, pp. 69–78.
Rihm, R., Henke, C.H., 1998. Geophysical studies on tectonic controls on Red Sea rifting, opening and segmentation. In: Purser, B.H., Bosence, D.W.J. (Eds.), Sedimentation and Tectonics of Rift Basins: Red Sea–Gulf of Aden. Chapman and Hall, London, pp. 27–49.
Rohling, E.J., Fenton, M., Jorissen, F.J., Bertrand, P., Ganssen, G., Caulet, J.P., 1998. Magnitudes of sea-level lowstands of the past 500,000 years. Nature 394, 162–165.
Rohling, E.J., Grant, K., Bolshaw, M., Roberts, A.P., Siddall, M., Hemleben, C., Kucera, M., 2009. Antarctic temperature and global sea level closely coupled over the past five glacial cycles. Nature Geoscience 2, 500–504.
Shackleton, N.J., 1987. Oxygen isotopes, ice volume and sea level. Quaternary Science Reviews 6, 183–190.
Shackleton, N.J., Opdyke, N.D., 1973. Oxygen isotope and palaeomagnetic stratigraphy of equatorial Pacific core V28-238: oxygen isotope temperatures and ice volumes on a 10^5 year scale and 10^6 year scale. Quaternary Research 3, 39–55.
Shaked, Y., Marco, S., Lazar, B., Stein, M., Cohen, C., Sass, E., Agnon, A., 2002. Late Holocene shorelines at the Gulf of Aqaba: migrating shorelines under conditions of tectonic and sea level stability. In: EGU Stephan Mueller Special Publication Series, vol. 2 105–111.
Siddall, M., Rohling, E.J., Almogi-Labin, A., Hemleben, C., Meischner, D., Schmelzer, I., Smeed, D.A., 2003. Sea-level fluctuations during the last glacial cycle. Nature 423, 853–858.
Siddall, M., Smeed, D.A., Hemleben, C., Rohling, E.J., Schmelzer, I., Peltier, W.R., 2004. Understanding the Red Sea response to sea level. Earth and Planetary Science Letters 225, 421–434.
Sivan, D., Wdowinski, S., Lambeck, K., Galili, E., Raban, A., 2001. Holocene sea-level changes along the Mediterranean coast of Israel, based on archaeological observations and numerical model. Palaeogeography, Palaeoclimatology, Palaeoecology 167, 101–117.
Sivan, D., Lambeck, K., Toueg, R., Raban, A., Porat, Y., Shirman, B., 2004. Ancient coastal wells of Caesarea Maritima, Israel, an indicator for sea-level changes during the last 2000 years. Earth and Planetary Science Letters 222, 315–330.
Stern, R.J., Johnson, P., 2010. Continental lithosphere of the Arabian Plate: a geologic, petrologic, and geophysical synthesis. Earth-Science Reviews 101, 29–67.
Stirling, C.H., Esat, T.M., Lambeck, K., McCulloch, M.T., 1998. Timing and duration of the last interglacial: evidence for a restricted interval of widespread coral reef growth. Earth and Planetary Science Letters 160, 745–762.
Strasser, A., Strohmenger, C., Davaud, E., Bach, A., 1992. Sequential evolution and diagenesis of Pleistocene coral reefs (South Sinai, Egypt). Sedimentary Geology 78, 59–79.
Strasser, T.F., Panagopoulou, E., Runnels, C.N., Murray, P.M., Thomson, N., Karkanas, P., McCoy, F.W., Wegmann, K.W., 2010. Stone Age seafaring in the Mediterranean: evidence from the Plakias region for Lower Palaeolithic and Mesolithic habitation of Crete. Hesperia 79, 145–190.
Stringer, C., 2000. Coasting out of Africa. Nature 405, 24–27.
Svendsen, J.I., Astakhov, V.I., Bolshiyanov, D.Y., Demidov, I., Dowdeswell, J.A., Gataullin, V., Hjort, C., Hubberten, H.W., Larsen, E., Mangerud, J., Melles, M., Möller, P., Saarnisto, M., Siegert, M.J., 1999. Maximum extent of the Eurasian ice sheets in the Barents and Kara Sea region during the Weichselian. Boreas 28, 234–242.
UKHO, 2000. Catalogue of Admiralty Charts and Publications, Charts. UK Hydrographic Office, Taunton, UK.
Van Andel, T.H., Shackleton, N.J., 1982. Late Paleolithic and Mesolithic coastlines of Greece and the Aegean. Journal of Field Archaeology 9, 445–454.
Veeh, H.H., 1966. $^{230}Th/^{238}U$ and $^{234}Th/^{238}U$ ages of Pleistocene high sea level stand. Journal of Geophysical Research 71, 3379–3386.

Vincent, P., 2008. Saudi Arabia: an Environmental Overview. Routledge, London, 309 pp.
Vita-Finzi, C., 1987. ^{14}C deformation chronologies in coastal Iran, Greece and Jordan. Journal of the Geological Society of London 144, 553–560.
Vita-Finzi, C., Spiro, B., 2006. Isotopic indicators of deformation in the Red Sea. Journal of Structural Geology 28, 1114–1122.
Waelbroeck, C., Labeyrie, L., Michel, E., Duplessy, J.C., McManus, J.F., Lambeck, K., Balbon, E., Labracherie, M., 2002. Sea-level and deep water temperature changes derived from benthonic foraminifera isotopic records. Quaternary Science Reviews 21, 295–305.
Walter, R.C., Buffler, R.T., Bruggemann, J.J., Guillaume, M.M.M., Berhe, S.M., Negassi, B., Libsekal, Y., Cheng, H., Edwards, R.L., von Gosel, R., Neraudeau, D., Gagnon, M., 2000. Early human occupation of the Red Sea coast of Eritrea during the Last Interglacial. Nature 405, 65–69.
Werner, G., Lange, K., 1975. A bathymetric survey of the sill area between the Red Sea and the Gulf of Aden. Geologisches Jarbuch D 13, 125–130.
Yokoyama, Y., de Dekker, P., Lambeck, K., Johnston, P., Fifield, L.K., 2001. Sea-level at the Last Glacial Maximum: evidence from northwestern Australia to constrain ice volumes for oxygen isotope stage 2. Palaeogeography, Palaeoclimatology, Palaeoecology 165, 281–297.